STABILIZATION OF MULTILOOP SYSTEMS VIA THE SENSITIVITY FUNCTION

by

R. Haddad

Research Report PIBMRI-944-61
Contract No. AF-18(603)-105

for

Office of Scientific Research
Washington, D. C.

August 30, 1961

POLYTECHNIC INSTITUTE OF BROOKLYN
MICROWAVE RESEARCH INSTITUTE

AFOSR-1420

Research Report No. PIBMRI-944-61
Contract No. AF-18(603)-105

STABILIZATION OF MULTILOOP SYSTEMS VIA THE SENSITIVITY FUNCTION

by

R. Haddad

Polytechnic Institute of Brooklyn
Microwave Research Institute
55 Johnson Street
Brooklyn 1, New York

Research Report PIBMRI-944-61

Contract No. AF-18(603)-105

August 30, 1961

Title Page
Acknowledgment
Abstract
Table of Contents (2 Pages)
Table of Figures (2 Pages)
List of Tables
112 Pages of Text

Richard A. Haddad

Approved: John G. Truxal
John G. Truxal
Head, Electrical Engineering Dept.

Prepared for

Office of Scientific Research
Washington, D.C.

ACKNOWLEDGMENT

The author wishes to express his gratitude to his advisor, Professor J. G. Truxal, for his encouragement and guidance through all phases of this investigation. He is also indebted to Professors E. Mishkin, L. Braun, Jr., J. J. Bongiorno, P. Dorato, and his other colleagues of the Systems and Control Group for their many helpful suggestions and criticisms.

Special thanks are extended to Mrs. Margaret Toldo, and Miss Jean Beirne who typed the manuscript, and to Mr. Joel Krinsky who sketched the diagrams.

The work reported herein was supported in part by the Air Force Office of Scientific Research under Contract No. AF-18(603)-105. Support of some of the initial research under AF-18(600)-1505 and DA-30-069-ORD-1560 Contracts is also acknowledged.

ABSTRACT

The problem studied in this thesis is the stabilization of multiloop systems against individual variations in one or more of the system parameters. A correlation between the stability of a multiloop configuration and the real-frequency behavior of the sensitivity function is derived. From this relationship, a set of stability margins is developed which provide a quantitative measure of the destabilizing effects of variations in each parameter. The margins, referred to as "parameter gain and phase margins" are shown to be generalizations of the familiar gain and phase margins of the single-loop, servo system.

The design objective is the realization of a set of specified stability margins; the relationship between these margins and the real-frequency behavior of the associated sensitivity functions gives rise to specification of the sinusoidal response of compensation networks at a set of discrete frequencies.

TABLE OF CONTENTS

TABLE OF CONTENTS
(continued)

TABLE OF FIGURES

TABLE OF FIGURES

(continued)

LIST OF TABLES

Chapter I - Introduction and Summary

1.1. Preliminary Remarks

After a decade of intensive work in the theory of linear feedback systems a great variety of linear control problems still remain largely unsolved. Much of the classical control theory is concerned with the single-loop, unity-feedback system. The system specifications are translated into certain "figures of merit" or design objectives and the synthesis proceeds accordingly. For a servo system, these figures of merit frequently take the form of the error coefficients, the gain and phase margins, the bandwidth, the sensitivity, the rise time and overshoot for a step input, etc.

But, when confronted by a difficult or non-conventional problem, the control engineer often has resorted to computer studies and extensive breadboarding in order to obtain a suitable design. Although large-scale computer facilities are a boon to any research establishment, they concommittantly foster an air of empiricism which may tend to stifle inquiries into novel approaches to system design. Experimental design procedures--unless motivated and guided by a core of underlying theory--eventually fail as the complexity of the process and the stringency of the specifications increase.

The present state of the art, however, does not admit of a straightforward synthesis procedure for a system of reasonable complexity. [The complexity of a linear system is measured by the number of interlocking feedback loops, the number of variable parameters and the order of the process to be controlled.] In fact, considerable difficulty is encountered even in translating the specifications into specific design objectives. For example, how does one insure the stability of a control system despite variations in a process gain or time constant over a known range of values. If only one parameter is involved, and the order of the process is "moderate", the root-locus technique, or the Nyquist test, may suggest some stabilization procedures. But, if variations in two or more parameters of a high-order, multiloop system are encountered, the conventional methods described in standard servomechanism texts usually leave the engineer groping in the dark for specific and suitable design objectives. Indeed, the frustration and ignorance in designing complex control systems have stimulated some of the recent developments in adaptive and computer-controlled systems.

1.2. Scope of the Thesis

The foremost consideration in the design of any feedback control system is stability. The system must be stable not only at the nominal design values, but also in the face of finite variations in one or more of the parameters. This thesis is concerned with the stabilization of multiloop systems which are subject to gross parameter variations.

Concisely stated, the problem considered in this thesis is: A multiloop system is assumed to have been designed to operate satisfactorily at the nominal values of the parameters, $x_1, x_2, \ldots, x_n$. What compensation should be introduced so that variations in no one parameter can cause instability, where the range of variations of the parameters is known a priori?

In general terms, the solution to this problem involves three steps:

(1) A quantitative evaluation of the effects of changes in the parameters of the controlled process on the stability of the overall system. This evaluation provides a set of "stability margins" which reflect the relative importance of each parameter in determining the stability.

(2) A formulation of specific design objectives based on the descriptions of (1) and the range of variations.

(3) Translation of the objectives into specifications on the behavior of compensation networks whose function is to improve the relative stability.

Two characterizations are frequently employed in analyzing the effects of parameter changes on the dynamics and stability of a system. These are:

(1) The sensitivity function, which measures the dependence of the transmission on a specified parameter, and

(2) The gain and phase margins, which measure the relative stability of a single-loop configuration in terms of the decibel gain and phase of the loop transmittance.

These two descriptions, which are found to be intimately connected with the stability of the system, constitute the basis for the design procedure developed.

1.3. Summary

In this dissertation, a correlation between the stability of a multiloop configuration and the real-frequency behavior of the sensitivity function is derived. From this relationship evolves a set of stability margins which provide a quantitative measure of the destabilizing effects of individual variations in the system parameters. These margins, referred to as "parameter gain and phase margins", are shown to be generalizations of the familiar gain and phase margins of the single-loop system.

The realization of a prescribed set of stability margins constitutes the design objective; the relationships between these margins and the real-frequency behavior of the associated sensitivity functions lead to specification of the sinusoidal response of the networks introduced for stabilization.

In particular, it is found that oscillations caused by variations in a single parameter can only occur at a frequency when the sensitivity function with respect to that parameter is real. The value of the sensitivity at that frequency yields a direct measure of the required change in the parameter to cause instability. The compensation network can be specified at this frequency to insure against instability caused by the parameter change. The procedure is repeated for each individually varying parameter, thereby leading to a specification of the compensation networks at a set of discrete frequenices.

Chapter II - Signal-Flow Graph Topology and Sensitivity

In 1949, S. J. Mason proposed that sets of simultaneous, linear, algebraic equations be represented pictorially by "signal-flow" graphs, thereby founding a basis for a topological interpretation of linear analysis. Since then, Mason* and other researchers† have refined and exploited the theory to such a degree that the flow-graph formalism has become fundamental to the study of linear feedback systems.

In this chapter, those aspects of graph theory germane to this dissertation are briefly reviewed; then the sensitivity function is introduced and related to the topological properties of the flow graph. These definitions and relationships furnish the background for the developments of Chap. III where a correlation between stability and sensitivity is established.

2.1 Definitions, and Properties of Flow Graphs†

A signal-flow graph is a graphical portrayal of a set of linear equations. The variables or "signals" correspond to the nodes of the graph, while the linear relationships between variables are represented by unilaterally directed branches connecting the appropriate nodes. The node serves a dual function: to sum the signals arriving along incoming branches and to transmit the sum signal to all outgoing branches. A node performing only the former function is said to be a sink node, while one that carries out only the latter is a source node. The transmittance T_{jk} from source node j to sink node k is defined as the signal appearing at k due to a unit signal injected at j.

A loop l, is a simple closed path along which no node is passed more than once per cycle of traversal. Two loops are said to be touching if any node or branch is common to both. Otherwise, they are disjoint. An open path, P_{jk}, from node j to node k is a successive and continuous traversal along the branches from j to k along which no node is encountered more than once.

---

*S. J. Mason, "Feedback Theory: Some Properties of Signal-Flow Graphs", Proc. IRE, Sept., 1953, and "Feedback Theory: Further Properties of Signal-Flow Graphs", Proc. IRE, July, 1956.

†E. Mishkin and L. Braun, Jr., Editors, "Adaptive Control Systems", McGraw-Hill Book Co., 1961, Chap. 2.

†R. F. Hoskins, "Signal Flow-Graph Analysis and Feedback Theory", Institution of Electrical Engineers, July, 1960.

The transmittance of a signal-flow graph as formulated by Mason is expressed wholly in terms of loops and open paths as follows:

$$T(s) = \frac{\sum_k P_k(s)\Delta_k(s)}{\Delta(s)} \tag{2.1}$$

where Δ, the graph determinant, is defined by

$$\Delta = \left[1 - \sum_p \ell_p + \sum_{p,q} \ell_p \ell_q - \sum_{p,q,r} \ell_p \ell_q \ell_r + \cdots\right]^* \tag{2.2}$$

In Eq. (2.2), ℓ_p is the transmittance of the pth loop of the graph; the summation is taken over all distinct combinations of pairs of loops, triplets of loops, etc.; and the star $*$ implies that only non-touching loops are included in any product term. P_k is the transmittance of the kth forward path from the specified source node (or input) to the specified sink node (or output). The path factor, Δ_k, is the same as Δ except that all loops that touch P_k are deleted. Alternately, the path factor may be viewed as the graph determinant after the k^{th} forward path has been removed from the graph.

An arbitrary node, y_k, is split into a source half y_k' and a sink half y_k'', by letting all outgoing branches of y_k originate from y_k' and all incoming branches of y_k terminate on y_k''. This node-splitting process is illustrated in Fig. 2.1 for a system with three disjoint loops.

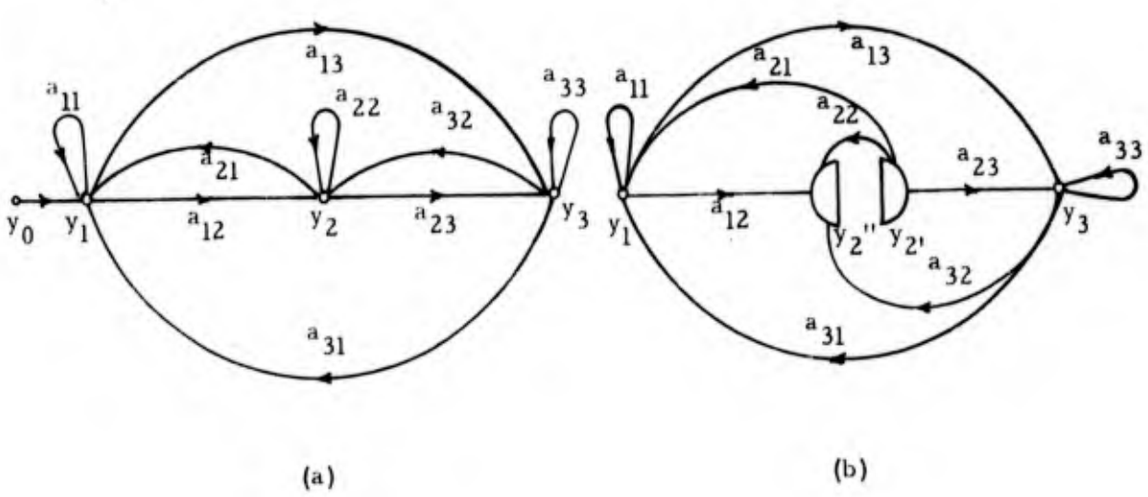

Fig. 2.1. Node y_2 is split into source half y_2' and sink half y_2''.

L_k, the loop transmittance with respect to node k, is defined as the transmittance from source to sink side of node k after it is split. Fig. 2.1b is redrawn as shown in Fig. 2.2 to illustrate that L_2 is the transmittance from y_2' to y_2''. L_k now can be evaluated by invoking the Mason reduction formula which must take the form

$$L_k = \frac{\sum_r P_r^k \Delta_r^k}{\Delta_k^o} \tag{2.3}$$

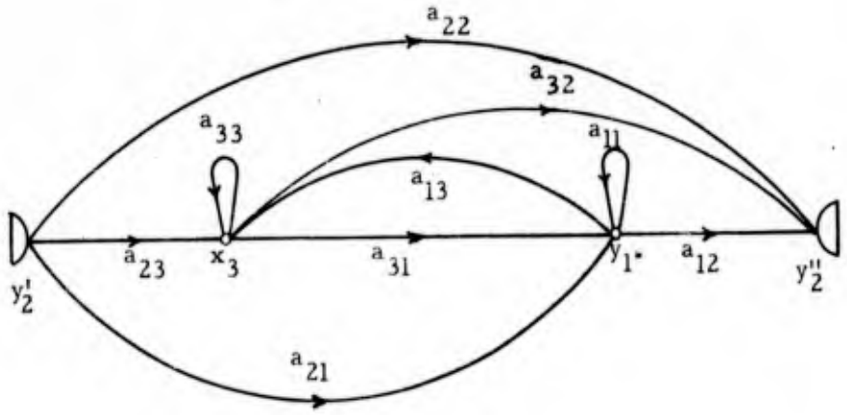

Fig. 2.2. Flow graph for computing loop transmittance with respect to node 2.

In Eq. (2.3), Δ_k^o is the graph determinant with node k split. But, since splitting k breaks all loops that formerly passed through node k, Δ_k^o must be the graph determinant obtained after node k is deleted from the graph. Δ_k^o is termed the residue of the node k. P_r^k is the forward path from y_k' to y_k'' and Δ_r^k is the cofactor of P_r^k, or the determinant with P_r^k removed. Once y_k' and y_k'' are recombined to form y_k, the P_r^k term is recognized as the r^{th} loop passing through k. Consequently, the $-P_r^k \Delta_r^k$ terms are identified with that part of the expansion of Δ which depends on k. (The minus sign takes account of the sign alternation in Δ). Therefore

$$\Delta = \Delta_k^o - \sum P_r^k \Delta_r^k \tag{2.4}$$

and

$$L_k = \frac{\Delta_k^o - \Delta}{\Delta_k^o} = 1 - \frac{\Delta}{\Delta_k^o} \tag{2.5}$$

The return difference with respect to k is defined as

$$F_k = 1 - L_k = \frac{\Delta}{\Delta_k^o} \tag{2.6}$$

and is seen to be the ratio of the graph determinant to the residue.

The loop transmittance, etc. can be referred to a branch of a graph rather than to a node. Let the branch be b. As shown in Fig. 2.3, a node β is inserted into the branch, and then split. The loop transmittance, etc. referred to the branch b are those evaluated with respect to the inserted node. In this case "splitting the node" at β is tantamount to "breaking the loop" at b. Thus L_b is the transmittance from β' to β'', and Δ_b^o, the residue of branch b, is the determinant computed after branch b is opened, or deleted from the graph.

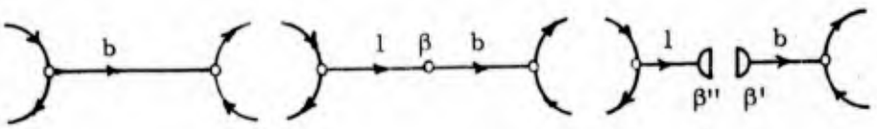

Fig. 2.3. Node insertion into a branch.

The loop gain and return difference provide a quantitative description of the feedback loops and their relationship to a selected node or branch. As defined, these quantities are wholly independent of input and output node designations. In order to afford a description of signal transmission through the forward or direct paths from input to output, and its dependence on a particular node or branch, a complementary set of functions called the null loop transmittance, L_k', and the null return difference, F_k', with respect to node k are defined as follows:

The node k is split and a unit signal is applied at the source half; the system input is then adjusted to make the system output zero. The resulting signal at the sink end of the split node is L_k'. And F_k' is given by

$$F_k' = 1 - L_k' \tag{2.7}$$

An arbitrary signal-flow graph with the k^{th} node split can be reduced[†] to the form shown in Fig. 2.4a. This reduction eliminates all internal nodes except the one of interest. The indicated transmittances are obtained by performing the operations

[†]J. G. Truxal, "Control System Synthesis", McGraw-Hill Co., N. Y., 1955, Chap. 2.

implicitly defined by the graph. For example, a_{1n} is the transmission from input to output of the original graph with node k removed.

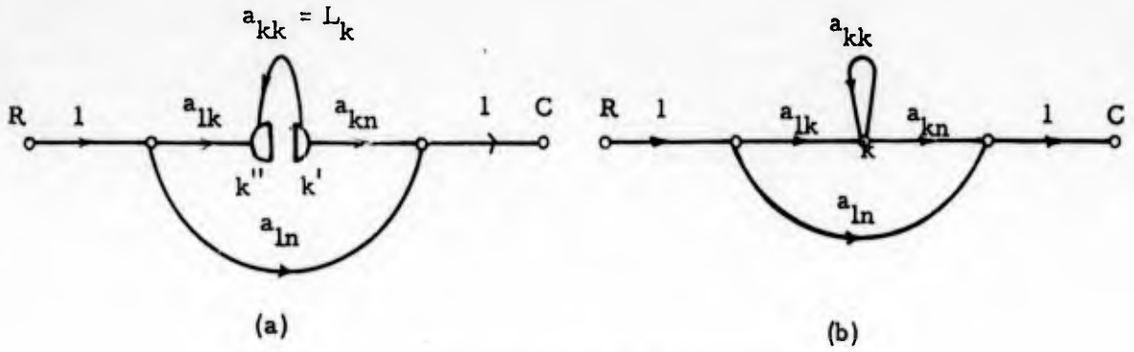

Fig. 2.4. Reduced forms of signal-flow graph.

L_k' can be visualized as the sum of two signals arriving at k'', one of which is due to the unit signal applied at k' (which must be L_k), and the other results from the input R. Thus

$$\left.\begin{aligned} L_k' &= L_k + \psi R^* \\ \text{and} \\ F_k' &= (1-L_k) - \psi R^* = F_k - \psi R^* \end{aligned}\right\} \qquad (2.8)$$

where ψ is the transmission from R to k'' and R^* is that value of R such that C = 0. From Fig. 2.4a, we have

$$\left.\begin{aligned} C &= a_{1n}R + a_{kn}\Big|_{R = R^*} = 0 \\ \text{and} \\ \psi &= a_{1k} \end{aligned}\right\} \qquad (2.9)$$

Consequently,

$$L_k' = a_{kk} - \frac{a_{1k}a_{kn}}{a_{1n}} \qquad (2.10)$$

and

$$\begin{aligned} F_k' &= (1 - a_{kk}) + \frac{a_{1k}a_{kn}}{a_{1n}} \\ &= \frac{a_{1n} + (a_{1k}a_{kn} - a_{kk}a_{1n})}{a_{1n}} \end{aligned} \qquad (2.11)$$

Coalescence of the split node yields the graph of Fig. 4.2b which is equivalent to the original at nodes R, C, and k. Inspection of Fig. 2.4b reveals that the numerator (or Σ term) of $T = C/R$ is

$$\begin{aligned}\Sigma &= a_{ln}(1 - a_{kk}) + a_{lk}a_{kn} \\ &= \underbrace{a_{ln}}_{\Sigma_k^o} + \underbrace{(a_{lk}a_{kn} - a_{ln}a_{kk})}_{\Sigma(k)}\end{aligned} \tag{2.12}$$

Σ is recognized as the numerator of F_k' and Σ_k^o as the denominator. Therefore,

$$F_k' = \Sigma/\Sigma_k^o \tag{2.13}$$

The return differences with respect to a node or branch as expressed in Eqs. (2.6) and (2.13) are perfectly general formulations. But, when the return differences are referred to a system parameter x, the situation is not quite so clear-cut. The distinction between the two cases arises from the possibility that the parameter may appear in several branches.* At this point, it is not obvious which branches should be broken, nor what should be evaluated.

The fundamental consideration is the linearity of the graph determinant in x. Thus, although Δ is a linear function of any branch gain, it is not necessarily linear in x. For example, if x is found in two non-touching loops, the expansion for Δ is quadratic in x. Sufficient conditions** for linearity are:

(1) there exist no two disjoint loops such that x appears as a linear term of each;

(2) x appears, at most, once in each loop.

For the purposes of this dissertation, the linearity of Δ is assumed. When Δ is linear, the return differences are defined on a topological basis by

$$\left.\begin{aligned}F_x &= \Delta/\Delta_x^o \\ F_x' &= \Sigma/\Sigma_x^o\end{aligned}\right\} \tag{2.14}$$

where Δ_x^o is the graph determinant evaluated after breaking all branches containing x, and Σ_x^o is Σ obtained similarly.

Two special cases frequently treated in this thesis are those of unity and infinite null return difference. If F_x' is infinite (or $\Sigma_x^o = 0$), the reference element is contained in all forward paths, and no forward path fails to touch all loops. If F_x' is unity (or $\Sigma_x = 0$), the reference parameter is not contained in any forward path and does not enter any path factor.

*It is assumed that by manipulation of the flow graph, the parameter is made to appear as the transmittance of one or more branches. Some examples of this technique are given in Fig. 3.6.

**Hoskins, op. cit.

2.2. Topological Formulation of Sensitivity[+]

The sensitivity function is a measure of the dependence of the overall transmission T on a specified system parameter x, and is defined as

$$S_x^T = \frac{\partial \ell n\, T}{\partial \ell n\, x} \tag{2.15}$$

Since $\frac{\partial \ell n\, T}{\partial \ell n\, x} = \frac{\partial T/T}{\partial x/x}$, S_x^T is interpreted as the ratio of the percent variation in T to the percent variation in x for small changes in the parameter. Therefore, an alternate form for Eq. (2.15) is

$$S_x^T = \frac{\partial T/T}{\partial x/x} = \frac{x}{T}\,\frac{\partial T}{\partial x} \tag{2.16}$$

Substituting the Mason Formula into Eq. (2.15) yields

$$\begin{aligned} S_x^T &= \frac{\partial \ell n(\Sigma/\Delta)}{\partial \ell n\, x} = \frac{\partial \ell n\, \Sigma}{\partial \ell n\, x} - \frac{\partial \ell n\, \Delta}{\partial \ell n x} \\ &= S_x^{\Sigma} - S_x^{\Delta} \end{aligned} \tag{2.17}$$

If T is a bilinear function of x -- that is to say, Σ and Δ are each linear in x of the form[++]

$$\left.\begin{aligned} \Sigma &= \Sigma_x^o + x\Sigma_x \\ \Delta &= \Delta_x^o + x\Delta_x \end{aligned}\right\} \tag{2.18}$$

the two components of the sensitivity function are

$$\left.\begin{aligned} S_x^{\Sigma} &= \frac{x}{\Sigma}\,\frac{\partial \Sigma}{\partial x} = \frac{x\Sigma_x}{\Sigma} = 1 - \frac{\Sigma_x^o}{\Sigma} \\ S_x^{\Delta} &= \frac{x}{\Delta}\,\frac{\partial \Delta}{\partial x} = \frac{x\Delta_x}{\Delta} = 1 - \frac{\Delta_x^o}{\Delta} \end{aligned}\right\} \tag{2.19}$$

[+] W. A. Lynch, "A Formulation of the Sensitivity Function" Correspondence, PGCT, vol. CT-4, no. 3, p. 289, Sept., 1957.

[++] If x is explicitly displayed as the gain of one or more branches of the flow graph, the bilinearity of T and the linearity of Δ and Σ are synonymous.

Hence, Eq. (2.17) becomes

$$S_x^T = \frac{\Delta_x^o}{\Delta} - \frac{\Sigma_x^o}{\Sigma} \tag{2.20}$$

or

$$S_x^T = \frac{1}{F_x} - \frac{1}{F_x'} \tag{2.21}$$

Equation (2.21) suggests the possibility of attaining zero sensitivity to a parameter. This somewhat utopian hope is exploded by the following considerations. If S_x^T is to be identically zero, then one possibility is to tentatively set $F_x' = F_x$ or equivalently $L_x' = L_x$. But Eqs. (2.8) and (2.10) point out the incompatibility of the latter condition (except for the trivial case wherein a_{1k} or a_{kn} is identically zero which in effect completely isolates node k from the graph). The only other alternative occurs when both $F_x' = \infty$ and $F_x = \infty$. The first requirement usually can be satisfied, as illustrated in the two examples below. The second condition implies that the loop gain L_x, must be infinite. To the author's knowledge all proposed zero sensitivity achemes have involved such a quest for an infinite loop gain. Two such configurations discussed by Truxal[*] are shown in Figs. 2.5a and 2.5b.

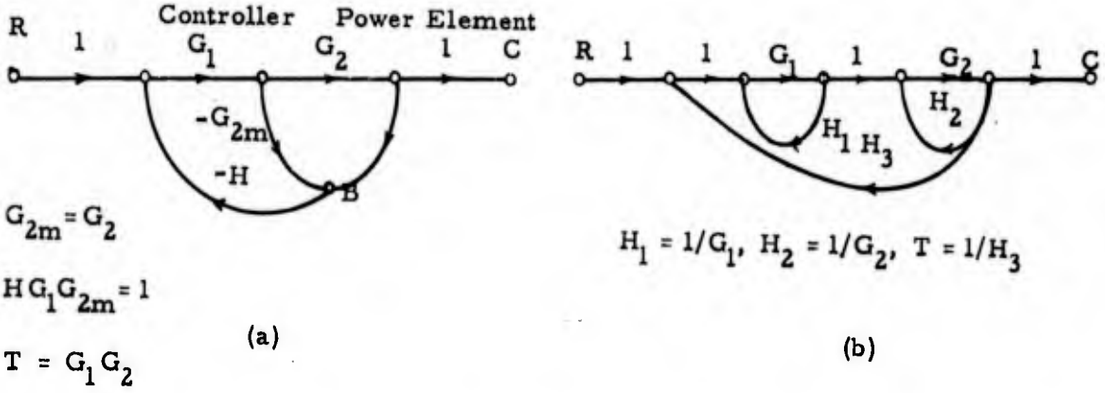

Fig. 2.5. Zero-sensitivity systems.

In Fig. 2.5a, G_{2m} represents a low-power model of the power stage, G_2. If G_{2m} is an accurate model of G_2, the signal B is zero and there is no net feedback (and no stability problem). The loop gain and sensitivity with respect to G_2 are

$$\left.\begin{aligned} L_{G2} &= \frac{-G_2HG_1}{1 - HG_1G_{2m}} \\ S_{G2}^T &= \frac{1 - HG_1G_{2m}}{1 + HG_1(G_2 - G_{2m})} \end{aligned}\right\} \tag{2.22}$$

[+]Mishkin and Braun, op. cit., Chapt. 4.

The loop gain is infinite and the sensitivity zero if H is selected to model $1/G_1G_{2m}$ over the significant frequency band. Under these conditions, the transmission is

$$T = G_1G_2 \tag{2.23}$$

In Fig. 2.5b, L_{G2} is made infinite by selecting $H_1 = 1/G_1$, thereby affording an infinite gain stage in the feedback loop about G_2. Moreover, if $H_2 = 1/G_2$, then L_{G1} is also infinite, thereby rendering the system transmission insensitive to both G_1 and G_2.

It should be noted, however, that zero sensitivity is attained only at the null conditions specified for each of the two configurations. If HG_1G_{2m} of Fig. 2.5a or H_1G_1 of Fig. 2.5b were to drift from the design values of unity, then the respective loop gains would become finite. More significantly, the stability problem occasioned by component drift at high levels of loop gain becomes quite critical.

The stability problems generated by these considerations require quantitative evaluation. A host of questions is immediately raised. What quantitative information is furnished by the sensitivity function other than the obvious definition involving percentage variations? Can criteria be derived which would insure satisfactory system operation despite large variations in one or more parameters? If so, then what specifications or tolerances on component blocks are required? How can multiloop configurations be employed to advantage and what is the underlying design philosophy for such systems? In short, of what value is the sensitivity function as a guide to the analysis and design of multiloop, multiparameter feedback systems?

In the chapters that follow, an attempt is made to answer, in part, some of these questions. In particular, a correlation between the formalism of flow-graph topology and the real frequency behavior of the sensitivity function is effected and then extensively employed in stability analysis and in obtaining design objectives in the real frequency domain. It is shown that the criteria so evolved are essentially generalizations of the design procedures normally followed in the single-loop, single-parameter case.

Chapter III - Stability and the Sensitivity Function

The stability of any linear, time-invariant system is wholly determined by the nature of the roots of the system's characteristic polynomial. The necessary and sufficient condition that a system be stable is, of course, that all zeros of the polynomial have negative real parts. The sundry stability tests and theorems must all reduce to this fundamental investigation.

In any case, the theorem invoked depends on the form of the available data describing the system and on the particular use to which the derived stability information will be put. Thus, the Routh-Hurwitz test may be employed if the coefficients of the polynomial are specified in numeric form. A "brute force" application of this technique yields stability boundaries if two or more variable coefficients are involved; but the test does not readily lead to stabilization methods. The root-locus method is particularly useful in describing the behavior of a system with one varying parameter; but, the loci are difficult to plot and interpret for high-order systems. The Nyquist and Bode plots are applicable and convenient when real (sinusoidal) frequency characterization of the component blocks is available. Frequently, however, the engineer must resort to computer simulation and, in many instances, empiricism is the principal guide to design.

The stability of a multiloop and/or multiparameter system is intimately connected with the topology of the configuration. Two generalizations of the Nyquist criterion which are sometimes employed in the analysis of such complex systems, are described in Se. 3.1. The practical limitations of these techniques point out the need for alternate and simpler approaches.

The sensitivity functions of Chap. II not only provide a particularly simple stability criterion for complex systems, but also suggest possible stabilization methods. Various aspects of sensitivity and stability are explored in this chapter; a correlation among such matters as sensitivity, stability, gain and phase margins, real frequency behavior, phase-angle loci, and topology is established.

3.1. Stability and Topology--Nyquist Criterion*

Since the transmission of any signal-flow graph is given by

$$T = \frac{\Sigma}{\Delta} \tag{3.1}$$

the stability of the system is determined by the zeros of Δ and the poles of Σ. If it is assumed that the graph is drawn so as to indicate explicitly all feedback loops, all branches of the graph are stable. [If an unstable branch exists, it can be replaced by a feedback loop with stable branches]. Since sums and products of stable transmittances

*J. G. Truxal, op. cit. Chap. 2

yield minimum phase poles and possibly, some non-minimum phase zeros, without loss of generality, it can be assumed that Σ is stable. Consequently, only the zeros of Δ need be examined for stability.

For a graph consisting of n nodes, F_1 is defined as the return difference with respect to node 1, F_2^+ as the return difference with respect to node 2 with node 1 split, F_3^+ as the return difference referred to node 3 with nodes 1 and 2 split, etc.. From the topological definition of return difference as expressed by Eq. (2.6), the F_j's are related to certain graph determinants by

$$\left.\begin{aligned} F_1 &= \Delta/\Delta_1^o \\ F_2^+ &= \Delta_1^o/\Delta_{1,2}^o \\ F_3^+ &= \Delta_{1,2}^o/\Delta_{1,2,3}^o \\ &\text{etc.} \end{aligned}\right\} \qquad (3.2)$$

where Δ_1^o is the graph determinant with node 1 deleted, $\Delta_{1,2}^o$ the determinant with nodes 1 and 2 split, and so forth.

From Eq. (3.2), Δ is expressed as the product of the partial return differences.

$$\Delta = F_1 F_2^+ \ldots F_m^+. \qquad (3.3)$$

[The last subscript in Eq. (3.3) is taken as m, the number of nodes which must be split to open all the loops. Obviously $m \leq n$, and the F_k^+ for $m < k \leq n$ are all unity.]

Alternately, Δ can be expressed in terms of "partial loop gains" as

$$\Delta = (1-L_1)(1-L_2^*) \ldots (1-L_m^*) \qquad (3.4)$$

The Nyquist test can now be applied successively to each of the m product terms in Eq. (3.3) in order to detect the presence of any right-half plane zeros. According to the familiar criterion, the number of clockwise origin encirclements in the F_j^+ plane equals the excess of zeros over poles of F_j^* in the right-half plane.

$$\text{i.e.,} \qquad N_j = Z_j - P_j \qquad (3.5)$$

where N_j is the number of clockwise encirclements, Z_j and P_j the number of non-minimum phase zeros and poles of F_j^+ respectively.

For $j = m$, we have $N_m = Z_m - P_m$. But P_m is zero since L_m^* can only consist of products of stable branches after nodes 1 through m are split. Furthermore, $N_{m-1} = Z_{m-1} - P_{m-1}$, where P_{m-1} is the number of right-half plane poles of L_{m-1}^*. These non-minimum phase poles can only arise from the non-minimum phase zeros of F_m^* since only node m has an operative loop. Hence $P_{m-1} = Z_m$, and $N_{m-1} = Z_{m-1} - Z_m = Z_{m-1} - N_m$. Therefore,

$$Z_{m-1} = N_m + N_{m-1} \tag{3.6}$$

Continuing in this fashion, we obtain

$$Z_1 = N_m + N_{m-1} + \ldots + N_1 = \sum_{j=1}^{m} N_j \tag{3.7}$$

But the total excess of zeros over poles in the right-hand plane of $F_1^* F_2^* \ldots F_m^*$ is simply the number of non-minimum phase zeros of Δ. Consequently for stability this number must be zero, and the criterion becomes

$$\sum_{k=1}^{m} N_k = 0 \tag{3.8}$$

where N_j is the number of clockwise origin encirclements of the F_j^* plot. [The shift to the +1 point in the L_j^* plane is trivial].

If $m > 2$, such plots become quite tedious to sketch, and rather difficult to interpret since variations in only one parameter may affect several of the Nyquist contours.

If two or more parameters vary simultaneously, then Meyer's[*] Convex Hull method can be employed in a stability analysis. A brief exposition of this method follows.

A flow graph has n variable branch parameters $x_1, x_2, \ldots x_n$ which are normalized so that each varies between zero and unity. Since the graph determinant is linear in all branch quantities, the most general form for Δ is

---

[*]B. R. Meyers, "A Useful Extension of the Nyquist Criterion to Stability Analysis of Mulitloop Feedback Amplifiers", Proc. Fourth Midwest Symposium on Circuit Theory, pp. J1 - J17, Dec. 1959, and "Two Theorems in Multi-Weighted Sums", Journal of the Society for Industrial and Applied Mathematics, March, 1961

$$\Delta(s) = 1 + x_1 G_1(s) + x_2 G_2(s) + \ldots + x_n G_n(s) + x_1 x_2 G_{12}(s) + x_1 x_3 G_{13}(s) + \ldots + \ldots + x_1 x_2 \ldots x_n G_{12..n}(s) \tag{3.9}$$

where

$$0 \leq x_i \leq 1 \quad , \text{ for } \quad 1 \leq i \leq n \tag{3.10}$$

Meyer's method determines if $\Delta(s)$ has any zeros in the right-half plane for any combination of x's within the range specified by Eq. (3.10), which can be imagined as defining a hyper-cube in n-dimensional parameter space with 2^n vertices. Each vertex of the hyper-cube corresponds to a possible binary combination of the x's, i.e., each vertex corresponds to the condition $x_i = 0$ or $x_i = 1$.

A Nyquist plot in the $\Delta(j\omega)$ plane is sketched for each vertex; since the origin of parameter space ($x_i = 0$, for all i) yields $\Delta = 1$, then $2^n - 1$ Nyquist contours are required. Points corresponding to equal frequencies on each of these contours are then connected to form a convex polygon or "hull". Thus as ω varies from 0 to ∞, the convex polygon pivots about the point 1 as shown in Fig. 3.1.

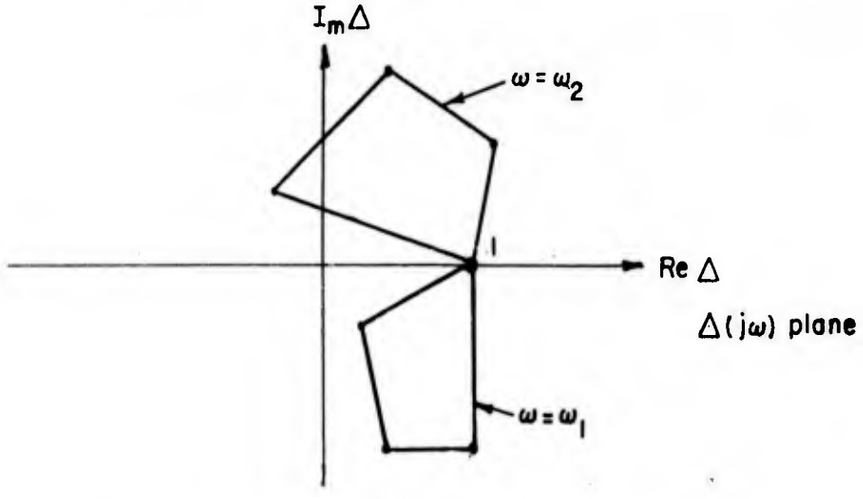

Fig. 3.1. Convex polygon method.

A sufficient condition for stability is that the area traced out by the convex polygon as ω varies from zero to infinity does not enclose the origin. The theorem is both necessary and sufficient for stability when the mapping from the hyper-cube onto the convex polygon is said to be "complete". Although the

conditions for completeness are not generally known, a sufficient condition is that the graph determinant take the form

$$\Delta = 1 + x_1 G_1 + x_1 x_2 G_{12} + \cdots + x_1 x_2 \cdots x_n G_{12\cdots n} \tag{3.11}$$

The major drawbacks of the convex hull method from the analysis standpoint are three-fold:

(1) Tedium in execution for high-order systems with $n > 2$.

(2) Difficulty of interpretation in terms of oscillation frequencies, relative damping and the like.

(3) Limitation of the theorem to a sufficiency condition except in very special circumstances.

From the design standpoint, the plots appear to yield little insight into possible stabilization techniques even if the system is simple enough at the outset.

Of the two Nyquist procedures described in this section, neither is particularly useful except in those rare situations wherein the engineer can visualize and easily perceive the effects of compensation networks on the contours. In control system analysis and design, the desideratum is a set of simple rules and criteria which may be exploited with relative ease. The techniques discussed above, and with them one might include the Routh test, fail in this respect. It is shown in the next section that a simple stability test, formulated in terms of the sensitivity functions of Chap. II, yields considerable insight into the behavior of complex systems.

3.2. Sensitivity-Stability Theorem[†]

This theorem relates the behavior of the sensitivity function along the $j\omega$ axis to the dependence of the stability on the parameter x. Two special cases are treated at first; the general situation is then reduced to one of the two special cases. In the discussion that follows it is assumed that the system transmittance T is a bilinear function of x so that the considerations of Sec. 2.2, and Eqs. (2.18) thru (2.21) are applicable.

(a) If F_x', the null return difference with respect to x, is unity, (or Σ_x is zero) the system transmittance is

$$T = \frac{\Sigma}{\Delta} = \frac{\Sigma_x^{\,o}}{\Delta_x^{\,o} + x\Delta_x} \tag{3.12}$$

[†]W. A. Lynch and J. G. Truxal, "The Significance of Sensitivity in Feedback Systems Studies", Research Report PIBMRI-866-60, Microwave Research Institute, Polytechnic Institute of Brooklyn, 1961.

and

$$S_x^T = \frac{\Delta_x^o}{\Delta} - 1 = -\frac{x\Delta_x}{\Delta} \tag{3.13}$$

T(s) is stable at $x = x_o$ the nominal setting of the parameter--i.e., the poles of $T(s, x_o)$, which are the poles of Σ_o and the zeros of $(\Delta_x^o + x_o\Delta_x)$, lie in the left-half plane. Then the necessary and sufficient condition that T become unstable as a consequence of a variation in x from its nominal value is that there exist a real frequency ω_x such that the sensitivity with respect to x evaluated at $x = x_o$ and $s = j\omega_x$ is real and finite--i.e.,

$$S_x^{T(s)}\Big|_{\substack{s = j\omega_x \\ x = x_o}} = \text{real, finite} \tag{3.14}$$

Proof: Only the zeros of $\Delta(s)$ change with x. If T becomes unstable the zeros of $\Delta(s)$ must cross the $j\omega$ axis at a point $\omega = \omega_x$ at the critical value of the parameter

$$x_{cr} = x_o + \delta_{cr} \tag{3.15}$$

That is to say, the equation

$$\Delta(x_{cr}, j\omega_x) = 0 \tag{3.16}$$

must be satisfied for real values of x_{cr} and ω_x. Equation (3.16) can be expanded into

$$\Delta(x_{cr}, j\omega_x) = \Delta_o(j\omega_x) + (x_o + \delta_{cr})\Delta_x(j\omega_x)$$

$$= \left[\Delta_o(j\omega_x) + x_o\Delta_x(j\omega_x)\right] + \delta_{cr}\Delta_x(j\omega_x) \tag{3.17}$$

The expression within the brackets of Eq. (3.17) is simply the graph determinant evaluated at ω_x and nominal x, and was tacitly assumed to be non-zero. Therefore, we obtain

$$\Delta(x_o, j\omega_x) = \Delta_o(j\omega_x) + x_o\Delta_x(j\omega_x) = -\delta_{cr}\Delta_x(j\omega_x) \tag{3.18}$$

Substituting Eq. (3.18) into Eq. (3.13) yields

$$S_x^{T(s)}\Big|_{\substack{s = j\omega_x \\ x = x_o}} = \frac{-x_o\Delta_x(j\omega_x)}{\Delta(x_o, j\omega_x)} = \frac{x_o}{\delta_{cr}} \tag{3.19}$$

Consequently, the fractional change in x required to cause instability is

$$\frac{\delta_{cr}}{x_o} = \frac{1}{S_{x_o}^{T}(j\omega_x)} \tag{3.20}$$

and the normalized critical value of the parameter is

$$\frac{x_{cr}}{x_o} = 1 + \frac{1}{S_{x_o}^{T}(j\omega_x)} \tag{3.21}$$

If x is real, Eq. (3.21) reveals that the condition $S_{x_o}^{T}$ be real at some point on the jω axis affords the only possibility for only possibility for oscillations. ω_x, of course, is then the frequency of oscillation. It is noted that nowhere in the derivation was any mention made of the magnitude of the change in the parameter. The theorem is valid for all variations in the parameter, however large.

(b) If F_x is infinite or, equivalently, $\Sigma_o = 0$, the system transmittance is

$$T = \frac{x\Sigma_x}{\Delta_x^{o} + x\Delta_x} \tag{3.22}$$

and

$$S_x^{T} = \frac{\Delta_x^{o}}{\Delta} = \frac{1}{F_x} \tag{3.23}$$

Again, if T is stable at $x = x_o$, the necessary and sufficient condition for instability is that $S_{x_o}^{T}(j\omega_x)$ be real.

Proof: The poles of T are the poles of $\Sigma_x(s)$ and the zeros of $\Delta(s)$; but only Δ depends on x. Consequently, as in part (a), instability arises if $\Delta(j\omega) = 0$ can be satisfied for real values of $\omega = \omega_x$ and $x = x_{cr}$. Therefore the condition

$$\Delta(x_{cr}, j\omega_x) = 0 \tag{3.24}$$

implies that

$$\Delta(x_o, j\omega_x) = -\delta_{cr}\Delta_x(j\omega_x) \tag{3.25}$$

or

$$\Delta_x^{o}(j\omega_x) = -x_{cr}\Delta_x(j\omega_x) \tag{3.26}$$

Substitution of Eqs. (3.25) and (3.26) into (3.23) yields

$$S_x^T(s)\Big|_{\substack{s = j\omega_x \\ x = x_o}} = \frac{-x_{cr}\Delta_x(j\omega_x)}{-\delta_{cr}\Delta_x(j\omega_x)} = \frac{x_{cr}}{\delta_{cr}} = \frac{x_o + \delta_{cr}}{\delta_{cr}} \tag{3.27}$$

A slight manipulation of this last equation gives the critical parameter change as

$$\frac{\delta_{cr}}{x_o} = \frac{1}{S_{x_o}^T(j\omega_x) - 1} \tag{3.28}$$

or

$$\frac{x_{cr}}{x_o} = 1 + \frac{1}{S_{x_o}^T(j\omega_x) - 1} \tag{3.29}$$

(c) In the general case, neither Σ_x^o nor Σ_x are identically zero, but T can be expressed as

$$T = \frac{\Sigma_x^o + x\Sigma_x}{\Delta} = \frac{\Sigma_x^o}{\Delta} + \frac{x\Sigma_x}{\Delta} = T_\alpha + T_\beta \tag{3.30}$$

where

$$\left.\begin{aligned} T_\alpha &= \Sigma_x^o/\Delta \\ T_\beta &= x\Sigma_x/\Delta \end{aligned}\right\} \tag{3.31}$$

For this situation the poles of Σ and the zeros of Δ must be examined. But if Σ is written as

$$\Sigma = \Sigma_x^o + x\Sigma_x = \frac{n_1}{d_1} + x\frac{n_2}{d_2} = \frac{n_1 d_1 + x n_2 d_2}{d_1 d_2} \tag{3.32}$$

it is clear that the poles of Σ are invariant with respect to x. Hence only the zeros of Δ need be studied, as was the case in parts (a) and (b) of the theorem. Furthermore, since T_α and T_β have the same denominator, both become unstable at the same value of $x = x_{cr}$. Thus S may be referred to either T_α or T_β. Use of $S_x^{T_\alpha}$ yields the criterion

of part (a) and Eqs. (3.20) and (3.21), while $S_x^{T_\beta}$ follows the development of part (b) and Eqs. (3.28) and (3.29).

In fact, we are not limited to T_α and T_β. We are free to choose any convenient, non-trivial set of source and sink nodes as system input and output respectively; the Mason formula assures us that all transmittances have the same Δ.

As an extension of the conventional servo gain-margin concept, the parameter gain margin is defined as

$$(G.M)_x = 20 \log_{10} \frac{x_{cr}}{x_o} \tag{3.33}$$

As defined, the parameter gain margin measures the required decibel change in the parameter which places the system on the verge of instability. A positive gain margin implies that the critical parameter value is greater than the nominal one, while a negative margin means that x_{cr} is less than x_o.

As an illustration of the application of the sensitivity theorem in the analysis of a multiloop configuration the system shown in Fig. 3.2 is considered. It is assumed that the system has been designed by conventional frequency-domain methods; the parameter gain margins with respect to τ_1, τ_2 and k are to be obtained in order to assess the effects of variations of these elements on system stability. The closed-loop gain and phase characteristics for T(s) are shown in Fig. 3.3.

$$G(s) = \frac{100}{s(\tau_1 s + 1)(\tau_2 s + 1)}$$

$$H(s) = \frac{k s^2}{(0.8 s + 1)}$$

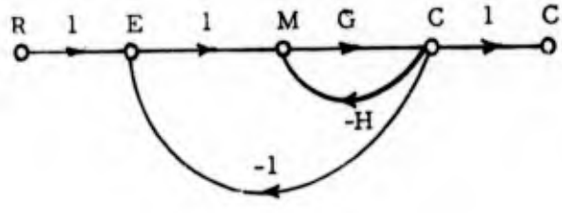

Nominal operating values: $\tau_1 = 1/4$, $\tau_2 = 1/16$, $k = 1/6$

Fig. 3.2. Two-loop control system with three variable parameters.

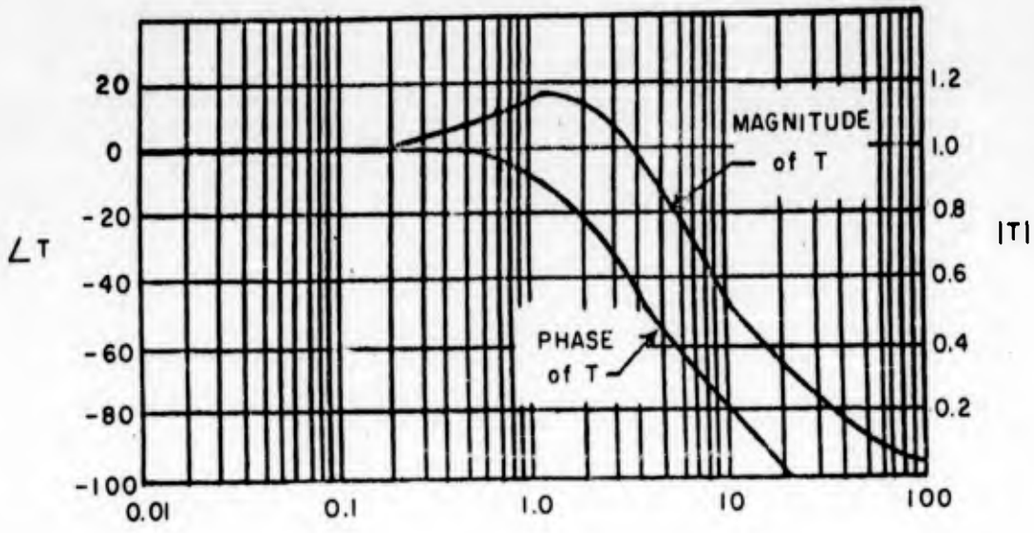

Fig. 3.3. Magnitude and phase plots for $T(j\omega)$

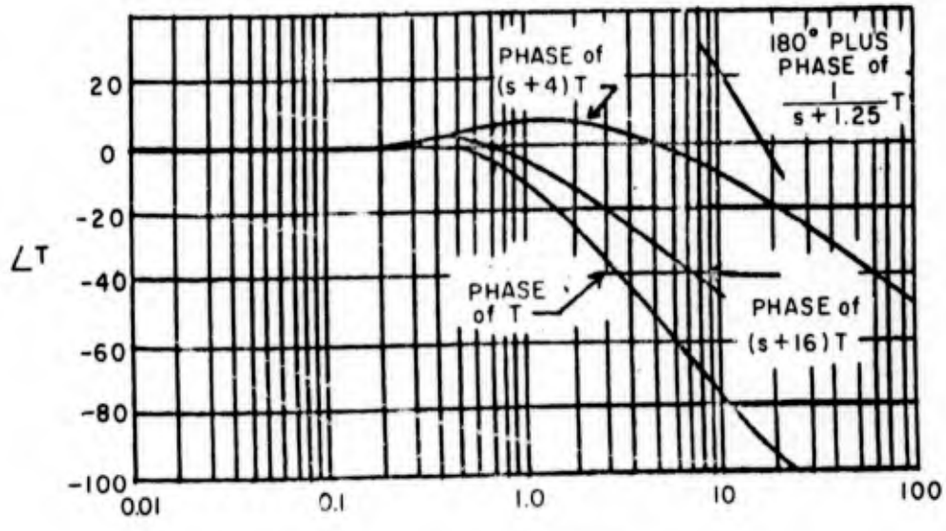

Fig. 3.7. Phase characteristics for evaluation of gain margins.

The study is initiated by determining the three sensitivity functions. But before this is attempted a few useful relations are first derived.

If a branch transmittance, B, contains the parameter x

$$S_x^T = \frac{x}{T}\frac{\partial T}{\partial x} = \left(\frac{B}{T}\frac{\partial T}{\partial B}\right)\left(\frac{x}{B}\frac{\partial B}{\partial x}\right) = S_B^T S_x^B \tag{3.34}$$

And if x is found in m branches, $B_1, B_2, \ldots, B_n$, partial differentiation gives

$$S_x^T = \sum_{i=1}^{m} S_{B_i}^T S_x^{B_i} \tag{3.35}$$

Furthermore, invoking the definition of sensitivity reveals

$$S_x^{\frac{n(s)}{d(s)}} = S_x^{n(s)} - S_x^{d(s)} \tag{3.36}$$

and

$$S_x^T = -S_{1/x}^T \tag{3.37}$$

For the system of Fig. 3.2, we have

$$S_{\tau_1}^T = S_{\tau_1}^G S_G^T \tag{3.38}$$

where

$$\left.\begin{aligned} S_{\tau_1}^G &= -S_{\tau_1}^{s(\tau_1 s+1)(\tau_2 s+1)} = -S_{\tau_1}^{(\tau_1 s+1)} = -\left(\frac{\tau_1 s}{\tau_1 s+1}\right) \\ S_G^T &= \frac{\Delta_G^o}{\Delta} - \frac{\Sigma_G^o}{\Sigma} = \frac{1}{1+G+GH} \end{aligned}\right\} \tag{3.39}$$

$$S_{\tau_1}^T = \frac{-\tau_1 s}{(\tau_1 s+1)}\,\frac{1}{(1+G+GH)} = \left(\frac{-\tau_1 s}{\tau_1 s+1}\,\frac{1}{G}\right)\left(\frac{G}{1+G+GH}\right) = \frac{-\tau_1 s^2(\tau_s s+1)}{100}\,T \tag{3.40}$$

Substituting the nominal parameter values in Eq. (3.40) gives

$$S_{\tau_1}^T = -\frac{s^2(s+16)}{6400}\,T \tag{3.41}$$

Before the sensitivity theorem can be applied, the pertinent category of null return difference ($F_x' = 1$ or ∞) is ascertained. This determination can be easily effected by inspection of the flow graph if the parameter can be made to appear as a

simple and single branch transmittance. The modification of the flow graph for τ_1 is illustrated in steps (a), (b), and (c) of Fig. 3.4, and the overall graph is shown in Fig. 3.5.

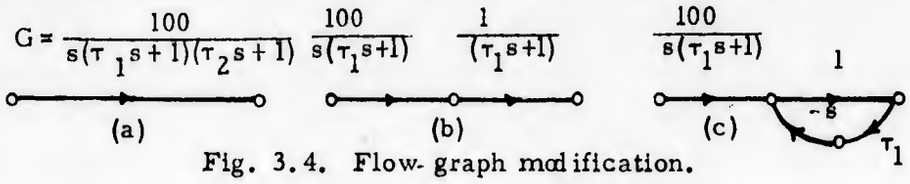

Fig. 3.4. Flow-graph modification.

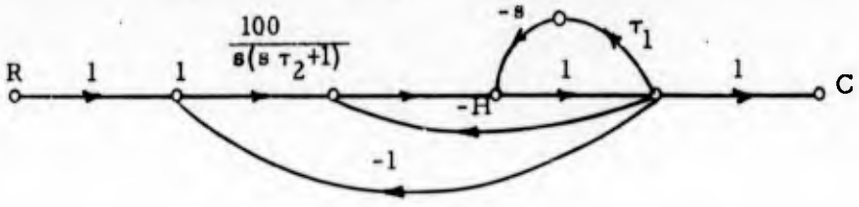

Fig. 3.5. Overall flow graph with τ_1 represented as a branch transmittance.

The flow graph in Fig. 3.4 is not the only possible representation of the factor $1/(\tau_1 s + 1)$. Instead, the analyst may choose to portray $1/\tau_1$ as a branch transmittance. Figure 3.6 illustrates this second alternative along with the graph representations for two other factors which are commonly encountered.

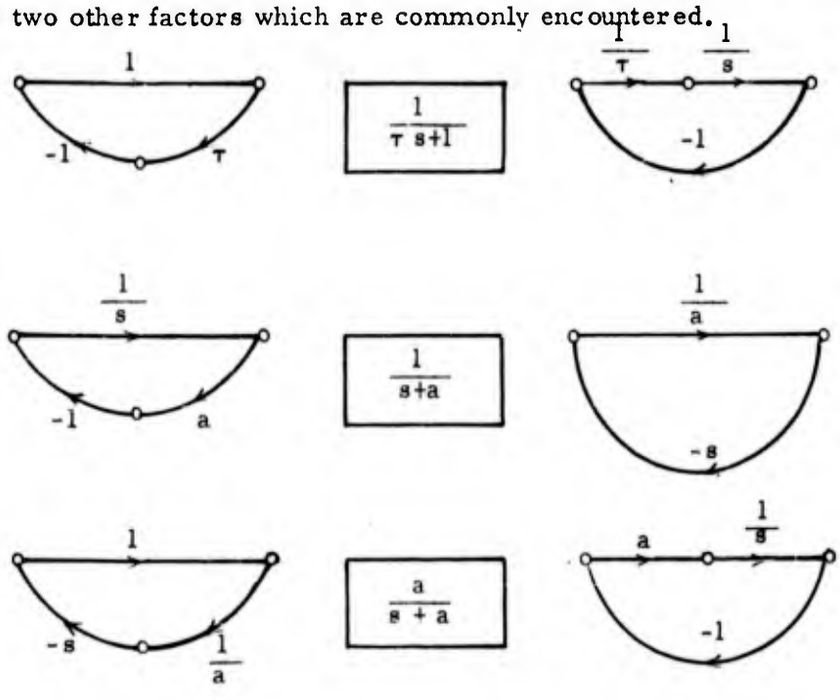

Fig. 3.6. Equivalent flow-graph representations.

In general, if F_x', the null return difference with respect to x, is infinite, then $F_{1/x}'$ is unity, and conversely. This assertion may be verified by noting that when F_x' is infinite, T is given by

$$T = \frac{x\Sigma_x}{\Delta_x^o + x\Delta_x}$$

If the substitution $x = 1/y$ is used, T becomes

$$T = \frac{\frac{1}{y}\Sigma_x}{\Delta_x^o + \frac{1}{y}\Delta_x} = \frac{\Sigma_x}{\Delta_x + y\Delta_x^o} = \frac{\Sigma_y^o}{\Delta_y^o + y\Delta_y} \qquad (3.42)$$

The form of Eq. (3.42) implies that

$$F_y' = F_{1/x}' = 1 \qquad (3.43)$$

If Eq. (3.37) is substituted into the expression for the gain margin on y, there results

$$\frac{y_{cr}}{y_o} = \frac{1}{x_{cr}/x_o} = 1 + \frac{1}{S_y^T} = 1 - \frac{1}{S_x^T} = \frac{1}{1 + \frac{1}{S_x^T \cdot 1}} \qquad (3.44)$$

Thus, the analyst manipulates the flow graph to express either x or 1/x as a branch gain and determines the applicable case of null return difference. The actual calculation of the sensitivity function is more easily effected by use of Eq. (3.34), as was done in obtaining $S_{\tau_1}^T$.

In Fig. 3.5, it is observed that $\Sigma = \Sigma_{\tau_1}^o$, and $\Sigma_{\tau_1} = 0$, so that $F_{\tau_1}' = 1$ and Eqs. (3.20) and (3.21) are applicable. According to the theorem the analyst seeks real values of $S_{\tau_1}^T = -s^2(s+16)/6400$ T, or more simply, real values of $(s + 16)T$. All that need be done is to add the phase angle of $(j\omega + 16)$ to that of $T(j\omega)$ in the frequency band where the sum is close to 0° or 180°. This sketch is shown in Fig. 3.7 where the 0° point is located at $\omega = 0.7$ rps. From Fig. 3.3, $|T(j0.7)|$ is found to be 1.07; hence the sensitivity is computed to be

$$S_{\tau_1}^T = \frac{\omega_1^2 |j\omega_1 + 16|}{6400} |T(\omega_1)| \cong \frac{0.5}{(6400)} (16)(1.07) = \frac{1}{748} \qquad (3.45)$$

$$\left.\begin{aligned} &\frac{\delta_{\tau_1}}{(\tau_1)_o} = 748 \\ \therefore\quad &\frac{(\tau_1)_{cr}}{(\tau_1)_o} = 749 \end{aligned}\right\} \qquad (3.46)$$

The gain margin for τ_1 is 20 log 749 = 57.5 db and the critical value is $(\tau_1)_{cr} = 749(\tau_1)_o = 749/4 = 187$.

In a similar fashion, the sensitivity functions for the other two parameters are

$$S_k^T = S_k^H S_H^T = S_H^T = \frac{\Delta_H^o}{\Delta} - 1 = \frac{-GH}{1 + G + GH} = -HT = \frac{-1}{4.8} \frac{s^2}{(s + 1.25)} T \quad (3.47)$$

$$S_{\tau_2}^T = S_{\tau_2}^G S_G^T = \frac{-\tau_1 s^2(\tau_2 s + 1)}{100} T = \frac{-s^2(s + 4)}{6400} T \quad (3.48)$$

The phase angles are sketched in Fig. (3.7); S_k^T is 180° at $\omega_k \cong 18$ while $S_{\tau_2}^T$ is 0° at $\omega_2 \cong 4.3$. The corresponding values of T are $|T(j18)| = 0.33$, and $|T(j4.3)| = 0.93$. The sensitivities are computed to be $S_k^T(j\omega_k) = 1/0.8$ and $S_{\tau_2}^T(j\omega_2) = 1/63$. Since the null return differences F_k' and F_{τ_2}' are each unity, then application of Eqs. (3.20) and (3.21) gives

$$\left.\begin{aligned} \frac{\delta_{\tau_2}}{(\tau_2)_o} &= 63 \\ \frac{(\tau_2)_{cr}}{(\tau_2)_o} &= 64 \quad \text{or 36 db gain margin} \\ (\tau_2)_{cr} &= 4 \end{aligned}\right\} \quad (3.49)$$

and

$$\left.\begin{aligned} \frac{\delta_k}{k_o} &= \frac{1}{-1/0.8} = -0.8 \\ \frac{(k)_{cr}}{(k)_o} &= 0.2 \quad \text{or -14 db gain margin} \\ (k)_{cr} &= 1/30 \end{aligned}\right\} \quad (3.50)$$

The example presented above indicates the relative simplicity of the sensitivity theorem. After a preliminary design configuration is proposed, the closed-loop gain and phase are normally plotted as a matter of course. The method then permits a rapid evaluation of all significant parameter margins. Attention can then be focussed on a sensitive or critical parameter with a small gain margin with a view toward possible system modification to increase the gain margin with respect to that parameter. The effect of such compensation on the stability margins for the other parameters can be immediately determined.

The stability margins so obtained afford a basis for comparison of proposed systems which exhibit satisfactory performance at nominal parameter values. The gain margins naturally lead to specification of component tolerances and thereby provide a basis for cost reduction.

An s-plane interpretation of these margins can be deduced through the medium of the familiar root-locus method. The graph determinant is written as

$$\Delta(x, s) = \Delta_x^{o}(s) + x\Delta_x(s) \tag{3.51}$$

and we seek the locus of the zeros of $\Delta(x, s)$ as x varies from its nominal value x_o. If

$$x = x_o + \delta \tag{3.52}$$

where δ is the variation in x, $\Delta(x, s)$ can be expressed as

$$\begin{aligned}\Delta(x, s) &= \left[\Delta_x^{o}(s) + x_o\Delta_x(s)\right] + \delta\Delta_x(s) \\ &= \Delta(x_o, s) + \delta\Delta_x(s)\end{aligned} \tag{3.53}$$

The first term on the right-hand side of Eq. (3.53) clearly represents the nominal positions of the determinant's zeros (or the nominal closed-loop poles), and the second term, the effect of the change in parameter value. Division of the last equation by $\Delta(x_o, s)$ and equating the result to zero gives the conventional root-locus form of

$$1 + \delta\,\frac{\Delta_x(s)}{\Delta(x_o, s)} = 0 \tag{3.54}$$

The stability problem is solved by finding the value of $\delta = \delta_{cr}$ which makes the "closed-loop" zeros, (the poles of T) of Eq. (3.53) cross the $j\omega$ axis at the point $\omega = \omega_x$, the frequency of oscillation. The diagram of Fig. 3.8 aids in clarifying these ideas. The system is assumed to possess a dominant pair of complex poles and two varying parameters x_1 and x_2. As one parameter is varied at a time with the other held at its nominal value, a root-locus is traced out in the s-plane. The intersection of the locus with the $j\omega$ axis yields the critical value of δ, and the oscillation frequency. Two such loci are shown in Fig. 3.8, each emanating from the nominal closed-loop positions. A basic limitation in the scope of the sensitivity theorem is immediately observed. Only one parameter is allowed to vary at a time--all others are fixed at the nominal settings. The inescapable inference is that the theorem, per se, yields no stability criterion if two or more parameters are varied simultaneously.

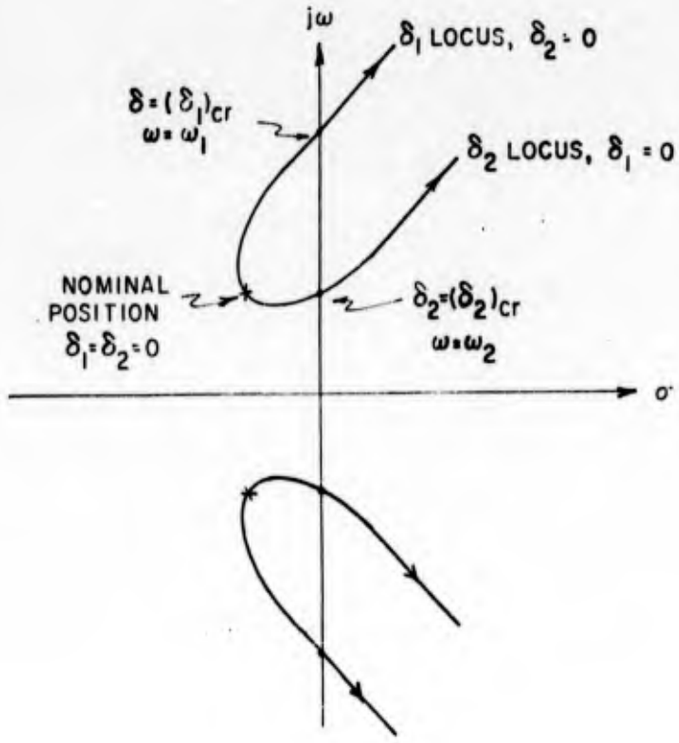

Fig. 3.8. Root loci for system with two varying parameters.

The scope of the theorem is more clearly delineated with the aid of Fig. 3.9, which portrays the parameter space for a system with two variable parameters x and y. In effect, the sensitivity test scans two orthogonal lines in the x-y plane. The lines intersect at (x_o, y_o), the nominal operating values. An unstable region within the x-y plane which does not intersect either of the scanning lines will be undetected. For example, in Fig. 3.9, region I is undetected while region II is detected at points P_1 and P_2. In particular, if the theorem were applied to a system characterized by

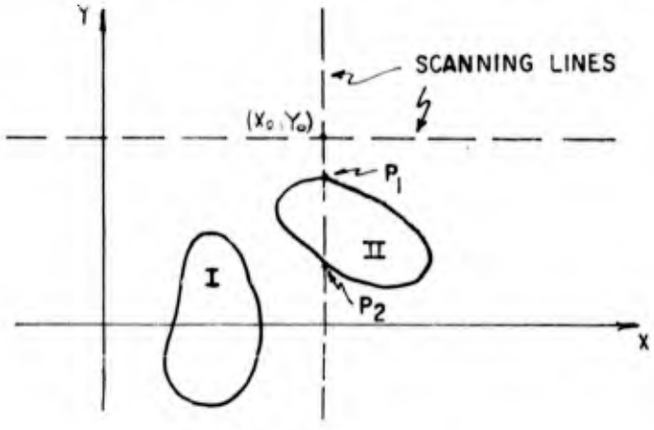

Fig. 3.9. Parameter plane with unstable regions.

the closed unstable areas shown in Fig. 3.9, we conclude that

(1) $S_x^T\Big|_{\substack{x=x_o \\ y=y_o}}$ is never real on the jω axis; consequently the root locus for **x** never crosses the jω axis, and the gain margin with respect to x is infinite.

(2) $S_y^T\Big|_{\substack{x=x_o \\ y=y_o}}$ is real at frequencies corresponding to P_1 and P_2, indicating two crossings of the jω axis and a conditionally stable system.

On the basis of this information, the root loci might be imagined as taking the form shown in Fig. 3.10.

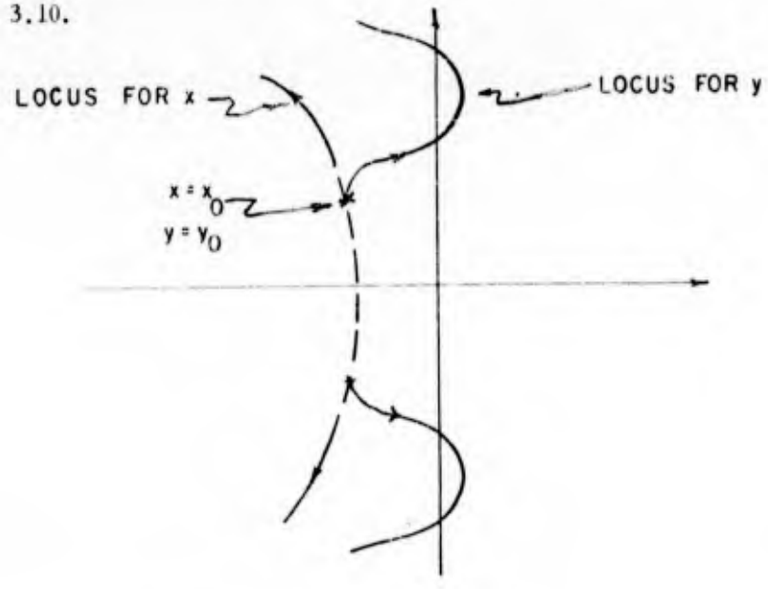

Fig. 3.10. Possible root loci for two-parameter system of Fig. 3.9.

More generally, let $\underline{x}$ be a parameter vector in k-dimensional space with components $x_1, x_2, \ldots, x_k$ and let $\underline{x}_o$ be the vector when all x_j's assume the nominal values $(x_j)_o$. The sensitivity theorem scans the parameter space along k orthogonal lines passing thru $\underline{x}_o$ in quest of unstable points. The same observations regarding the detection of unstable regions apply in this general situation.

The scope of the theorem can be extended somewhat if a set of m nominal parameter vectors are used to scan across km lines in parameter space. But the computational work involved is prohibitive. The ease of calculating the gain margins depends on the availability of gain and phase plots of T(jω) or some other closed-loop transmission function. Each $\underline{x}_0$ would define a new T(jω). Hence, if a set of m $\underline{x}_o$'s were used, one gain-phase plot (or its equivalent) would be required for each of the m T(jω)'s-- an exceedingly difficult task to be performed by hand. Even so, unstable regions can still remain undetected unless fortuitously, they all intersect some of the km scanning lines.

Despite the limitations set forth above, the theorem (along with parameter pole sensitivities to be discussed in Chap. V) affords considerable insight into system behavior. The magnitude and sign of the gain margins, and the respective oscillation frequencies permit one to visualize in qualitative terms the relative effects of two or more simultaneously varying parameters on the stability of the system, on the frequency and time responses, on the relative damping and on the root locus.

3.3. Parameter Phase Margin via the Sensitivity Function

Just as the gain-margin concept was generalized and related to the sensitivity function, so it is also possible to extend the conventional concept of phase margin. In this context, the phase margin with respect to a parameter x is interpreted as the phase angle which the parameter must assume to place the control system on the verge of instability. The magnitude of x is fixed at its nominal value x_o, while the nominal phase angle is taken as zero. More explicitly, the parameter phase margin is defined as that value of ϕ_m which satisfies the equation

$$\Delta(s,x)\Big|_{\substack{s = j\omega \\ x = x_o e^{j\phi_m}}} = 0 \tag{3.55}$$

provided that the system is stable at the nominal value $x = x_o$ -- that is, the zeros of $\Delta(s,x_o)$ are minimum phase.

In any physical system, the parameter x is always real, and the phase margin expressed by Eq. (3.55) appears to be a mathematical fiction. But, as discussed in Sec. 3.4, this somewhat "artificial" margin is indicative of the relative stability of the system, and is shown to be intimately associated with the root and phase-angle loci for the varying parameter. The conventional gain and phase margins for the single-loop, unity-feedback system are shown to be special cases of the parameter gain and phase margins for an arbitrary multiloop configuration. In Chap. VI, the parameter-margin characterization of multiloop systems suggests the basis for the compensation schemes discussed there.

In this section, various expressions relating the phase margin to the real-frequency behavior of the sensitivity function and to the topology of the flow graph are derived. As before, the two special cases of unity and infinite null return difference are studied, and the general situation is reduced to one of the two special propositions.

(a) If Γ_x' is unity, the necessary and sufficient condition that T become unstable due to a change in the phase of x is that there exist a real frequency ω_p such that

$$\text{Re } S_x^T(j\omega_p)\Big|_{x=x_o} = -\frac{1}{2} \tag{3.56}$$

Proof: Only the zeros of Δ determine the stability. Let ϕ_m be the phase angle which x must take on to place the zeros of Δ on the $j\omega$ axis. Consequently at crossover,

$$\Delta(x_o e^{j\phi_m}, j\omega_p) = \Delta_x{}^o(j\omega_p) + x_o e^{j\phi_m}\Delta_x(j\omega_p) = 0 \tag{3.57}$$

or

$$\Delta_x{}^o(j\omega_p) = -x_o e^{j\phi_m}\Delta_x(j\omega_p) \tag{3.58}$$

Substituting Eq. (3.58) into the expression for S_x^T and evaluating the latter at $x = x_o$ yields

$$S_x^T\Big|_{\substack{x=x_o \\ s=j\omega_p}} = \frac{\Delta_x^o}{\Delta} - 1 = \frac{-x_o\Delta_x(j\omega_p)}{\Delta_x{}^o(j\omega_p) + x_o\Delta_x(j\omega_p)} = \frac{-x_o\Delta_x(j\omega_p)}{-x_o e^{j\phi_m}\Delta_x(j\omega_p) + x_o\Delta_x(j\omega_p)}$$

$$= \frac{1}{e^{j\phi_m} - 1} = -\frac{1}{2} - \frac{j}{2}\cot\frac{\phi_m}{2} \tag{3.59}$$

The real part of Eq. (3.59) is seen to be - 1/2 as stated in the theorem, and ϕ_m is identified as the parameter phase margin with respect to x. From Eq. (3.59), the phase margin is

$$\frac{-\phi_m}{2} = \cot^{-1} 2\,\mathrm{Im}\, S_{x_o}^T(\omega_p) \tag{3.60}$$

Equations (3.56) and (3.60) define the frequency crossover and the required phase change in the parameter; on the other hand, Eqs. (3.14) and (3.20) yield the crossover frequency and the required amplitude change in the parameter. In this sense, the two sets of equations may be considered as complementary.

(b) If F_x' is infinite, the stability criterion is that the real part of $S_{x_o}^T(j\omega_p)$ be $+\frac{1}{2}$.

Proof: At crossover, Eq. (3.58) is satisfied; substitution into the expression for S_x^T gives

$$S_x^T\Big|_{\substack{x=x_o \\ s=j\omega_p}} = \frac{\Delta_x^o(\omega_p)}{\Delta(x_o, \omega_p)} = \frac{1}{1 - e^{-j\phi_m}} = \frac{1}{2} - j\left(\frac{1}{2}\right)\cot\frac{\phi_m}{2} \tag{3.61}$$

Therefore

$$\mathrm{Re}\, S_{x_o}^T(j\omega_p) = \frac{1}{2} \tag{3.62}$$

and

$$\frac{-\phi_m}{2} = \cot^{-1} 2 \operatorname{Im} S_{x_o}^{T}(j\omega_p) \tag{3.63}$$

(c) In the general case, $F_x' \neq 1$ and $F_x' \neq \infty$. T is split into two parts, T_α and T_β as was done in Sec. 3.2, Eq. (3.30), and either T_α or T_β can be used in the S formulation. It is noted that since

$$\left.\begin{aligned} S_x^{T_\alpha} &= \frac{\Delta_x^o}{\Delta} - 1 \\ S_x^{T_\beta} &= \frac{\Delta_x^o}{\Delta} \end{aligned}\right\} \tag{3.64}$$

then

$$S_x^{T_\alpha}(s) = S_x^{T_\beta} - 1 \tag{3.65}$$

Equations (3.64) and (3.65) indicate the reason for the change in sign of the real part of S at crossover for the two special cases of (a) and (b).

An alternate form and interpretation of the sensitivity function is obtained if T(s) is expressed as

$$T(s) = |T(s)|\, e^{j\theta(s)} \tag{3.66}$$

so that

$$\ell n\, T(s) = \ell n|T(s)| + j\theta(s) \tag{3.67}$$

and

$$S_x^T = \frac{\partial \ell n T}{\partial \ell n x} = \frac{\partial \ell n|T|}{\partial \ell n x} + j\frac{\partial \theta}{\partial \ell n x} \tag{3.68}$$

If x is real, as it is at nominal values, then Eq. (3.68) can be expressed as

$$S_x^T = \operatorname{Re} S_x^T + j \operatorname{Im} S_x^T \tag{3.69}$$

where

$$\left.\begin{aligned} \operatorname{Re} S &= \frac{\partial \ell n|T|}{\partial \ell n x} = S_x^{|T|} \\ \operatorname{Im} S &= \frac{\partial \theta}{\partial \ell n x} = \theta S_x^{\theta} \end{aligned}\right\} \tag{3.70}^{+}$$

+Equation (3.70) was first derived by E. J. Angelo, "Design of Feedback Systems", Polytechnic Institute of Bklyn, Microwave Research Institute, Research Rpt. R449-55, PIB 379, 1956.

Therefore at crossover,

$$\text{Re } S_x^T = S_x^{|T|} = \frac{1}{2} S_x^{|T|^2} = \begin{cases} -1/2, \text{ if } \Sigma_x = 0 \\ +1/2, \text{ if } \Sigma = 0 \end{cases} \tag{3.71}$$

and

$$\frac{-\phi_m}{2} = \cot^{-1} 2 \, \text{Im} \frac{\Delta_x^o}{\Delta} (\omega_p) \tag{3.72}$$

Equation (3.70) reveals that the real part of the sensitivity is the sensitivity of $|T|$ to changes in x while the imaginary part of S_x^T is related to the sensitivity of the phase shift.

Still another, and more interesting formulation, of the conditions set down in Eq. (3.71) is possible. If $F_x' = 1$, then at crossover, $\omega = \omega_p$,

$$\text{Re } S_{x_o}^T = \text{Re}\left(\frac{\Delta_x^o}{\Delta} - 1\right) = \text{Re}\left(\frac{-x_o \Delta_x}{\Delta}\right) = -\frac{1}{2} \tag{3.73}$$

or

$$-1 + \text{Re} \frac{\Delta_x^o}{\Delta} = -x_o \frac{\text{Re}\, \Delta_x}{\Delta} = -\frac{1}{2} \tag{3.74}$$

From Eq. (3.74), it is evident that ω_p occurs for

$$x_o \text{Re} \frac{\Delta_x(\omega_p)}{\Delta(x_o, \omega_p)} = \text{Re} \frac{\Delta_x^o(\omega_p)}{\Delta(x_o, \omega_p)} = \frac{1}{2} \tag{3.75}$$

If $F_x' = \infty$, then crossover occurs when

$$\text{Re } S_{x_o}^T = \text{Re}\left(\Delta_x^o/\Delta\right) = \text{Re}(1 - x_o \Delta_x/\Delta) = 1 - x_o \, \text{Re}(\Delta_x/\Delta) = 1/2 \tag{3.76}$$

or

$$x_o \, \text{Re} \frac{\Delta_x(\omega_p)}{\Delta(x_o, \omega_p)} = \text{Re} \frac{\Delta_x^o(\omega_p)}{\Delta(x_o, \omega_p)} = \frac{1}{2} \tag{3.77}$$

But Eqs. (3.75) and (3.77) are identical in form and may be construed as an alternate phrasing for Eq. (3.71). It is shown in Appendix A that Eq. (3.77) is tantamount to requiring that

$$x_o^2 \frac{|\Delta_x|^2}{|\Delta_x^o|^2} = 1 \tag{3.78}$$

or

$$\left| \frac{x_o \Delta_x}{\Delta_x^o} \right| = 1 \tag{3.79}$$

Equation (3.79) is recognized as the logical generalization of the phase-margin condition $\left|k \frac{n(j\omega)}{d(j\omega)}\right| = 1$ for the single-loop unity feedback system. From a root-locus standpoint, the result is not at all surprising, since the locus equations have the forms $1 + k \frac{n(s)}{d(s)} = 0$ for the single-loop case, and $1 + x\Delta_x(s)/\Delta_x^o(s) = 0$ for the arbitrary system.

Since Eq. (3.79) corresponds to the "zero db" crossing, then the parameter phase margin[†] may be taken as

$$\phi_m = 180^o - \Delta_x/\Delta_x^o(\omega_p) \tag{3.80}$$

Thus Eqs. (3.79) and (3.80) serve as a compact generalization of the phase margin concept, while Eqs. (3.71) and (3.72) explicitly relate these to the sensitivity function.

A major drawback from the computational point of view is that the form of the equation (Re $S = \pm 1/2$) does not permit a simple, rapid evaluation of the phase margins in terms of available gain-phase plots for $T(j\omega)$. The procedure involves two operations. From the Bode plot for $T(j\omega)$, $S(j\omega)$ is obtained both magnitude and phase. The $S(j\omega)$ plots are then translated into real and imaginary parts which are sketched vs. ω. These then furnish all the data for the implementation of Eqs. (3.71) and (3.72).

3.4. Phase-Angle Loci Interpretation of Gain and Phase Margins

The concept of the phase-angle loci[††] permits an s-plane interpretation of the parameter gain and phase margins. After a brief exposition of this technique, a simple example is discussed which illustrates the correlation between these loci and the parameter margins.

The conventional root loci are the loci of the zeros of

$$\Delta(s) = \Delta_x^o(s) + x\Delta_x(s) \tag{3.81}$$

as x varies over all real values. If x has a constant phase angle but variable amplitude, the loci of the zeros of Δ define the phase-angle loci. The loci are also defined by those values of s and x satisfying

$$1 + \frac{x\Delta_x(s)}{\Delta_x^o(s)} = 0$$

[†]The parameter phase margin as defined here reduces to the negative of the phase margin commonly referred to in the servo literature for the single-loop, unity feedback system.

[††]J. G. Truxal, op. cit., Chap. 4.

or

$$\frac{x\Delta_x(s)}{\Delta_x^{o}(s)} = -1 \tag{3.82}$$

If

$$G(s) \equiv \frac{\Delta_x}{\Delta_x^{o}}(s) = |G(s)|\, e^{j\theta(s)} \tag{3.83}$$

then

$$\ell n\, G(s) = \ell n\, |G(s)| + j\theta(s) \tag{3.84}$$

If G(s) is represented as the ratio of two factored polynomials in s,

$$G(s) = \frac{\Pi(s + b_i)}{\Pi(s + a_i)} \tag{3.85}$$

Combining Eqs. (3.85) and (3.84) gives

$$\ell n\, G(s) = \left[\Sigma \ell n \left| s + b_i \right| - \Sigma \ell n |s + a_i|\right] + j\left[\Sigma \angle(s + b_i) - \Sigma \angle(s + a_i)\right] \tag{3.86}$$

In Eq. (3.86), $\ell n|G(s)|$ has the form of a logarithmic potential caused by an array of unit line charges in the s-plane with a plus charge representing the poles and a minus charge for the zeros.

If W(s) is an analytic function of s given by

$$W(s) = V(s) + j\psi(s) \tag{3.87}$$

then V and ψ are harmonic functions satisfying Laplace's equation (or the Cauchy-Riemann conditions), and the contours of V = constant and ψ = constant are everywhere orthogonal in the s-plane.

Now since G(s) of Eq. (3.85) is an analytic function, $\ell n|G(s)|$ is analytic. If $\ell n|G(s)$ is taken to correspond to the logarithmic potential V, θ must correspond to $\psi(s)$. Consequently $\ell n|G(s)|$ and $\theta(s)$ are harmonic functions and the contours of θ = constant and $\ell n|G(s)|$ = constant (or equivalently $|G(s)|$ = constant) must be orthogonal. Furthermore, the shapes correspond to the two-dimensional constant-V lines and the stream lines of ψ = constant.

---

*Throughout this section, the potential analogy is employed. See, for example, J. G. Truxal, op. cit., Chap. 1, and
S. Darlington, "The Potential Analogue Method of Network Synthesis", Bell System Tech. J, Vol. 30, pp. 315-365, April, 1951.

To describe explicitly the phase-angle loci,

$$x = |x| e^{j\phi} \tag{3.88}$$

is substituted into Eq. (3.82) to obtain

$$xG(s) = |x| e^{j\phi} G(s) = -1 = e^{j180} \tag{3.89}$$

or

$$|x| G(s) = e^{j(180-\phi)}$$

If $\phi = 0$, or $\phi = 180$, then Eq. (3.89) reduces to the conventional root locus equation for positive and negative feedback respectively. As ϕ takes on values from 0° to 360°, Eq. (3.89) generates a family of phase-angle loci.

As an illustration of these ideas, the loci for

$$G(s) = \frac{1}{s(s+1)(s+2)} \tag{3.90}$$

are sketched in Fig. 3.12 and the corresponding values of the parameter are shown in the complex x plane in Fig. 3.11.

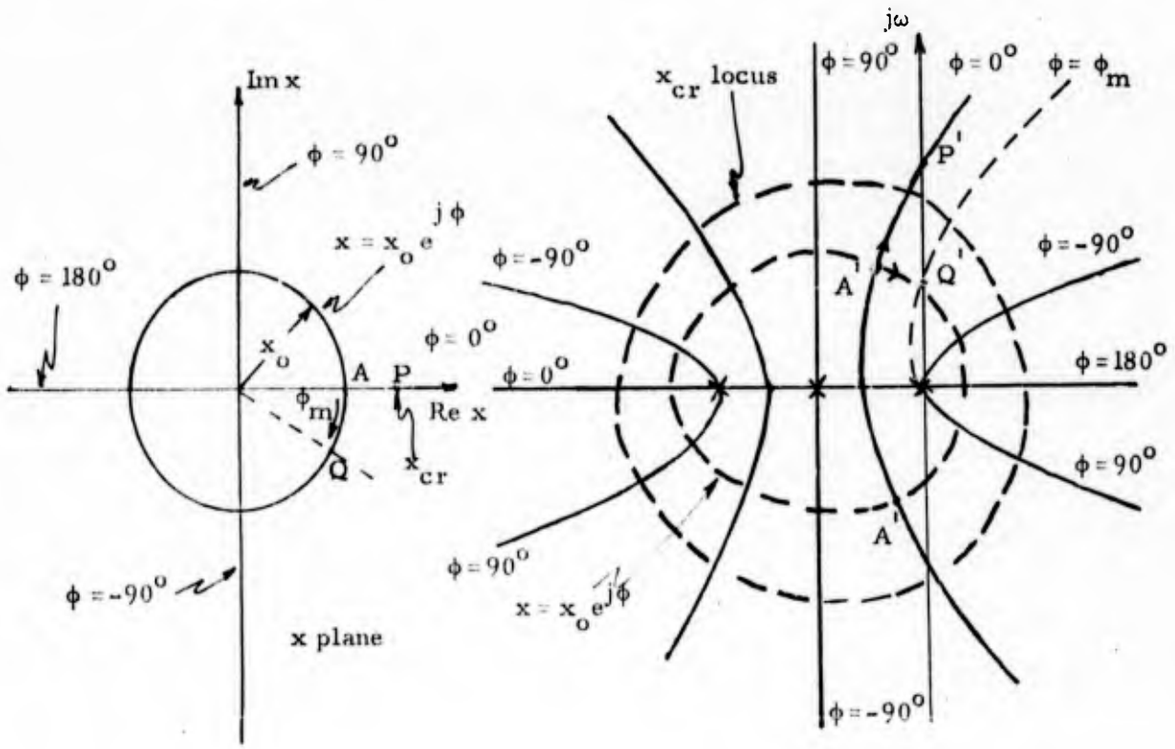

Fig. 3.11. Complex x plane.

Fig. 3.12. Phase-angle loci.

The phase-angle loci in the s-plane satisfying the condition

$$|x|\, G(s) = G(s) = 180 - \phi = \text{constant} \qquad (3.91)$$

are seen to correspond to the stream lines. Along a circle in the x-plane, $|x|$ is a constant; since the loci of $|G(s)|$ = constant corresponding to the equipotential lines are orthogonal to the stream lines, the loci of constant $|x|\ |G(s)|$ must be likewise orthogonal to the phase-angle loci.

Two elliptical loci corresponding to circles in the x-plane of radii x_o, the nominal parameter value, and x_{cr}, the critical value, are shown in Fig. 3.12. Points P' and Q' determine the parameter gain and the parameter phase margin respectively. For the nominal setting $x = x_o \angle 0^o$, the system poles are located at points A' in the s-plane. An increase in the magnitude of x to the value x_{cr} places the poles on the $j\omega$ axis at P'. Hence $(GM)_x = 20 \log x_{cr}/x$. If x has a constant modulus x_o, but changes in phase by an angle ϕ_m, the poles move along the elliptical contour from A' to point Q' on the $j\omega$ axis. At Q' the system is on the verge of instability and the parameter phase is ϕ_m. The whole procedure may be viewed as a conformal mapping from the complex x plane into the s-plane, where orthogonal contours in the parameter plane generate orthogonal contours in the frequency plane.

From the diagram of Fig. 3.12, some qualitative notions regarding the behavior of the root locus may be deduced. Thus if the gain margin is large but the phase margin small, the root locus must be moving almost parallel to the $j\omega$ axis; the frequencies of crossover ω_p and ω_x are fairly well separated; the system poles are probably lightly damped; and, as a first approximation $\omega_p \cong \beta$ as indicated in Fig. 3.13.

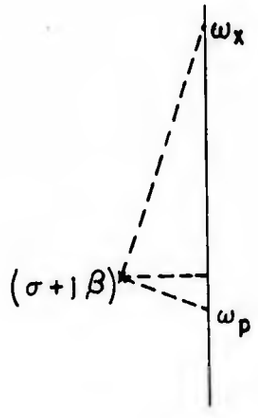

Fig. 3.13. Gain and phase margin crossover frequencies.

If both gain and phase margins are small, the system is very close to instability with $\omega_g = \omega_x = \beta$.

A small gain margin and large phase margin indicates that the locus is moving almost normal to the jω axis; $\omega_x = \beta$, but ω_p is likely quite different from β.

3.5. Extension of the Sensitivity Theorem to "Relative" Stability

In essence, the sensitivity theorem dictates a scanning of the jω axis in the s-plane in quest of points at which S_x^T is real (0° or 180° phase shift). At these frequencies the poles of T cross into the right half plane with a changing parameter. This theorem can readily be extended to lines other than the jω axis.

The two lines under consideration are depicted in Figs. 3.14 and 3.15. At the nominal value $x = x_o$, the poles of T(s) are assumed to be to the left of the indicated lines--i.e., the real part of each pole is $-a$ in Fig. 3.14 and the damping of each pole is $> \zeta_m$ in Fig. 3.15.

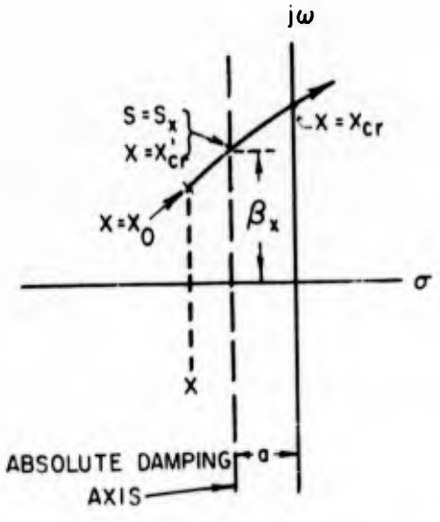

Fig. 3.14. Absolute damping as a measure of stability.

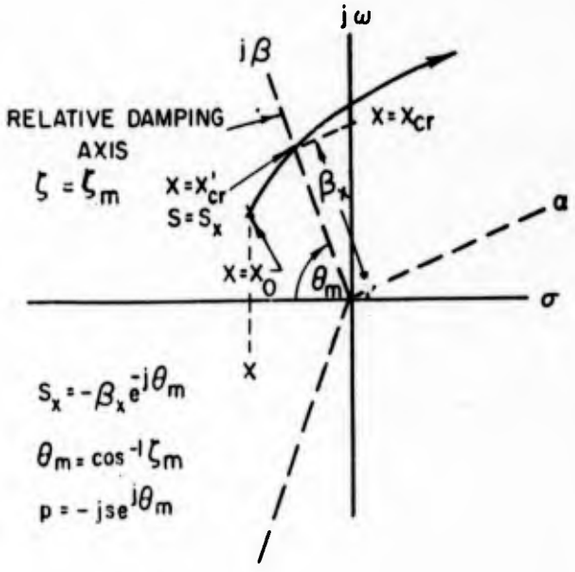

Fig. 3.15. Relative damping as a measure of stability.

The theorems derived previously in Secs. 3.2 and 3.3 are applicable in these cases. The only modification is that the line $s = -a$, or the line $\zeta = \zeta_m$, is scanned rather than the jω axis. If $S_{x_o}^T$ is real at some point, (s_x), along these axes, the value of the parameter that causes a pole to cross these axes is given by

$$\frac{x'_{cr}}{x_o} = \begin{cases} 1 + 1/S_{x_o}^{T}(s_x), & \text{if } F_x' = 1 \\ 1 + 1/\left|S_{x_o}^{T}(s_x) - 1\right|, & \text{if } F_x' = \infty \end{cases} \qquad (3.92)^*$$

where

$$s_x = \begin{cases} -a + j\beta_x, & \text{for Fig. 3.14} \\ \beta_x e^{j\theta_m}, & \text{for Fig. 3.15} \end{cases} \qquad (3.93)$$

Similarly, the parameter phase margins can be extended to indicate the nexessary change in the phase of the parameter which causes crossings of the relative or absolute damping axes. The axes are scanned to find frequencies where the real part of $S_{x_o}^{T}(s)$ is $+1/2$ or $-1/2$. The "damping" phase margins are then found by computing the imaginary part of S_x^T at these frequencies and invoking Eq. (3.63).

The results of this section demonstrate that the sensitivity theorem, suitably modified, can be used to compute the parameter margins when the prime interest lies in the absolute or relative damping of the system. But, the usefulness and simplicity of the method are greatly compromised by the attendant change of variable dictated by the translation, and by the rotation of the axes for the two cases considered. In particular, the rotation generates complex coefficients in the polynomial for S_x^T. In either case, the change in variable precludes the direct use of available frequency-response data.

This chapter establishes the relationship between the stability of a multiloop system and the sensitivity function and presents an s-plane, root-locus interpretation of the parameter gain and phase margins. Stability analysis via the sensitivity functions is particularly applicable when the only system description available is a set of experimentally-derived, sinusoidal-response characteristics. The next chapter introduces a method, based on the sensitivity functions, for the realization of a set of specified parameter gain margins.

---

*Equations (3.92) and (3.93), obtained by a translation of the axes in Fig. 3.14 and by a rotation of the axes in Fig. 3.15 are derived in Appendix B.

Chapter IV - Frequency Specifications for Prescribed Stability Margins

In the preceding chapters, the relationship between stability and sensitivity is established, and the destabilizing effects of variations in the elements of the system are evaluated quantitatively in terms of the parameter gain and phase margins. The relative ease of applying the theorem and calculating the gain margins is illustrated by the example of Sec. 3.2. In Sec. 4.1 of this chapter two additional examples are discussed. These point out the need for evaluating the gain margins, even with respect to parameters which are expected to vary only slightly.

The theorems of Chaps. II and III are next applied to a prototype single-loop system with a view toward establishing a design philosophy which would guide the engineer in the solution of the general problem which is stated as: given the configuration and a description of the fixed elements, which compensation networks should be used to realize a set of specified stability margins? The method which emerges involves an attempt to realize prescribed values of the sensitivity functions at discrete points on the $j\omega$ axis.

The compatibility of the stability margin specifications with the flow-graph configuration is studied in Sec. 4.3 and, in this regard, the multiloop system is shown to be more flexible than the single-loop configuration.

4.1 Two Examples Which Illustrate the Importance of Stability Margins

In many instances the gain margin with respect to only one parameter is a poor indication of the relative stability of the system. There may be other parameters with such small gain margins that even the slightest variation causes instability. Two systems illustrating this theme are depicted in Fig. 4.1; Fig. 4.2 shows the respective pole-zero patterns.

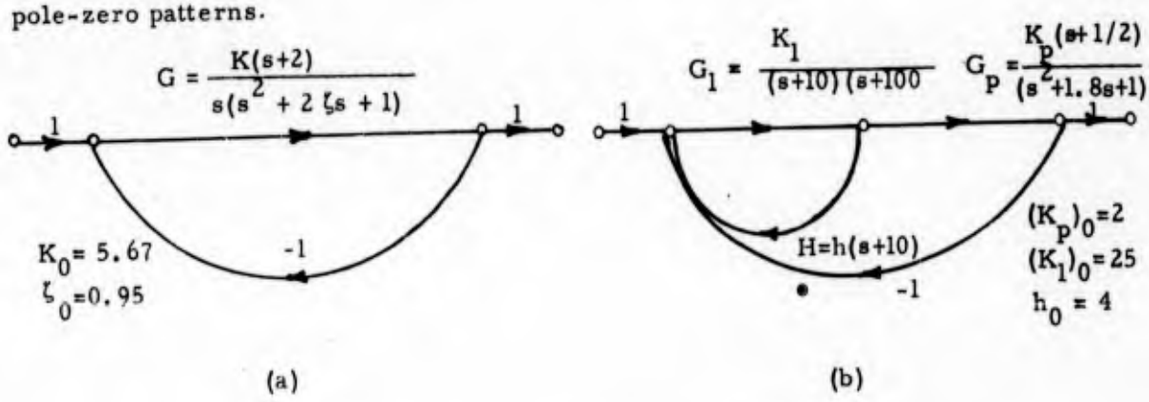

Fig. 4.1 Two feedback systems with interesting gain margins

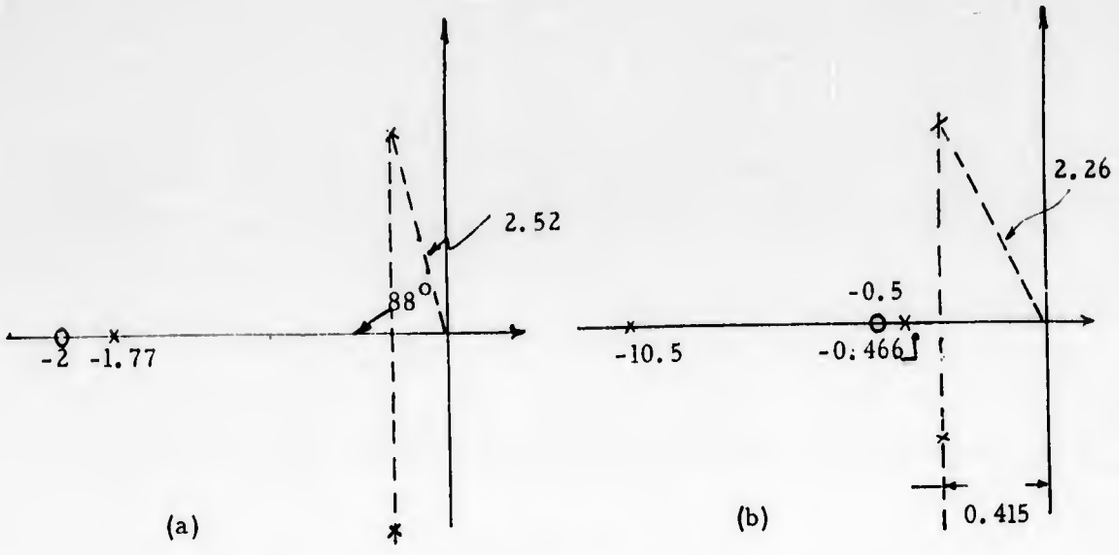

Fig. 4.2 Pole-zero patterns

The stability margins and some of the corresponding crossover frequencies are summarized in Table 4.1.

	Parameter	Gain Margin and Freq.	Phase Margin and Freq.
System (a)	K	10.5 db at $\omega = 4.5$	-3° at $\omega = 2.5$
	ζ	-1 db at $\omega = 2.5$	-10° at $\omega = 2.6$
System (b)	K_p	9.5 db at $\omega = 3.7$	-23° at $\omega = 2.1$
	h	0.08 db at $\omega = 2.0$	
	K_1	0.2 db at $\omega = 0$	

Table 4.1 Stability margins and crossover frequencies

For the system of Fig. 4.1a, the gain margin on K is a comfortable 10.5 db; yet, only a -1 db change in ζ causes instability. In this case, the small phase margin for K leads one to suspect that the poles are very lightly damped--which is indeed the case as seen from the pole-zero pattern of Fig. 4.2a.

On the other hand, the process gain, K_p, of Fig. 4.1b has a gain margin of 9.5 db, and a respectable -23° phase margin. On the basis of these data alone, the designer may be lulled into thinking that the system is reasonably stable. Even the pole-zero pattern of Fig. 4.2b seems reassuring since the relative damping of the complex poles is 0.2 -- not an exceptionally low figure. Yet the gain margins for the other parameters h and K_1 reveal that the system is dangerously close to instability.

The latter system is similar, in some respects, to the zero-sensitivity systems mentioned in Chap. II. At low frequencies the loop gain, G_1H, of the positive-feedback minor loop is close to unity and the transmittance of the first stage is very large. Hence, the loop gain around K_p is large and $S^T_{K_p}$ is small. At d-c, $S^T_{K_p}$ is zero, but S^T_h and $S^T_{K_1}$ are quite large. Large values of the sensitivity lead one to suspect that the stability margins are small, especially if the phase of the sensitivity is also near 0^o or 180^o.

These examples indicate the usefulness and importance of the stability margins as analytical tools. Use of these margins as a guide to design is the next logical step.

4.2 Specification of Sensitivity for Prescribed Gain and Phase Margins -- Single-Loop System

The problem considered in this thesis is the stabilization of feedback systems in the face of expected parameter variations. The single-loop configuration illustrated in Fig. 4.3 is deliberately chosen in order to illustrate a design procedure and to yield simple results with a minimum of effort. $G_p(s)$ represents the fixed elements, $G_c(s)$ the compensation networks, and K is the only varying parameter.

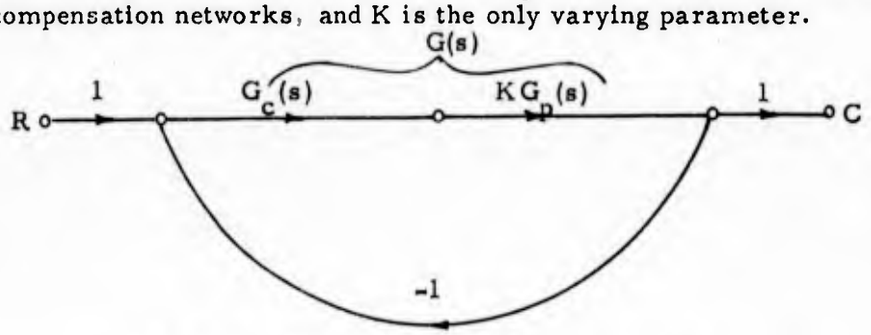

Fig. 4.3 Classical feedback control system

During normal operation, the gain K is expected to vary by as much as a factor of 2 from its nominal value K_o, i.e.,

$$\frac{1}{2} \leq \frac{K}{K_o} \leq 2 \tag{4.1}$$

If K_{cr} is the value of K which makes the system oscillate, the conditions

$$\left.\begin{aligned} \frac{K_{cr}}{K_o} &> 2 \\ \frac{K_{cr}}{K_o} &< 2 \end{aligned}\right\} \tag{4.2}$$

insure the stability of the system despite variations in the parameter within the range given in Eq. (4. 1). Through the medium of the sensitivity function, K_{cr}/K_o can be related to the component transfer function, and eventually to specifications on the compensation networks. Thus,

$$S^T_{K_o} = \frac{1}{1 + K_o G_c G_p} = \frac{1}{1 + G} \tag{4. 3}$$

$S^T_{K_o}(j\omega_x)$ is real when $G(j\omega_x)$ is real. When the latter condition obtains,

$$\frac{K_{cr}}{K_o} = 1 + \frac{1}{S^T_{K_1} - 1} = 1 + \frac{1}{\frac{1}{1+G} - 1} = -\frac{1}{G}$$

$$= \begin{cases} -\dfrac{1}{|G|}, & \text{if } \angle G = 0^\circ, 360^\circ, \text{ etc.} \\ \dfrac{1}{|G|}, & \text{if } \angle G = 180^\circ, 540^\circ, \text{ etc.} \end{cases} \tag{4. 4}$$

The first part of Eq. (4. 4) indicates a negative value for the critical gain, and is applicable for the positive feedback case. For positive values of the parameter only the second half need be considered. Combining Eqs. (4. 2) and (4. 3) gives $|G| < 1/2$ and $|G| < 2$. Consequently, the specification required to satisfy Eq. (4. 2) is

$$\left.\begin{array}{l} |G(j\omega_x)| < \frac{1}{2} \\ \text{or} \\ |G(j\omega_x)|\,\text{db} < -6\ \text{db} \\ \text{when} \\ \angle G(j\omega_x) = 180^\circ \end{array}\right\} \tag{4. 5}$$

The requirement expressed in Eq. (4. 5) is simply the conventional servo gain margin.

Similarly, the parameter phase margin for K as obtained from Eq. (3. 61) is

$$S^T_K(j\omega_p) = \frac{1}{1 - e^{-j\phi_m}} = \frac{1}{1 + G(j\omega_p)} \tag{4. 6}$$

Equation (4.6) is satisfied by

$$\left.\begin{aligned} &|G(j\omega_p)| = 1 \\ &\text{and} \\ &\phi_m = -180^\circ - \angle G(j\omega_p) \end{aligned}\right\} \tag{4.7}$$

If the parameter phase margin with respect to K is specified as

$$\phi_m < -30^\circ \tag{4.8}$$

the requirement on G becomes

$$\left.\begin{aligned} &\angle G(j\omega_p) > -150^\circ \\ &\text{when} \\ &|G(j\omega_p)| = 1 \end{aligned}\right\} \tag{4.9}$$

The requirements of Eqs. (4.5) and (4.9) are recognized as the familiar gain and phase margin specifications for servo-systems, and the design procedure evolves along conventional lines. The gain level K_o is normally selected to satisfy the steady-state accuracy requirements usually stated in terms of the positional or velocity constant. Then $G_c(s)$ is selected so that G(s) meets the desired stability margins. Considerable freedom is permitted in the choice of an appropriate compensation network, since the stability margins specify the behavior of G(s) at only two frequencies. Of course, other system specifications (such as noise bandwidth) may further restrict the allowable $G_c(s)$. In some instances, simple lead-lag compensation suffices.

The steps involved in the stabilization of this simple system are indicative of a general procedure which is followed in more complex configurations. The central idea in the proposed scheme is to force the critical values of the parameter to fall outside the range of expected variation, thereby insuring against instability. The steps in the procedure are:

(1) The sensitivity function with respect to the parameter x is formulated and expressed in terms of the plant and compensation network transfer functions.

(2) The sensitivity function is specified so that the critical parameter values fall outside the range of expected variations.

For example, if F'_x is unity,

$$\frac{x_{cr}}{x_o} = 1 + \frac{1}{S^T_{x_o}(j\omega_x)} \tag{4.10}$$

The range of expected variation is

$$a \leq \frac{x}{x_o} \leq b \tag{4.11}$$

with a, b > 0, and b > 1, a < 1.

Hence, in order to insure stability,

$$\left.\begin{aligned} &\frac{x_{cr}}{x_o} > b \\ \text{and} \quad &\\ &\frac{x_{cr}}{x_o} < a \end{aligned}\right\} \tag{4.12}$$

or

$$\left.\begin{aligned} &\left|S^T_{x_o}(j\omega_a)\right| < \frac{1}{(b-1)}, \text{ when } \angle S^T_x(j\omega_a) = 0^\circ, 360^\circ, \text{ etc.} \\ \text{and} \quad &\\ &\left|S^T_{x_o}(j\omega_b)\right| < \frac{1}{|a-1|}, \text{ when } \angle S^T_x(j\omega_b) = 180^\circ, 540^\circ, \text{ etc.} \end{aligned}\right\} \tag{4.13}$$

(3) The compensation networks are selected so that they, in conjunction with the fixed plant, satisfy the specifications on the sensitivity function at the frequencies where $S^T_{x_o}$ is real (e. g., Eq. 4. 13). By choosing the compensation the designer can control the frequencies ω_a and ω_b.

(4) Steps (1) through (3) can be repeated if another parameter, y, is involved. In general, each varying parameter, x_i, yields a sensitivity function, $S^T_{x_i}$, which is constrained by the expected range of that parameter's variation (as in Step (2)). These constraints are then introduced as specifications on the behavior of the compensating networks at a set of discrete frequencies corresponding to the 0° and 180° points for each $S^T_{x_i}$.

The steps outlined above serve more as a guide to the stabilization of the system rather than as a straightforward, step-by-step synthesis procedure. Much is left to

the imagination and inventiveness of the engineer. A detailed example of this procedure is carried out in Chap. VI in connection with a multiloop, multiparameter system. A criticism of the method is deferred until Chap. VI.

4.3 Compatibility of Stability Margin Specifications

Before the procedures discussed in the preceeding section can be applied, a determination must first be made of the compatibility of the parameter margin specifications with the given configuration. The two examples considered here serve to indicate the salient aspects of the problem, rather than attain conclusive, far-reaching results.

The first system under consideration is the single-loop structure shown in Fig. 4.4, where the parameters of interest are x_1 and x_2.

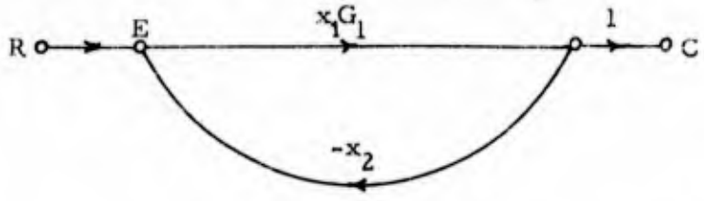

Fig. 4.4 Single-loop feedback system with two variable parameters

Since both parameters appear as tandem branches in the same loop,

$$\left.\begin{aligned} L_{x_1} &= L_{x_2} \equiv L \\ F_{x_1} &= F_{x_2} \equiv F \end{aligned}\right\} \qquad (4.14)$$

Furthermore, x_1 appears only in the forward path, and x_2 only in the return path. Hence,

$$\left.\begin{aligned} F'_{x_1} &= \infty \\ F'_{x_2} &= 1 \end{aligned}\right\} \qquad (4.15)$$

Consequently,

$$\left.\begin{aligned} S^T_{x_1} &= \frac{1}{F} \\ S^T_{x_2} &= \frac{1}{F} - 1 \end{aligned}\right\} \qquad (4.16)$$

Equation (4.16) reveals that the sensitivities with respect to the elements are not independent, but rather are related by

$$S^T_{x_1}(s) - 1 = S^T_{x_2}(s) \qquad (4.17)$$

Moreover, both sensitivities become real at the same frequency ω_x, yielding respective gain margins of

$$\frac{\delta_1}{(x_1)_o} = \frac{1}{S^T_{x_1}(\omega_x) - 1} = \frac{1}{S^T_{x_2}(\omega_x)} = \frac{\delta_2}{(x_2)_o} \qquad (4.18)$$

Letting R_j and I_j represent the real and imaginary parts of $S^T_{x_j}$, one obtains from Eq. (4.17)

$$\left.\begin{aligned} R_2(s) &= R_1(s) - 1 \\ I_2(s) &= I_1(s) \end{aligned}\right\} \qquad (4.19)$$

In Eq. (4.19) when $R_1(\omega_p) = 1/2$, $R_2(\omega_p) = -1/2$. Thus each of the respective phase margin criteria is satisfied at the same frequency, ω_p. Also, $I_2(\omega_p) = I_1(\omega_p)$, and the parameter phase margin with respect to x_1 and x_2 are equal. Thus

$$\phi_{m_1} = \phi_{m_2} \qquad (4.20)$$

This example clearly points out the fact that it is impossible to specify arbitrarily the sensitivity function and the parameter margins for more than one tandem element in a single-loop system. The parameter margins are equal, and the sensitivities are dependently related by Eq. (4.17). The equality of the stability

margins with respect to x_1 and x_2 is obvious in terms of the root-locus, a plot of the equation

$$1 + x_1 x_2 G_1(s) = 0 \tag{4.21}$$

The root-locus contours are the same whether x_1 or x_2 varies.

The influence of x_1 and x_2 on the transmission, however, are quite different. For example, if G(s) has a single pole at the origin, L and F are each characterized by an origin pole. Consequently $S^T_{x_1}$ has an origin zero, and at d-c:

$$\left.\begin{aligned} S^T_{x_1}(o) &= 0 \\ S^T_{x_2}(o) &= -1 \end{aligned}\right\} \tag{4.22}$$

The steady-state accuracy is wholly determined by x_2. Of course, this conclusion also could be drawn by simply evaluating the system transmission at zero frequency which is

$$T(o) = \frac{1}{x_2} \tag{4.23}$$

Another indication of the differing effects of x_1 and x_2 on the system behavior is revealed if, at some frequency ω_1

$$R_1(\omega_1) = 1 \tag{4.24}$$

From Eq. (4.19),

$$\left.\begin{aligned} R_2(\omega_1) &= 0 \\ \text{and} \\ I_2(\omega_1) &= I_1(\omega_1) \neq 0 \end{aligned}\right\} \tag{4.25}$$

In this instance, $|T|$, the magnitude of the transmission, is independent of x_2 at the frequency ω_1 although the phase of T is dependent on both x_1 and x_2.

If the stability specifications for two or more parameters are incompatible with the given configuration, additional degrees of freedom can be obtained via a multiloop system, an example of which is shown in Fig. 4.5

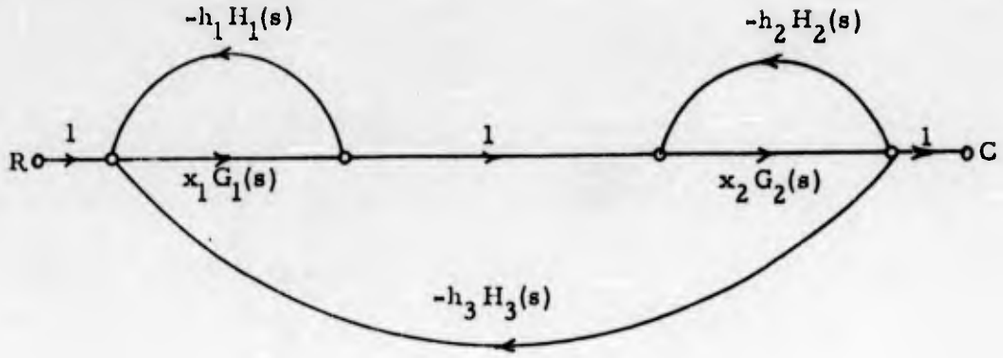

Fig. 4.5 A multiloop feedback system

For the multiloop configuration, we have

$$\left.\begin{aligned} \Delta &= \Delta^o_{x_1}\,\Delta^o_{x_2} + x_1x_2h_3\,G_1G_2H_3 \\ \text{and} \qquad \textstyle\sum &= x_1x_2G_1G_2 \end{aligned}\right\} \tag{4.26}$$

where

$$\left.\begin{aligned} \Delta^o_{x_1} &= (1 + x_2h_2G_2H_2) \\ \Delta^o_{x_2} &= (1 + x_1h_1G_1H_1) \\ \Delta^o_{h_3} &= \Delta^o_{x_1}\,\Delta^o_{x_2} \\ \Delta^o_{h_1} &= \Delta^o_{x_1} + x_1x_2h_3G_1G_2H_3 \\ &\text{etc.} \end{aligned}\right\} \tag{4.27}$$

The various sensitivity functions are

$$\left.\begin{aligned} S^T_{x_1} &= \frac{\Delta^o_{x_1}}{\Delta} \\ S^T_{h_1} &= \frac{\Delta^o_{h_1}}{\Delta} - 1 \\ S^T_{h_3} &= \frac{\Delta^o_{h_3}}{\Delta} - 1 \\ &\text{etc.} \end{aligned}\right\} \tag{4.28}$$

From Eq. (4.28) various relationships among the sensitivity functions may be noted, the most significant of which is

$$S^T_{x_1}(s) - S^T_{h_1}(s) - S^T_{h_3}(s) = 1 \tag{4.29}$$

If $S^T_{x_1}$, $S^T_{h_1}$, $S^T_{h_3}$ are real at frequencies ω_{x_1}, ω_{h_1}, ω_{h_3}, respectively, the parameter gain margins are

$$\left.\begin{aligned} \frac{\delta_{x_1}}{(x_1)_o} &= \frac{1}{S^T_{x_1}(\omega_{x_1}) - 1} \\ \frac{\delta_{h_1}}{(h_1)_o} &= \frac{1}{S^T_{h_1}(\omega_{h_1})} \\ \frac{\delta_{h_3}}{(h_3)_o} &= \frac{1}{S^T_{h_3}(\omega_{h_3})} \end{aligned}\right\} \tag{4.30}$$

If any one of the sensitivities in Eq. (4.29) is real at some point on the $j\omega$ axis, each of the other two need not be real at this frequency to satisfy the equation. Consequently, the crossover frequencies ω_{x_1}, ω_{h_1}, ω_{h_3} are generally distinct, and the gain margins of Eq. (4.30) are independent. A similar argument demonstrates that the corresponding parameter phase margins are also independent. Therefore in this example, there is no inherent incompatibility in arbitrarily specifying the stability margins for x_1, h_1, and h_3. There should be no confusion, however, regarding the independence of the sensitivity functions themselves. From Eq. (4.29), obviously only two sensitivities are independent. The basic difference is that Eq. (4.29) must be satisfied for all values of the argument, while the stability margins of Eq. (4.30) are evaluated at a set of discrete and distinct frequencies. This discussion points out two significant conclusions:

(1) The multiloop system is much more flexible than the single-loop. In some instances, the flexibility so afforded allows one to prescribe simultaneously a set of arbitrary stability margins.

(2) The compatibility of the stability margin specifications with the configuration must be carefully examined in each case. There appear to be no general rules which

guarantee a consistent set. Each configuration, of course, can be readily investigated on its own merits.

Throughout this chapter the sensitivity functions and the parameter margins are observed to serve a dual purpose:

(1) As a tool of analysis, the parameter margins clearly indicate the relative importance of each parameter in determining the stability, as illustrated in Sec. 4. 1.

(2) As a design tool, they guide rather than dictate stabilization procedures. More is said about the second function of the margins in Chap. VI, after the matter of pole sensitivities is taken up in Chap. V.

Chapter V - Parameter Pole Sensitivity

The considerations of Chaps. II and III demonstrate how the sensitivity-stability theorem logically evolves from a fusion of the root-locus method with Lynch's topological formulation of sensitivity. The theorem affords a rigorous quantitative evaluation of the destabilizing effects of variations in any one system parameter. There is no restriction on the magnitude of the change.

On the other hand, the pole sensitivity* describes the change in pole position caused by an incremental change in a parameter. If several parameters vary simultaneously, the change in pole position can be computed approximately by superposing the effects of each parameter increment. The pole-sensitivity concept, to an extent, supplements the sensitivity theorem; the latter is applicable when the consequence of large variations in a single parameter are studied, while the former is useful in analyzing the effects of small changes in several parameters.

The purpose of this chapter is to extend the pole-sensitivity concept in several directions. Specifically, our attention is focussed on:

(1) A topological formulation of parameter pole sensitivity. This formalism leads to a correlation between pole sensitivity and the sensitivity function.

(2) An approximate analysis of the effects of simultaneous parameter variations on the pole position, the pole residue, and the impulsive response.

(3) An interpretation of pole sensitivities in terms of gain and phase margins for lightly damped systems.

(4) Parameter tolerance specifications for systems with a stringently prescribed dynamic behavior.

5.1 Topological Formulation of Parameter Pole Sensitivity

An arbitrary feedback configuration is characterized by n poles $p_1, p_2, \cdots p_n$, which depend on a parameter x. As x varies, the k^{th} pole, (p_k), traces out a continuous locus in the s-plane. There is a certain analogy between a pole "moving" along a root-locus contour and a point mass moving along a trajectory. The "velocity" of the pole at any point on the contour is the parameter rate of change of pole position or $\frac{dp_k}{dx}$, and the "pole acceleration" is the rate of change of velocity or $d^2 p_k/dx^2$.

---

*E. J. Angelo, op. cit.

The angle and magnitude of dp_k/dx directly measure the slope of the root-locus and the "instantaneous" speed respectively. In this context, the parameter pole sensitivity* defined as

$$Q_x^{p_k} \equiv \frac{d\,p_k}{d\,\ell n\,x} = \frac{d\,p_k}{dx/x} \tag{5.1}$$

can be interpreted as a normalized complex velocity of the pole p_k as it traverses the s-plane along the root-locus contour.

Our immediate objective is to relate this "velocity" to the graph topology. The transmission is

$$T = \frac{\sum}{\Delta} = \frac{\sum_x^o + x \sum_x}{\Delta_x^o + x \Delta_x} \tag{5.2}$$

Clearly, the only poles of T(s) which depend on x are those contributed by the zeros of $\Delta(s, x)$. The root loci are defined as the continuous sets of points in the s-plane satisfying

$$\Delta_x^o(s) + x\,\Delta_x(s)\Big|_{s\,=\,p_k} = 0 \tag{5.3}$$

or

$$x = \frac{-\Delta_x^o(p_k)}{\Delta_x(p_k)} \tag{5.4}$$

Hence

$$\ell n\,x = j\pi + \ell n\,\Delta_x^o - \ell n\,\Delta_x \tag{5.5}$$

Differentiation of Eq. (5.5) with respect to p_k gives

$$\frac{d\,\ell n\,x}{d\,p_k} = \left.\frac{\Delta_x^{o\,\prime}}{\Delta_x^o} - \frac{\Delta_x^{\prime}}{\Delta_x}\right|_{s\,=\,p_k} \tag{5.6}$$

---

*Hanoch Ur, "Root Locus Properties and Sensitivity Relations in Control Systems", I. R. E. Trans. on Automatic Control, Jan. 1960.

Equation (5. 6) is recognized as the reciprocal of the pole sensitivity, so that

$$Q_x^{p_k} = \frac{1}{\frac{\Delta_x^{o\,\prime}}{\Delta_x^o} - \frac{\Delta_x^{\prime}}{\Delta_x}} = \frac{\Delta_x^o}{\Delta_x^{o\,\prime} - \Delta_x^{\prime}\frac{\Delta_x^o}{\Delta_x}}\Bigg|_{s\,=\,p_k} \tag{5.7}$$

Substitution of Eq. (5. 4) into Eq. (5. 7) yields

$$Q_x^{p_k} = \frac{\Delta_x^o}{\Delta_x^{o\,\prime} + x\,\Delta_x^{\prime}}\Bigg|_{s\,=\,p_k} = \frac{\Delta_x^o}{\Delta^{\prime}}\Bigg|_{s\,=\,p_k} = \frac{-x\,\Delta_x}{\Delta^{\prime}}\Bigg|_{s\,=\,p_k} \tag{5.8}$$

Usually, the pole sensitivity is defined at the nominal value of the parameter--i. e., when $x = x_o$, $p_k = p_{k_o}$, and Eq. (5. 8) becomes

$$Q_{x_o}^{p_k} = \frac{d\,p_k}{dx/x_o} = \frac{\Delta_x^o}{\Delta^{\prime}}\Bigg|_{\substack{s\,=\,p_{k_o} \\ x\,=\,x_o}} \tag{5.9}$$

Equation (5. 8) is perfectly general and valid at any point on the locus. In particular, as the pole crosses the $j\omega$ axis, $x = x_{cr}$, $s = j\omega_x$, and the normalized velocity is

$$Q_{x_{cr}}^{p_k} = \frac{d\,p_k}{dx/x_{cr}} = \frac{\Delta_x^o}{\Delta^{\prime}}\Bigg|_{\substack{s\,=\,j\omega_x \\ x\,=\,x_{cr}}} \tag{5.10}$$

A diagram depicting Eqs. (5. 9) and (5. 10) is shown in Fig. 5. 1.

Obviously, from Eq. (5. 8), the pole sensitivity depends only on the graph determinant Δ, and is completely independent of the choice of sink and source nodes in the signal-flow graph. When the null return difference with respect to x is either unity or infinite, the sensitivity function, S_x^T, is also found to depend only on Δ. For these cases, the pole sensitivity bears a particularly simple relationship to S_x^T. The usual three cases are considered below.

(a) $F_x^{\prime}$ is infinite (or $\Delta_x^o = 0$). Then

$$S_x^T = \frac{\Delta_x^o}{\Delta} = \frac{\Delta_x^o}{\Delta_x^o + x\,\Delta_x} \tag{5.11}$$

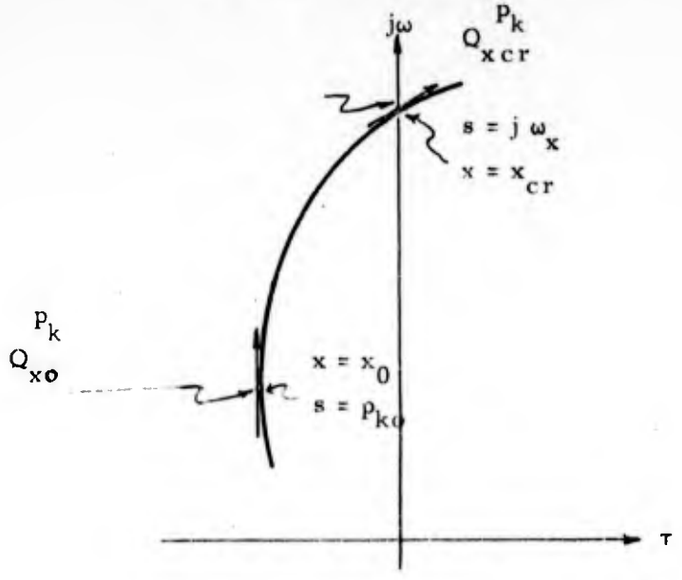

Fig. 5.1 Pole-sensitivity diagram

If the pole at p_k is simple, S_x^T can be expanded in partial fractions as

$$S_x^T(s) = \frac{a_k}{(s - p_k)} + \cdots \tag{5.12}$$

where

$$a_k = (s - p_k)\, S_x^T \Big|_{s = p_k} = \frac{\Delta_x^o}{\frac{d}{ds}(\Delta)} \Big|_{s = p_k} = Q_x^{p_k} \tag{5.13}$$

Hence the pole sensitivity is simply the residue of S_x^T at p_k. The pole sensitivity can be related to the transmission T(s). Since T and S_x^T have common poles, T may be written as

$$T(s) = \frac{x \sum_x}{\Delta} = \frac{r_k}{(s - p_k)} + \cdots \tag{5.14}$$

where

$$r_k = \left. \frac{x \sum_x}{\Delta'} \right|_{s = p_k} \tag{5.15}$$

is the transmission residue at the pole in question. A combination of Eqs. (5.13) and (5.15) yields

$$Q_x^{p_k} = (r_k) \left. \frac{\Delta_x^o}{x \Sigma_x} \right|_{s=p_k} = -(r_k) \left. \frac{\Delta_x}{\Sigma_x} \right|_{s=p_k} \tag{5.16}$$

As expressed in Eq. (5.8), $Q_x^{p_k}$ depends only on Δ and not on $\sum$. The form of Eq. (5.16) facilitates computation in some instances, but additionally, the equation seems to indicate the extent to which the transmission residue is dependent on $Q_x^{p_k}$. For example, if x is the gain of the forward path in a single-loop, unity feedback system (Fig. 5.2a), $\sum_x = \Delta_x$ and $r_k = -Q_x^{p_k}$. On the other hand, if there is attenuation in the return path as shown in Fig. 5.2b, then $r_k / Q_x^{p_k} = -1/h$.

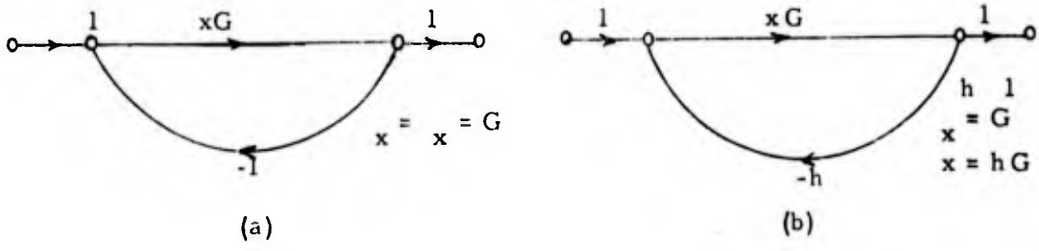

Fig. 5.2 Two single-loop systems

Apparently, the only meaning to be drawn from a comparison of the graphs in Fig. 5.2 is that for equal pole sensitivities at the same position p_k, the r_k of (b) is 1/h times that of (a). But this is obvious at the outset since, at this setting, the transmission of (b) is simply that of (a) multiplied by 1/h.

(b) F'_x is unity, or $\sum_x = 0$. For a simple pole at p_k,

$$S_x^T = \frac{-x \Delta_x}{\Delta} = \frac{a_k}{(s - p_k)} + \cdots \tag{5.17}$$

"Comparison of Eq. (5.19) with Eq. (5.8) gives"

$$Q_x^{p_k} = a_k \tag{5.18}$$

Similarly, T is expanded as

$$T = \frac{\sum_x^o}{\Delta} = \frac{r_k}{(s - p_k)} + \cdots \tag{5.19}$$

and

$$Q_x^{p_k} = \frac{\Delta_x^o}{\sum_x^o}\Bigg|_{s = p_k} (r_k) \qquad = \frac{-x\,\Delta_x}{\sum_x^o}\Bigg|_{s = p_k} (r_k) \tag{5.20}$$

(c) For the general case, F'_x is neither unity nor infinite, and T is expressed as

$$T = \frac{\sum_x^o}{\Delta} + \frac{x \sum_x}{\Delta} \tag{5.21}$$

$$= T_\alpha + T_\beta$$

For this case, it can be shown that

$$Q_x^{p_k} = \begin{cases} a_{k_\alpha} = \dfrac{\Delta_x^o}{\sum_x^o}\Big|_{s = p_k} (r_{k_\alpha}) \\ a_{k_\beta} = \dfrac{-\Delta_x}{\sum_x}\Big|_{s = p_k} (r_{k_\beta}) \end{cases} \tag{5.22}$$

where a_{k_α} and a_{k_β} are the residues of $S_x^{T_\alpha}$ and $S_x^{T_\beta}$ at p_k, respectively, and r_{k_α} and r_{k_β} are the residues at p_k of T_α and T_β.

Equation (5.22) summarizes the topological formulation of the pole sensitivity and clearly indicates the condition under which the pole sensitivity and the transmission residue are independent. The equation also serves as the basis for reducing the pole sensitivity with respect to some critical system parameter.

In order to insure the stability of the system the horizontal (or σ) component of the pole sensitivity should approach zero as the pole draws near the $j\omega$ axis. This ideal implies that

$$\angle Q_x^{p_k} \longrightarrow 90^\circ \quad \text{as Re } p_k \longrightarrow 0 \tag{5.23}$$

From root-locus considerations, however, the condition of Eq. (5.23) can not be attained if the system has an asymptotic order of three or more. In most practical situations, all attempts to satisfy (5.23) are futile. Furthermore, since $Q_x^{p_k}$ can never be zero (except in trivial cases) it is clearly impossible to guarantee the stability of the system with one varying parameter. Of course, the practical alternative involves an attempt to control the pole sensitivity in a limited region of the s-plane and only over the expected range of variation of the parameter.

5.2 Approximate Gain and Phase Margins

In Sec. 3.3, it is argued that orthogonal lines in the complex parameter plane map into orthogonal lines in the s-plane. This contention is also supported by the following considerations.* The magnitude of x is fixed at its nominal value x_o, but the phase changes by a small angle $d\alpha$ as shown in Fig. 5.3a.

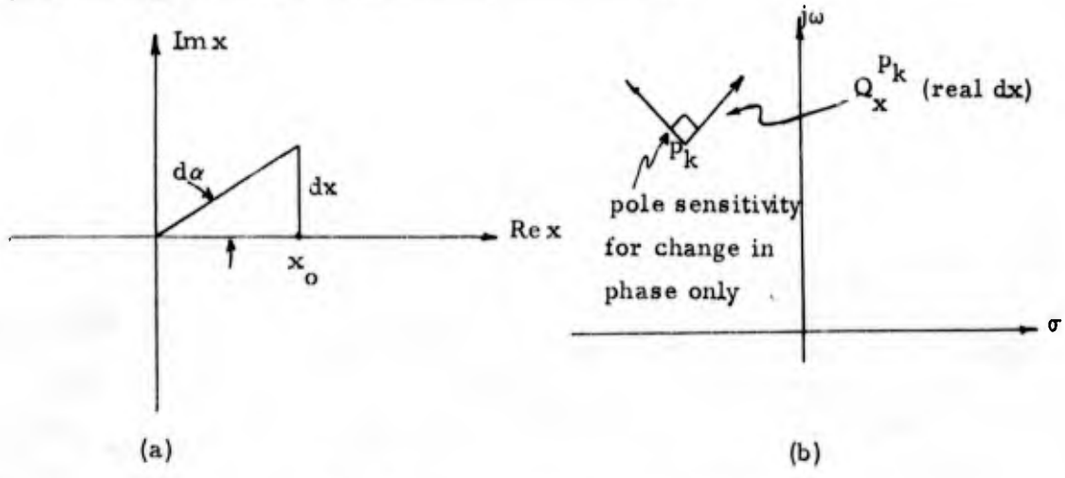

Fig. 5.3 Orthogonal properties

From the diagram, it follows that

$$\left.\begin{aligned} dx &= j x_o \, d\alpha \\ \text{or} \qquad \frac{dx}{x_o} &= j \, d\alpha \end{aligned}\right\} \tag{5.24}$$

Therefore,

$$Q_{x_o}^{p_k} = \frac{d p_k}{dx/x_o} = \frac{d p_k}{j \, d\alpha} \tag{5.25}$$

*H. Ur, op. cit.

The pole displacement is

$$d\,p_k = (j\,Q_{x_o}^{p_k})\,d\,a \tag{5.26}$$

and is clearly at right angles to the displacement for a real increment in x, as portrayed in Fig. 4.3b.

These orthogonal properties of the pole sensitivity can be used to indicate the order of magnitude of the parameter gain and phase margins. If the curvature* of the root locus about the lightly damped pole p_k is assumed small, a linear extrapolation of the phase and magnitude pole sensitivities until they intersect the $j\omega$ axis yields a first, albeit crude, approximation to the gain and phase margins. (From the mechanical analogy, we are assuming that the pole is moving with almost constant velocity.) The situation is portrayed in Fig. 5.4 with

$$\left.\begin{aligned} Q_{x_o}^{p_k} &= \left|Q_{x_o}^{p_k}\right| e^{j\phi_k} \\ p_k &= -\sigma_k + j\beta_k \end{aligned}\right\} \tag{5.27}$$

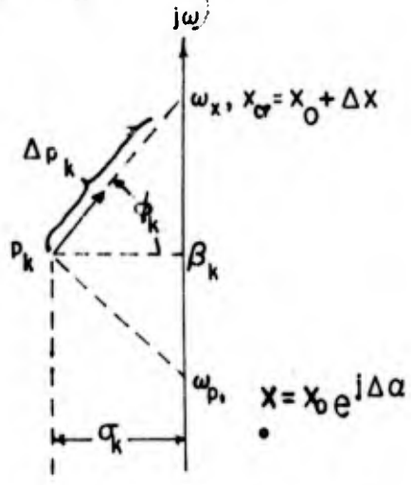

Fig. 5.4 Gain-phase margin diagram.

---

* Ibid.

From the geometry, it follows that

$$\left.\begin{aligned} \frac{\Delta x}{x_o} &\cong \frac{\sigma_k/\cos\,\phi_k}{\left|Q_{x_o}^{p_k}\right|} \\ \Delta\alpha &\cong \frac{-\sigma_k/\sin\,\phi_k}{\left|Q_{x_o}^{p_k}\right|} \end{aligned}\right\} \qquad (5.28)$$

and also

$$\left.\begin{aligned} (\omega_x - \beta_k) &\cong \sigma_k \tan\,\phi_k \\ (\beta_x - \omega_p) &\cong \sigma_k \cot\,\phi_k \end{aligned}\right\} \qquad (5.29)$$

In Eq. (5.28), $(1 + \Delta x/x_o)$, and $\Delta\alpha$ are first-order approximations to the gain and phase margins for lightly-damped systems.

A combination of the pole sensitivity concept and the sensitivity-stability theorem enables the designer to visualize, to an extent, the motion of the pole through the s-plane. For example in Fig. 5.1, the stability theorem predicts the values of x_{cr} and ω_x, while the pole sensitivity indicates the direction and "speed" of the pole as x is perturbed from x_o. The two techniques should be employed in conjunction with each other, rather than to the exclusion of one or the other. As a case in point, the gain margin and crossover frequency ω_p are more easily and accurately computed by means of the stability theorem, while an approximation to the crossover frequency is readily found from Eq. (5.28) or from a construction similar to that in Fig. 5.4.

5.3 Effect of a Small Parameter Change on the Impulse Response

The impulsive response of a system is determined wholly by the distribution of poles and zeros in the complex plane. As the parameter x takes on an increment dx, the shift in positions of some of the poles and zeros causes the impulse response to change. The perturbation of the impulse response can be computed approximately by means of the pole sensitivity, and, an extension of this concept, the zero sensitivity.

Specifically, the impulse response for an arbitrary system with simple poles is

$$g(t) = \sum_{k=1}^{n} r_k e^{p_k t} = \sum_{k=1}^{n} g_k(t) \tag{5.30}$$

where r_k, the residue of $T(s)$ at p_k, is given by

$$r_k = (s - p_k)\, T(s)\Big|_{s = p_k} = \frac{\prod_{j=1}^{m} (p_k - z_j)}{\prod_{\substack{u=1 \\ u \neq k}}^{n} (p_k - p_u)} \tag{5.31}$$

and

$$T(s) = \frac{\sum_x^o(s) + x \sum_x(s)}{\Delta_x^o(s) + x\, \Delta_x(s)} = \frac{\prod_{j=1}^{m} (s - z_j)}{\prod_{u=1}^{m} (s - p_u)} \tag{5.32}$$

At the nominal value of the parameter $x = x_o$, the poles p_{k_o}, the zeros z_{j_o}, and the residues r_{k_o} are known, and the nominal impulse response is

$$g_o(t) = \sum_{k=1}^{n} r_{k_o} e^{p_{k_o} t} = \sum_{k=1}^{n} g_{k_o}(t) \tag{5.33}$$

As x changes incrementally, the response becomes

$$g(t) = g_o(t) + \Delta g(t) = \sum (r_{k_o} + \Delta r_k) e^{(p_{k_o} + d\, p_k)t}$$

$$= \sum r_{k_o} e^{(p_{k_o} + d\, p_k)t} + \sum \Delta r_k\, e^{(p_k + d\, p_k)t} \tag{5.34}$$

The first term on the left-hand side of Eq. (5.34) is approximately the unperturbed impulse response (except for the $e^{d\, p_k t}$ factor), and the second must correspond to $\Delta g(t)$. Hence,

$$\Delta g(t) \cong \sum \Delta r_k e^{(p_k + d\, p_k)t} \approx \sum \Delta r_k e^{p_k t} = \sum \frac{\Delta r_k}{r_{k_o}}\, g_{k_o}(t) \tag{5.35}$$

Alternately, if the residue sensitivity is defined as

$$S_x^{r_k} = \frac{d\, r_k / r_{k_o}}{d\, x / x_o} \tag{5.36}$$

Eq. (5.35) can be expressed as

$$\Delta g(t) = \frac{\Delta x}{x_o} \sum_{k=1}^{n} S_x^{r_k} g_{k_o}(t) \tag{5.37}$$

or

$$\frac{\Delta g(t)}{\Delta x / x_o} = \sum_{k=1}^{n} S_x^{r_k} g_{k_o}(t) \tag{5.38}$$

The last equation, representing the normalized change in the impulse response, consists of a weighted sum of the components of the unperturbed response. In the Appendix, the weighting factor or residue sensitivity is shown to be

$$S_x^{r_k} = \sum_{j=1}^{m} \frac{Q_x^{p_k} - U_x^{z_j}}{(p_k - z_j)} + \sum_{\substack{u=1 \\ u \neq k}}^{n} \frac{Q_x^{p_k} - Q_x^{p_u}}{(p_k - p_u)} \tag{5.39}$$

In Eq. (5.39), the term $U_x^{z_j}$ is the transmission zero sensitivity for the $j^{\underline{th}}$ zero, and is defined by

$$U_x^{z_j} = \frac{d\, z_j}{d\, x / x_o} \tag{5.40}$$

By analogy with the pole sensitivity, $U_x^{z_j}$ is found to be

$$U_x^{z_j} = \left. \frac{\sum_x^o}{\sum'} \right|_{s = z_j} = \left. \frac{-x \sum_x}{\sum'} \right|_{s = z_j} \tag{5.41}$$

If the null return difference with respect to x is either unity or infinite, the transmission zeros do not depend on x, and $U_x^{z_j}$ is identically zero.

Equation (5.37) represents only the linear term in the series expansion for $\Delta g(t)$, and the approximation is valid for Δx sufficiently "small". But, there is no a priori indication of a permissible range for $d x / x_o$ unless the higher-order terms

involving $d^2 p_k / dx^2$, etc., are computed. As a rule of thumb, the higher-order derivatives are large if the root-locus has a sharp bend or twist in the vicinity of the pole.

Although Eq. (5.39), expressing the residue sensitivity in terms of the pole-zero sensitivities, appears quite formidable, it can be reduced considerably in most practical situations. For example, quite frequently the transmission zeros are independent of x. Moreover, in any specific case, there are system poles far removed from the jω axis and the origin of the s-plane. Terms of Eq. (5.39) with such distant poles in the denominator often can be neglected. Furthermore, in most practical cases, the components of the impulse response arising from these distant poles can be ignored in Eq. (5.37). The implication here is that only the control poles near the jω axis are of any real concern or significance. Engineering intuition should guide the analyst in making suitable approximations in these situations.

As an example, the perturbed impulse response for the system of Fig. 5.5a is calculated. The closed-loop pole-zero pattern for T(s) is shown in Fig. 5.5b.

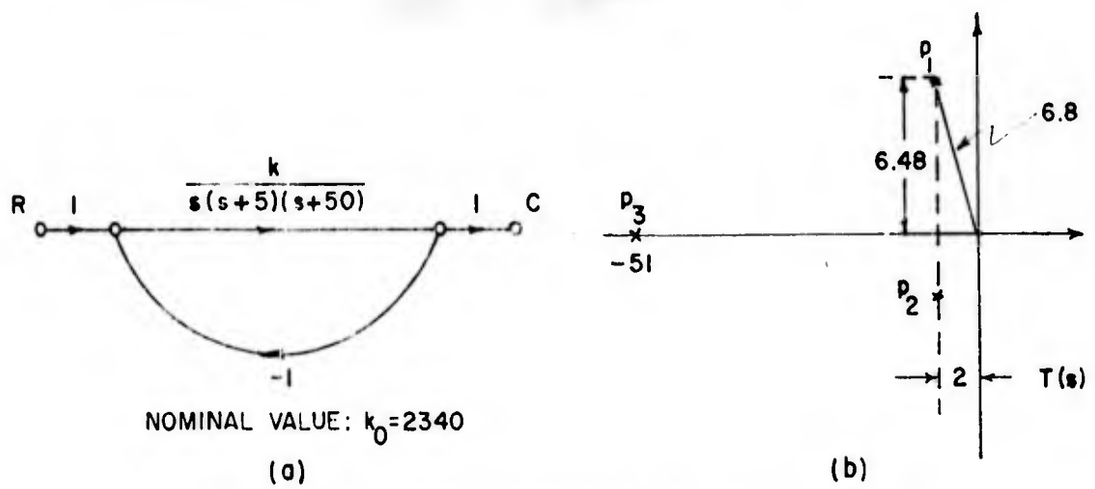

Fig. 5.5 Flow graph and pole-zero plot for example

The pole sensitivities are found to be:

$$\left.\begin{aligned} Q_k^{p_3} &= -0.94 \\ Q_k^{p_1} &= -3.7\, e^{-j\,97.5} \\ Q_k^{p_2} &= (Q_k^{p_1})^* \end{aligned}\right\} \qquad (5.42)$$

The residue sensitivities and perturbed response are calculated by using all the terms in Eqs. (5.37) and (5.39), then they are compared with the results obtained by making judicious approximations. Thus,

$$S_k^{r_1} = \frac{Q_k^{p_1}}{p_1} + \sum_{u=2}^{3} \frac{Q_k^{p_1} - Q_k^{p_u}}{p_1 - p_u} = 1.1\, e^{-j\,8^o}$$

$$S_k^{r_2} = (S_k^{r_1})^* \tag{5.43}$$

$$S_k^{r_3} = \frac{Q_k^{p_3}}{p_3} + \sum_{u=1}^{2} \frac{Q_k^{p_3} - Q_k^{p_u}}{p_3 - p_u} = 0.096$$

Substitution of Eq. (5.43) into Eq. (5.37) gives

$$\Delta g(t) = \frac{\Delta k}{k_o}\left[8.15\, e^{-2t} \sin(6.5t - 15^o) + 0.1\, e^{-51t}\right] \tag{5.44}$$

The pole at p_3 contributes negligibly to the impulse response of Eq. (5.44) and to the residue sensitivities, $S_k^{r_1}$ and $S_k^{r_2}$. If p_3 is completely ignored, there results

$$S_k^{r_1} = 1.1\, e^{-j\,12^o}$$

$$\Delta g(t) = \frac{\Delta k}{k_o}\left[8.15\, e^{-2t} \sin(6.5\, t - 19^o)\right] \tag{5.45}$$

A comparison of Eqs. (5.44) and (5.45) justifies completely neglecting the distant pole at p_3.

5.4 Damping and Radial Sensitivities

If the effects of a parameter perturbation on the relative damping ζ and on the undamped natural frequency ω_n of a complex pole are to be determined,* the complex pole sensitivity can be resolved into two orthogonal real components:

*For example, many servomechanisms are approximated by a second-order system with control poles characterized by ζ and ω_n. These parameters are used to determine the overshoot, rise time, the bandwidth, etc., of the system.

(1) along the radial or ω_n direction, and

(2) along the direction of increasing θ (or decreasing ζ).

The situation envisaged is portrayed in Fig. 5.6 with $\omega_n \equiv \rho$.

$$\rho_k = |p_k|$$

$$\zeta_k = \cos^{-1} \theta_k$$

$$Q_x^{p_k} = |Q_x^{p_k}| e^{j\phi_k}$$

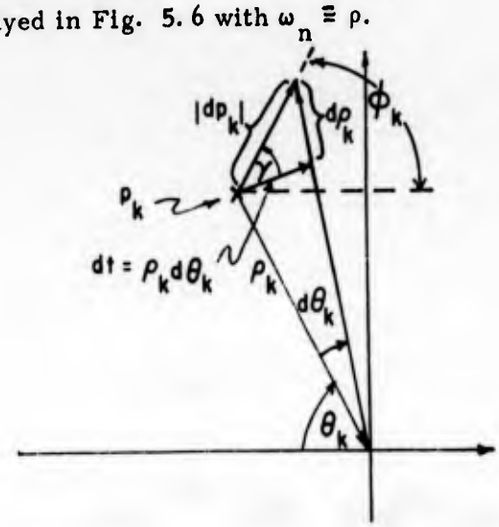

Fig. 5.6 Radial and damping sensitivities

The damping and radial sensitivities which are proportional to the projections of $Q_x^{p_k}$ along these orthogonal directions, are defined by

$$\left.\begin{aligned} S_x^{\zeta_k} &\equiv \frac{d\zeta_k/\zeta_k}{dx/x} \\ S_x^{\rho_k} &\equiv \frac{d\rho_k/\rho_k}{dx/x} \end{aligned}\right\} \qquad (5.46)$$

From Fig. 5.6 and the expression for pole sensitivity, these sensitivities can be shown to be

$$\left.\begin{aligned} S_x^{\rho_k} &= \frac{-|Q_x^{p_k}|}{\rho_k} \cos(\theta_k + \phi_k) \\ S_x^{\zeta_k} &= \frac{-|Q_x^{p_k}|}{\rho_k} (\tan\theta_k) \sin(\theta_k + \phi_k) \end{aligned}\right\} \qquad (5.47)$$

In Sec. 5.6, these sensitivities are employed in the formulation of an optimum parameter specification problem. Thus far, pole-zero sensitivities and some of the ramifications have been studied from the standpoint of a single perturbed parameter. Our attention is now turned to the more challenging problem encountered when several parameters vary simultaneously.

5.5 Multiparameter Pole Sensitivities

The results of the preceding sections are generalized to take into account simultaneous perturbations in several parameters. The general case of a system characterized by n poles, m zeros, and q parameters $x_1, x_2 \cdots, x_q$ is considered. For small changes in each of the q parameters, the pole or zero displacement is obtained by linearly superposing the displacement caused by each parameter perturbation. Thus, if the component pole-zero sensitivities are

$$\left.\begin{aligned} Q_{x_i}^{p_k} &= \frac{d\,p_k}{d\,x_i/x_i} \\ U_{x_i}^{z_j} &= \frac{d\,z_j}{d\,x_i/x_i} \end{aligned}\right\} \quad \begin{aligned} &1 \le i \le q \\ &1 \le k \le n \\ &1 \le j \le m \end{aligned} \tag{5.48}$$

the net displacements of the pole p_k and the zero z_j from the nominal positions are

$$\left.\begin{aligned} d\,p_k &= \sum_{i=1}^{q} Q_{x_i}^{p_k} \left(\frac{d\,x_i}{x_i}\right) \\ d\,z_j &= \sum_{i=1}^{q} U_{x_i}^{z_j} \left(\frac{d\,x_i}{x_i}\right) \end{aligned}\right\} \tag{5.49}$$

Similarly, if the component of the residue sensitivity is

$$S_{x_i}^{r_k} = \frac{d\,r_k/r_k}{d\,x_i/x_i} \tag{5.50}$$

the percent change in the residue at the $k^{\underline{th}}$ pole when all parameters vary simultaneously is

$$\frac{d\,r_k}{r_k} = \sum_{i=1}^{q} S_{x_i}^{r_k} \left(\frac{d\,x_i}{x_i}\right) \tag{5.51}$$

The change in the impulse response when the $i^{\underline{th}}$ parameter changes is

$$\Delta\,g(t) = \frac{\Delta\,x_i}{x_i} \sum_{k=1}^{n} S_{x_i}^{r_k}\, g_k(t) \tag{5.52}$$

When all the parameters vary, Eq. (5.52) becomes

$$\Delta g(t) = \sum_{i,k}' \left(\frac{\Delta x_i}{x_i}\right) S_{x_i}^{r_k} g_k \tag{5.53}$$

Similarly, the damping and radial sensitivities yield

$$\left.\begin{aligned} \frac{d\zeta_k}{\zeta_k} &= \sum_{i=1}^{q} S_{x_i}^{\zeta_k} \left(\frac{d x_i}{x_i}\right) \\ \frac{d\rho_k}{\rho_k} &= \sum_{i=1}^{q} S_{x_i}^{\rho_k} \left(\frac{d x_i}{x_i}\right) \end{aligned}\right\} \tag{5.54}$$

It was mentioned in the first section of this chapter in connection with the discussion of Eq. (5.23) that since $Q_x^{p_k}$ is non-zero, $d p_k$ is non-zero. An inspection of Eq. (5.49) for the multiparameter case, however, reveals that the possibility exists for a net pole displacement of zero. One such possibility for a three-parameter system is shown in Fig. 5.7.

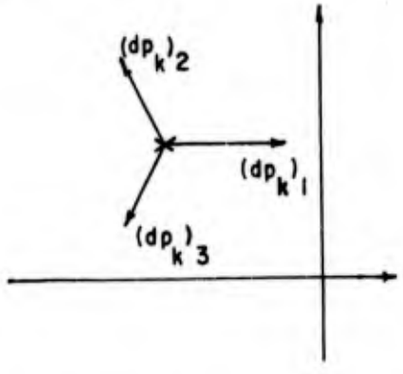

Fig. 5.7 A null pole displacement

But, the lengths of the phasors in Fig. 5.7 are proportional to the respective $d x_i/x_i$. (The $Q_{x_i}^{p_k}$ are constants.) Consequently, the null condition can be obtained only for certain combinations of the $d x_i/x_i$ and if the parameters vary independently the null can never be maintained. In the example considered, if any of the $d x_i$ is zero, $d p_k$ must be non-zero.

On the other hand, if all three parameters are dependent on some environmental variable, say temperature, and if two arise from the controlled process, the third can be selected to vary in such a manner as to minimize the effects of the other two.

Indeed, the tailoring of thermistors in the transistor circuits serves this express purpose. Ur has shown that the derivative $d\,p_k/dT$, where T represents the environmental variable, can be made zero, by suitably selecting the compensation parameters as follows. Equations (5.48) and (5.49) are combined to give

$$d\,p_k = \sum_i \frac{\partial p_k}{\partial x_i}\, d\,x_i \tag{5.55}$$

or

$$\frac{d\,p_k}{d\,T} = \sum \frac{\partial p_k}{\partial x_i}\, \frac{d\,x_i}{d\,T} \tag{5.56}$$

The $\partial p_k/\partial x_i$ terms are constants determined by the flow-graph topology. The $d\,x_i/d\,T$ corresponding to the plant elements are evaluated at the nominal value of the environmental variable (e.g., at room temperature). Then the $d\,x_i/d\,T$ corresponding to the compensation elements are tailored so that the sum of the terms in Eq. (5.56) is zero. This procedure yields a true null only for infinitesimal changes in the environmental variable, but certainly minimizes the pole displacement in most practical situations when the $d\,x_i/d\,T$ are reasonably well-behaved functions of T.

Even if $d\,p_k$ is zero, the residue increment, $d\,r_k$, need not be. A shift in the positions of the other poles and zeros changes r_k, resulting in a change in the impulsive response. In fact, in the absence of more information regarding the other poles and zeros, there is no assurance that the change in r_k is less than that for the uncompensated system for a given variation in T. This observation is not intended to be a criticism of the merits of the zero $d\,p_k$ objective, but rather to point out the obvious fact that the time response can vary even though the important control poles are stationary.

Control over the positions of the significant poles is certainly a worthy objective, since these determine the stability and the bandwidth of the system. Indeed, any attempt to maintain a zero $d\,r_k$ (or zero $d\,r_k/d\,T$) is not only senseless, but almost impossible because of the complexity of Eq. (5.39) and Eq. (5.51). In the following section, a somewhat different approach to the problem of small parameter variations is taken.

5.6 An Application of Pole Sensitivities to Optimum Tolerance Specifications

The problem studied in this section is the determination of a set of parameter tolerances which insures that the closed-loop poles remain within specified regions in the s-plane, and which minimizes a certain cost function related to the tolerances. It is presumed that the system has been designed to operate satisfactorily at the nominal values of the parameters, and that the pole positions at these values are known. The only remaining problem is the specification of the tolerances.

The system under consideration has r pairs of complex poles which depend on q parameters. At the nominal parameter values, $\{(x_i)_o\}$, the pole positions are described by $\{(\zeta_k, \rho_k)_o\}$. The bounds on the tolerable variations of the pole positions are set by

$$\left.\begin{aligned} (\zeta_k)_m \leq \zeta_k \leq (\zeta_k)_M \\ (\rho_k)_m \leq \rho_k \leq (\rho_k)_M \end{aligned}\right\} \qquad (5.57)$$

where

$$\left.\begin{aligned} \zeta_k = (\zeta_k)_o + d\,\zeta_k \\ \rho_k = (\rho_k)_o + d\,\rho_k \end{aligned}\right\} \qquad (5.58)$$

The region envisaged for the k^{th} pole is portrayed in Fig. 5.8.

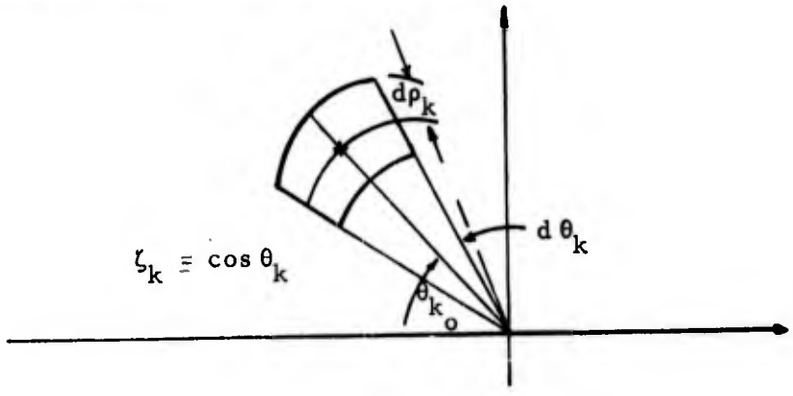

Fig. 5.8 Permissible region for k^{th} pole

The inequalities of Eq. (5.57) are normalized upon substitution of Eq. (5.58)

to yield

$$(a_k)_m \triangleq \frac{(\zeta_k)_m}{(\zeta_k)_o} - 1 \leq \frac{d\zeta_k}{(\zeta_k)_o} \leq \frac{(\zeta_k)_M}{(\zeta_k)_o} + 1 \triangleq (a_k)_M$$

$$(\beta_k)_m \triangleq \frac{(\rho_k)_m}{(\rho_k)_o} - 1 \leq \frac{d\rho_k}{(\rho_k)_o} \leq \frac{(\rho_k)_M}{(\rho_k)_o} + 1 \triangleq (\beta_k)_M \qquad (5.59)$$

where

$$\left.\begin{aligned} &(a_k)_M, (\beta_k)_M \geq 0 \\ &(a_k)_m, (\beta_k)_m \leq 0 \end{aligned}\right\} \qquad (5.60)$$

The inequalities of Eq. (5.59) are related to the parameter variations by the damping and radial sensitivities defined in Sec. 5.4. Combining Eq. (5.59) with Eq. (5.54) and defining $y_i \triangleq dx_i/(x_i)_o$ gives a set of 2 r inequalities of the form

$$\left.\begin{aligned} (a_k)_m &\leq \sum_{i=1}^{q} S_{x_i}^{\zeta_k} y_i \leq (a_k)_M \\ (\beta_k)_m &\leq \sum_{i=1}^{q} S_{x_i}^{\rho_k} y_i \leq (\beta_k)_M \end{aligned}\right\} \qquad (5.61)$$

The inequalities of Eq. (5.61) define a volume in a normalized q-dimensional parameter space. If the parameter variations are confined to this volume, the closed-loop poles remain within the bounds prescribed by Eq. (5.57).

Moreover, the weighted cost function is selected as

$$C = \frac{w_1}{|y_1|} + \cdots + \frac{w_q}{|y_q|} = \sum_{j=1}^{q} \frac{w_j}{|y_j|} \qquad (5.62)$$

C represents the "cost" or effort expended in constraining the parameter variations to lie within the designated volume, or alternately, C may be viewed as the expenditure required to keep the components represented by the parameters within the tolerances $|y_j| = \left|dx_j/(x_j)_o\right|$. The w_j's are appropriate positive constant weighting factors.

Thus, w_j would be relatively large if the component or parameter in question is costly (e. g. , a power element), whereas it would be small if x_j corresponds to an inexpensive, low-power element. The form of the cost equation is "reasonable", since zero tolerance in any parameter implies infinite cost. Nevertheless, the form seems somewhat artificial or forced, and the cost equation might just as well take a number of other forms (e. g. , $w_i/|y_i|^2$, or $w_i/|y_i| + |y_i|^2$, etc.).

Our objective is to minimize C subject to the constraints of Eq. (5. 61), and to solve for the resulting set of optimum tolerances $\{|y_i|\}$. Intuition (and the cost equation) suggests that $|y_j|$ be made large; but Eq. (5. 61) must be satisfied, and is obviously satisfied for $\{|y_j| = 0\}$ but at an infinite cost. Hence, an optimum set of $\{|y_i|\}$ compatible with Eq. (5. 61) is sought.

If the pole sensitivity formulation is to be valid, the parameter variation must be "small". Consequently, in addition to Eq. (5. 61), one might add

$$|y_i| \leq \gamma_i < 1 \tag{5. 63}$$

But the latter condition is usually fulfilled if the permissible s-plane region in which the p_k may wander is sufficiently restricted. This would be the case if the system designer wanted to maintain a stringently prescribed dynamic behavior.

Because of the nonlinear form of the cost function, the linear programming techniques cannot be directly applied to the solution of this problem. Consequently, surface-searching methods must be used to find the minimum compatible C. That is to say, the problem requires computer solution when more than three parameter variables are involved.

For example, if two varying parameters are involved, the inequalities of Eq. (5. 61) give rise to an area of feasible solutions in the y_2 -- y_1 plane as indicated in Fig. 5. 9. The minimum cost corresponds to the vertices of one of the family of symmetric rectangles which can be inscribed within the boundary. The boundary of the area must be scanned in quest of a minimum cost point.

Each boundary segment is a straight line of the form

$$y_2 + a\, y_1 = b \tag{5. 64}$$

A straight line passing through the origin of the form

$$y_2 = k\, y_1 \tag{5. 65}$$

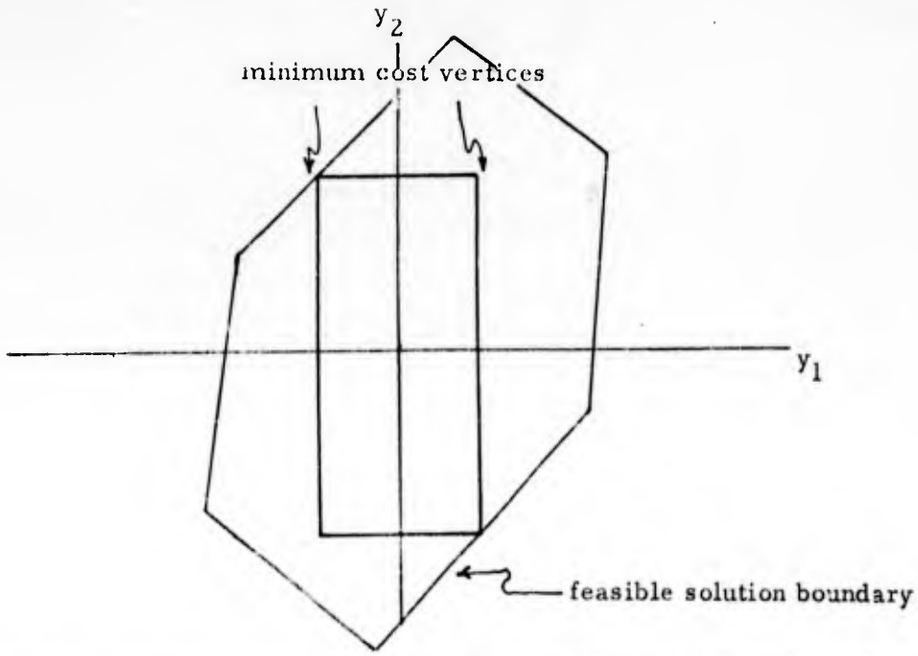

Fig. 5.9 Feasible solution boundary in parameter plane with symmetric constraints

intersects the boundary segment at

$$y_1 = \frac{b}{(a + k)}$$

$$y_2 = \frac{k\,b}{(a + k)} \qquad (5.66)$$

where a and k have the same sign (here assumed > 0).

Substitution of Eq. (5.66) into the cost equation gives

$$C = \frac{w_1}{|y_1|} + \frac{1}{|y_2|} = \frac{w_1(a + k)}{|b|} + \frac{(a + k)}{|b|} = \frac{(a + k)}{|b|}\,\frac{(k\,w_1 + 1)}{k} \qquad (5.67)$$

The cost equation as a function of the slope k is plotted in Fig. 5.10.

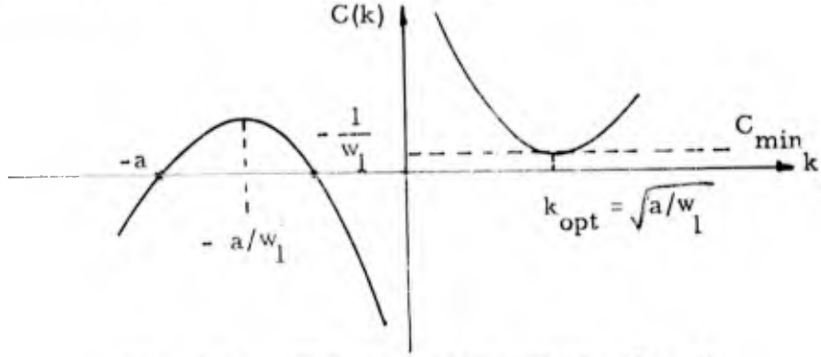

Fig. 5.10 Plot of cost function vs. slope k

Setting $\frac{\partial C(k)}{\partial k} = 0$ yields

$$k_{opt}^2 = \frac{a}{w_1} \tag{5.68}$$

Therefore,

$$\left.\begin{aligned} |y_1| &= \frac{|b|}{(a + k_{opt})} \\ |y_2| &= k_{opt}\ \frac{|b|}{(a + k_{opt})} \\ C_{min} &= \frac{(a + k_{opt})}{|b|}\ (w_1 + \frac{1}{k_{opt}}) \end{aligned}\right\} \tag{5.69}$$

As indicated in Fig. 5.10, k_{opt} is the geometric mean between the zeros of C(k) on the negative k axis. By these means, the two-parameter cost minimization problem has been reduced to one involving a single variable, k.

The procedure described is repeated along each of the straight-line segments which bound the area of feasible solution. A comparison of the minimum C's along each segment then specifies the optimum tolerances ($|y_1|$, $|y_2|$).

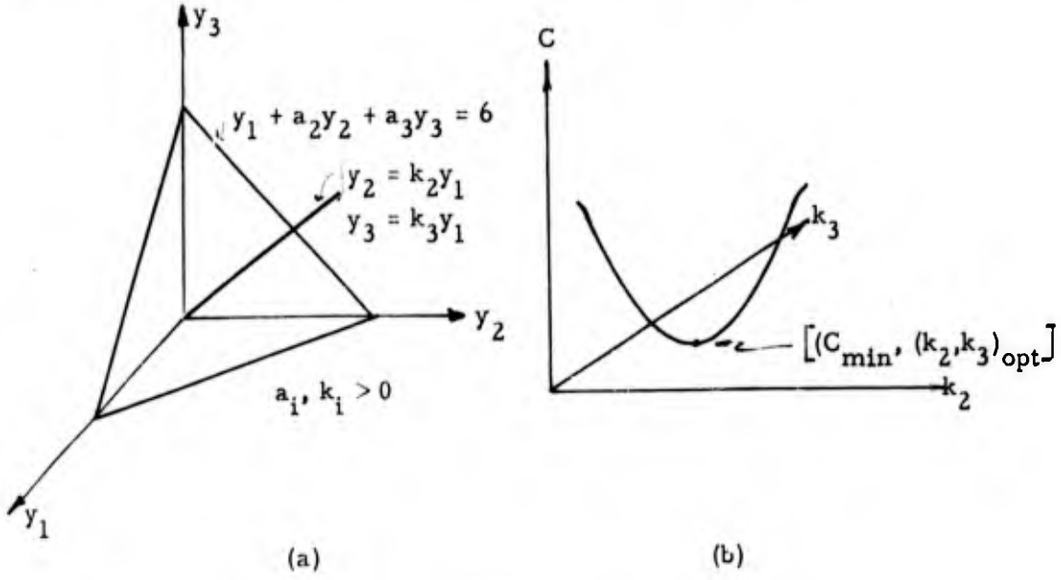

Fig. 5.11 Three-parameter minimization

For the three-parameter case, the boundaries are planes, and the cost equation is converted into a surface as indicated in Fig. 5.11. Four or more parameters give rise to hyperplane boundaries in parameter space and to a hypersurface cost function. The solution of the minimization problem in these instances requires use of surface-searching techniques.

From the discussions of this section, two criticisms of the whole procedure emerge:

(1) The formulation is of limited applicability since the accuracy of the pole-sensitivity approximations depends on "small" variations in all parameters. In most real situations, some one parameter is likely to vary over wide ranges, thereby violating the constraints of Eq. (5.63).

(2) The cost-minimization procedure does not yield a design method which reduces the undesired effects of a parameter's variations. Nevertheless, the techniques of this section can be used in conjunction with the design method (tailoring of components) mentioned briefly in Sec. 6.5 to view the multiparameter design problem in a new light.

In contrast to the objections raised above, the sensitivity function and the gain margins suggest design methods for systems whose parameters vary grossly. A detailed example of the design of such a system follows in Chap. VI.

Chapter VI - Use of the Sensitivity Function in Stabilization of Multiloop, Multiparameter System

In Chap. IV, the stability of the single-loop, unity-feedback system is examined from the standpoint of the sensitivity function. The parameter gain and phase margins for the forward-path gain are found to be identical to the conventional gain and phase margins of the servomechanism literature, and consequently compensation via tandem networks can evolve along familiar lines. The most significant and exciting aspect of the simple example, however, is that analysis via the sensitivity function suggests a general stabilization procedure which can be employed in more complex situations.

Our objective here is to indicate how the sensitivity function approach outlined in Sec. 4.2 can guide the design of compensation networks for multiloop, multiparameter systems. The particular case of a multiloop radar-tracking system is examined from the sensitivity standpoint and stabilized against the variations of two parameters. From this example, general conclusions regarding the scope and power of the method, and its inherent limitations are drawn.

6.1 Multiloop Radar-Tracking System

The example to be studied in detail in this chapter is the radar-tracking, signal recovery system* illustrated in the flow graph of Fig. 6.1.

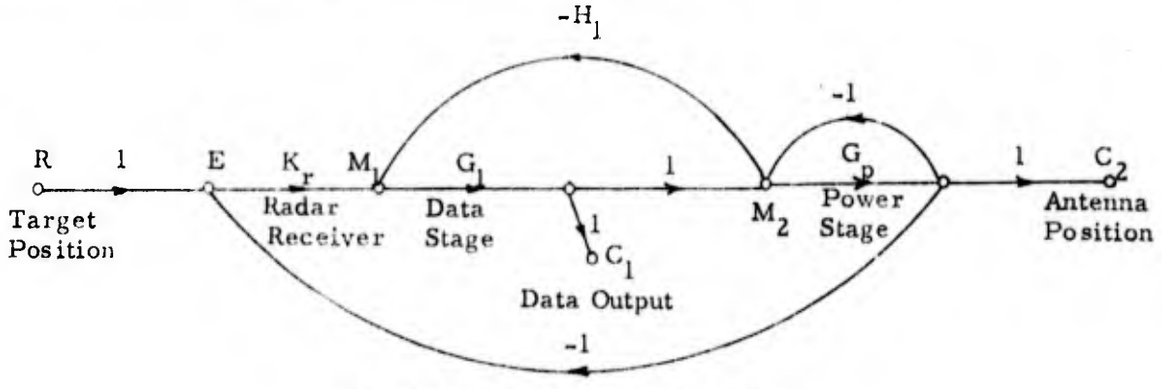

Fig. 6.1 Radar-tracking system

The primary objective of the tracking system is the recovery of the input signal R with as high an accuracy as possible -- that is to say, the desideratum, in this instance, is an accurate evaluation of the target position. Although the antenna position could provide an estimate of the target position, it need not be used if another

*Mishkin and Braun, op. cit., Chap. 4, pp. 111-115.

signal in the system can be found which more accurately approximates R. If such is the case, the actual position of the antenna is relevant only to the extent that the target must remain within the radar beam.

The system operates as follows. By lobe switching or other means, the antenna system detects the error E between the target angle R and the antenna position C_2; the radar receiver with effective gain K_r receives and demodulates E to provide an electrical signal M_1; G_1 represents a controller which processes M_1 to furnish the data output C_1; G_p, representing the power elements and load, is linearized by the negative-feedback minor loop around it, and is actuated by M_2, the difference between C_1 which is an estimate of R, and C_2, the antenna position; and H_1 is selected to be a model of K_r for reasons set forth below.

The point of view may be taken that the tracking system is inherently multiloop. The principal feedback path from C_2 to E exists by virtue of the nature of the antenna lobe switching, and the minor loop around G_p is needed to reduce the effects of nonlinearities in G_p and to improve the static and dynamic accuracy of the power stage as a whole. Furthermore, the signals R and E are not directly measureable; the data-recovery elements can only operate on the accessible signals M_1, M_2, C_1, and C_2.

If H_1 is chosen to be a model of K_r,

$$H_1 = K_r \tag{6.1}$$

the feedback signals from C_2 to M_1 along the (-1) ($-H_1$) path and along the (-1) (K_r) path cancel exactly. When this condition holds, M_1 has no component arising from C_2 and depends only on the input signal R. Consequently, the data output signal $C_1 = G_1 M_1$ yields a measure of the target position without " contamination" by C_2. Hence, when Eq. (6.1) is satisfied, the flow graph of Fig. 6.1 reduces to that of Fig. 6.2, an arrangement of two, tandem, non-touching feedback loops.

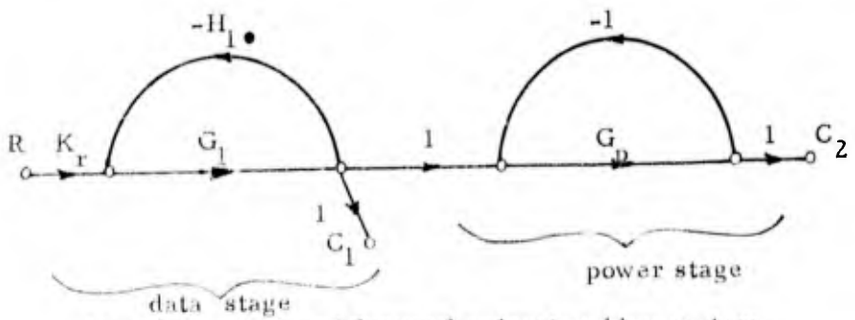

Fig. 6.2 Reduced form of radar-tracking system

The configuration of Fig. 6.2 can be verified by reference to Fig. 6.1. The data-stage and overall transmissions are defined as

$$\left.\begin{aligned} T_1 &= \frac{C_1}{R} = \frac{\sum_1}{\Delta} \\ T &= \frac{C_2}{R} = \frac{\sum}{\Delta} \end{aligned}\right\} \qquad (6.2)$$

The terms in Eq. (6.2), obtained by inspection of Fig. 6.1, are

$$\Delta = 1 + G_1H_1 + G_p + K_r G_1G_p \qquad (6.3)$$

and

$$\left.\begin{aligned} \sum_1 &= K_r G_1(1 + G_p) \\ \sum &= K_r G_1G_p \end{aligned}\right\} \qquad (6.4)$$

At the null setting, $H_1 = K_r$, the graph determinant is factored into

$$\Delta\Big|_{H_1 = K_r} = 1 + G_1H_1 + G_p + H_1G_1G_p = (1 + G_p)(1 + H_1G_1) \qquad (6.5)$$

and the transmissions are

$$\left.\begin{aligned} T_1\Big|_{H_1 = K_r} &= \frac{K_rG_1}{(1 + H_1G_1)} \\ T\Big|_{H_1 = K_r} &= \frac{K_rG_1}{(1+H_1G_1)} \frac{G_p}{(1+G_p)} = T_1 T_p \end{aligned}\right\} \qquad (6.6)$$

where T_p is the transmission of the power stage.

The form of Eq. (6.6) corroborates the reduced configuration of Fig. 6.2. The topological implication of the cancellation of feedback signals is the conversion of a system with three touching loops (of index one) into one with two non-touching loops (of index two). The analytical significance of this reduction is that the transmissions T_1 and T_p can be treated independently in the formulation of design criteria and in

stability studies despite extreme variations in G_1 and G_2 -- so long as Eq. (6.1) is satisfied. Unfortunately, the receiver gain K_r is known to vary widely with signal level, thereby upsetting the balance of Eq. (6.1) and invalidating the reductions. Moreover, any attempt to measure K_r while the system is in operation is almost futile since the signal E is not accessible. This limitation frustrates any effort to have H_1 adaptively track K_r. Consequently, the original flow graph of Fig. 6.1 and Eqs. (6.3) and (6.4) must be employed whenever variations in K_r or H_i invalidate Eq. (6.1).

For the basic configuration of Fig. 6.1, the plant elements are assumed to have a third-order transfer function of the form

$$G_p = \frac{K_p}{s(s+b)(s+c)} \tag{6.7}$$

with nominal values*

$$\left.\begin{aligned} K_p &= 538 \\ b &= 5 \\ c &= 20 \end{aligned}\right\} \tag{6.8}$$

At these values, the power-stage transmission is

$$T_p = \frac{G_p}{1+G_p} = \frac{538}{(s+21.5)(s^2+3.5s+25)} \tag{6.9}$$

The corresponding velocity constant for the power stage is

$$K_v = \lim_{s \to 0} s\,G_p(s) = \frac{K_p}{bc} = 5.38 \tag{6.10}$$

The velocity constant, as defined above, plays a slightly different role compared with that for a conventional servo system. In the single-loop, unity-feedback system, the process actuating signal is exactly the error between the input R and the output C. In our system, the actuating signal is M_2, the error between the data output C_1, and the antenna output C_2. If C_1 is a "reasonable" reproduction of R (as is required in our system), M_2 is approximately the difference between the target and antenna positions,

*The transfer functions and values used in this chapter are chosen primarily for convenience.

and K_v is a good measure of the follow-up capability or accuracy of the antenna controls. For comparable performance, the velocity constant for the multiloop system of Fig. 6.1 consequently would be somewhat larger than that required for the prototype single-loop configuration. Since the accuracy of the antenna position is only a secondary consideration in a data-recovery system, K_v need only be large enough to keep the target within range of the radar beam.*

At the null setting, C_1 is related to R by Eq. (6.6). If G_1 is chosen to be a constant gain K_1, the data output is directly proportional to the target position, and the system of Fig. 6.2 reduces to that of Fig. 6.3.

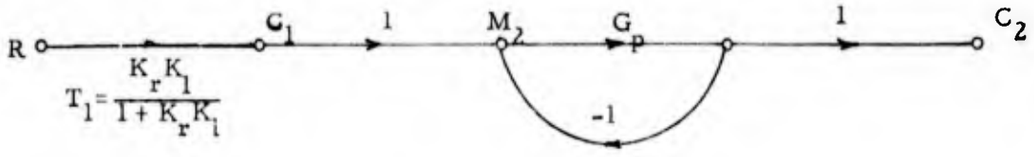

Fig. 6.3 Reduced system for G_1 = constant

The proportionality of c_1 to r is not necessarily a desirable characteristic as demonstrated by the following argument. Even if $K_r K_1$ is made large, there is, nevertheless, a small but non-zero error between c_1 and r. If r(t) is a unit ramp, c_1 has a slope $a = K_r K_1 / 1 + K_1 K_r < 1$, and c_2 has a slope less than unity, resulting in an infinite steady-state positional error between r and c_2. To avoid this pitfall, G_1 should have at least one integration. But, more importantly, T_1 is required to be essentially a low-pass filter in order to reduce the level of wide-band noise which contaminates R. For the system at hand, the data-stage bandwidth is to be about 1.5 cps. or roughly 9.4 radians per second (rps).** Therefore, G_1 is selected to be

$$G_1(s) = \frac{K_1}{s(s + a)} \tag{6.11}$$

The nominal gain of the radar receiver is

$$K_r = 22.5 \tag{6.12}$$

---

*Nonlinearities, such as static friction, are neglected in these considerations.

**This value for the required bandwidth is actually quite low.

Suitable values for H_1, K_1, and $\underline{a}$ which satisfy the null condition of Eq. (6.1) and the bandwidth requirement are

$$\left.\begin{aligned} H_1 &= 22.5 \\ K_1 &= 1.88 \\ a &= 5.2 \end{aligned}\right\} \qquad (6.13)$$

Hence, the data-stage transmission is

$$T_1(s) = \frac{K_r G_1}{1 + H_1 G_1} = \frac{(6.5)^2}{s^2 + 5.2\, s + (6.5)^2} \qquad (6.14)$$

The pole-zero patterns for the transmissions T_1, T_p, and T at nominal settings of all parameters are shown in Fig. 6.4 and the gain and phase plots are given in Figs. (6.5) and (6.6). These plots provide the data for the stability analysis and the stabilization schemes which are presented in the following two sections.

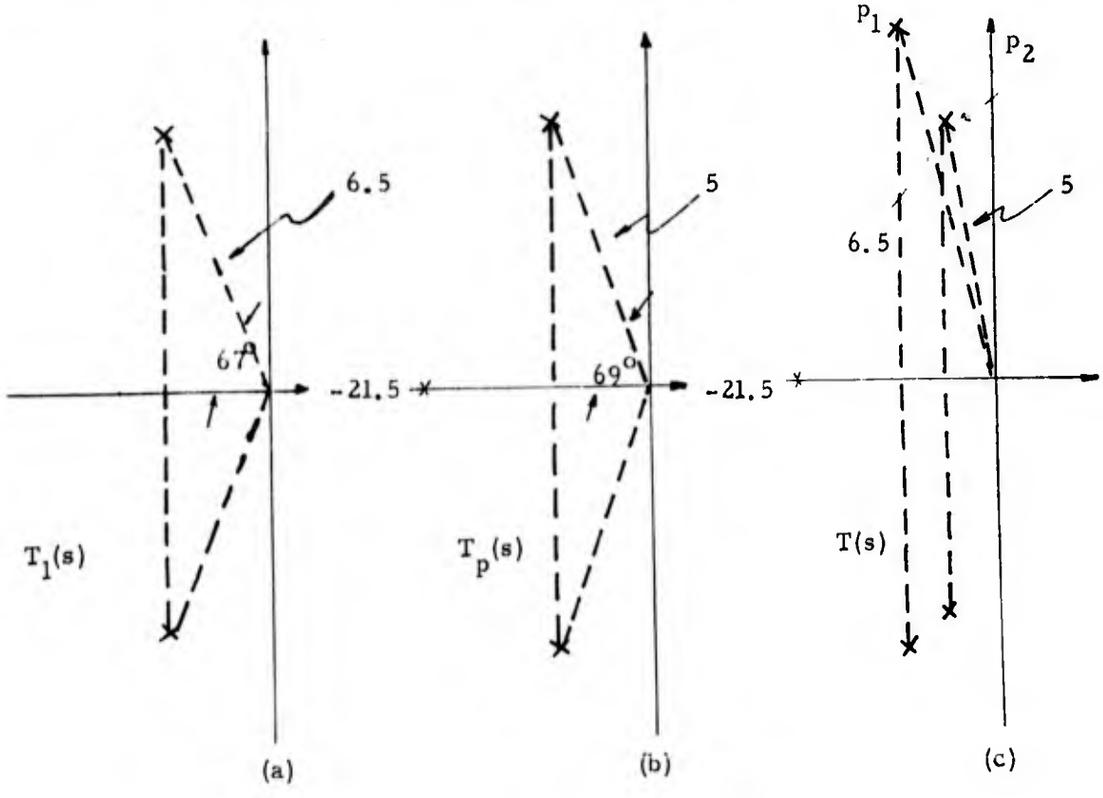

Fig. 6.4 Pole-zero plots

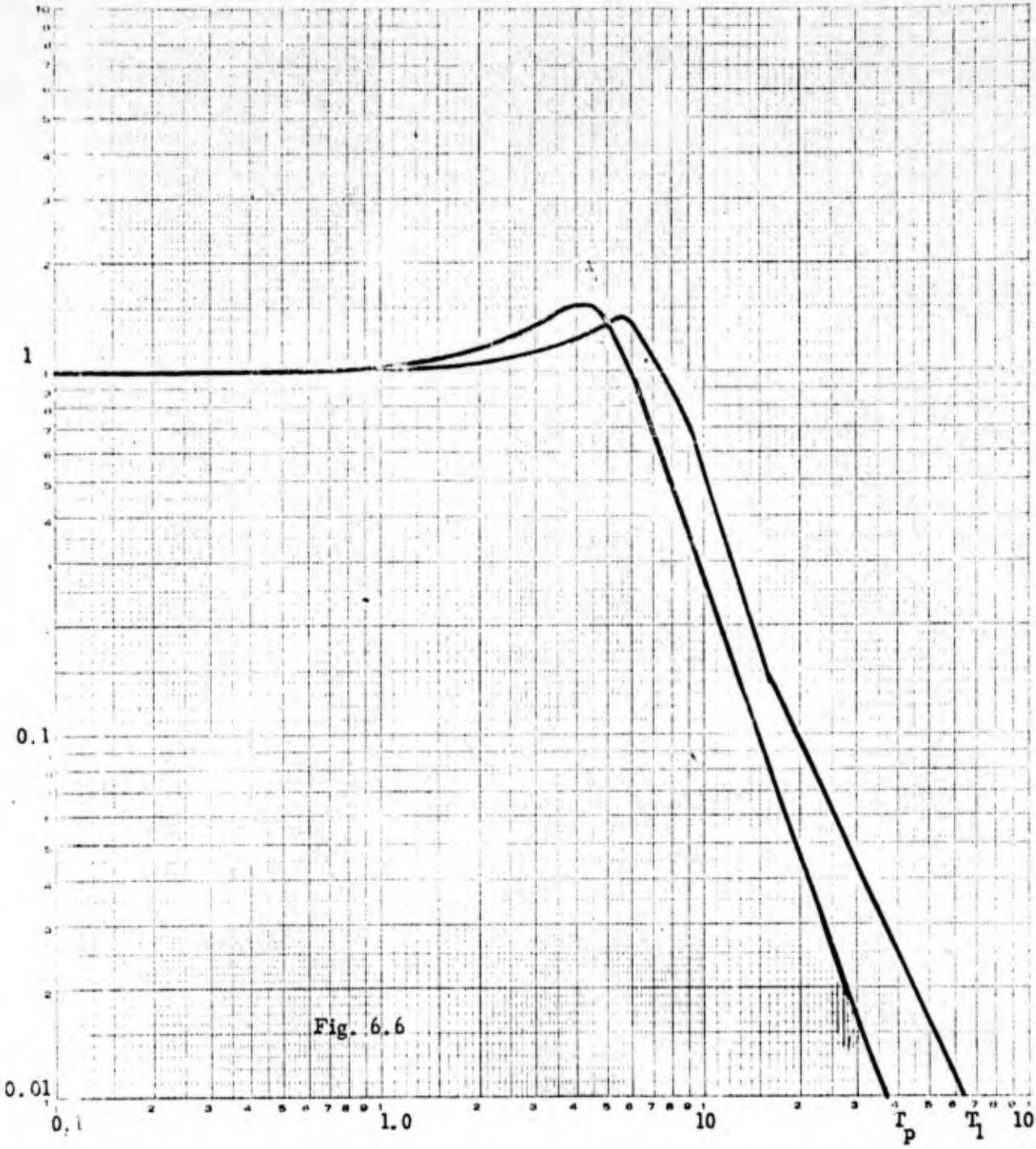

Fig. 6.6

Fig. 6.6. Magnitude characteristics.

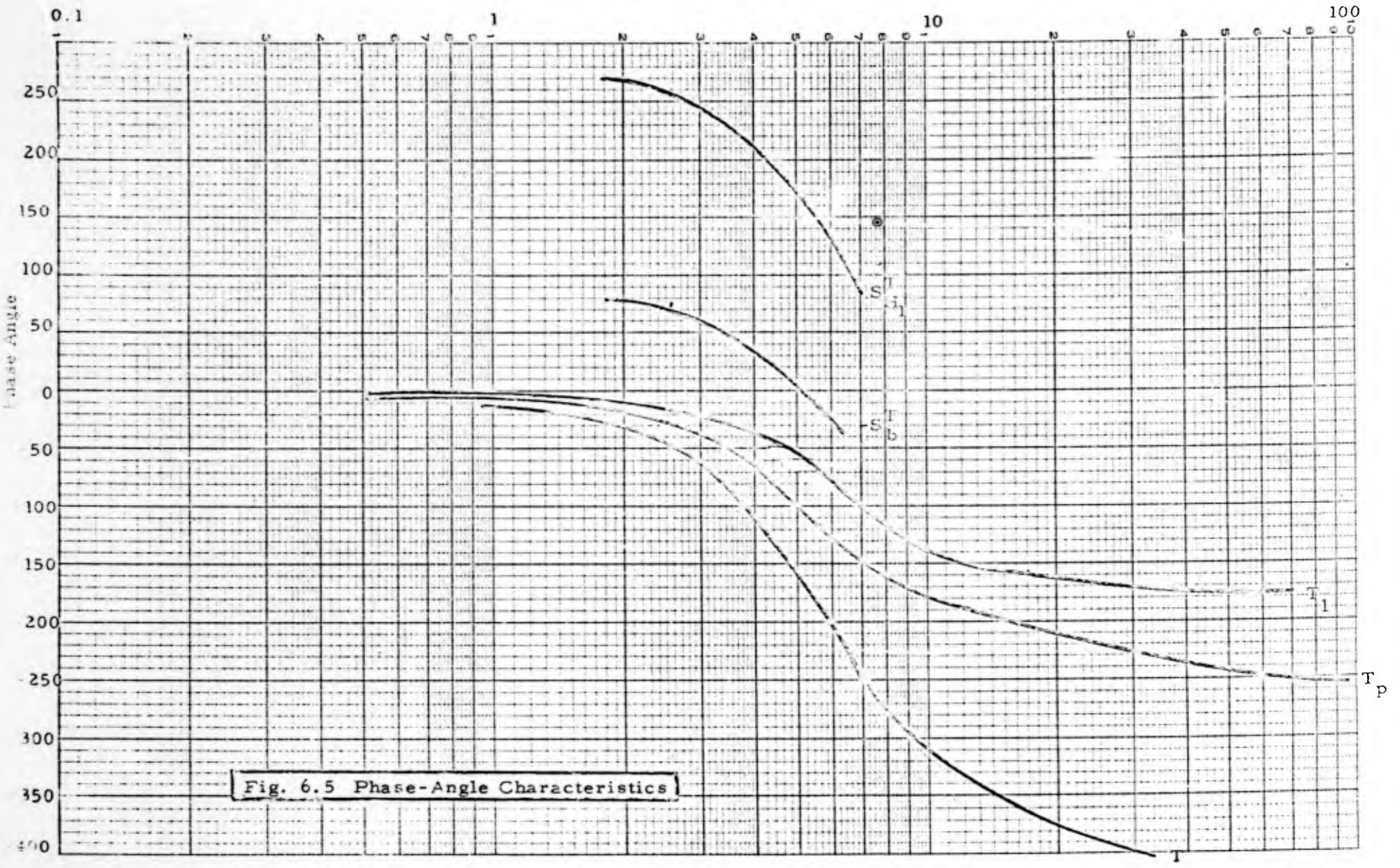

Fig. 6.5 Phase-Angle Characteristics

6.2 Stability Analysis

Our purpose here is to investigate the destabilizing effects of parameter variations. There are a total of seven system parameters, K_r, H_1, K_1, a, K_p, b, and c. Two of them, K_r and K_p, are expected to vary over wide ranges; b and c, the poles of the process, over a much smaller range; and K_1, a, and H_1 only over incremental bands. Since the feedback cancellation depends only on the $H_1 = K_r$ condition and no other, variations in K_1, K_p, a, b, and c can be studied with reference to the reduced configuration of Fig. 6.2.

The root-loci for the latter set of parameters involve only second and third-order polynomials and can be sketched with ease. On the other hand, the loci for H_1 and K_r, involving fifth-order polynomials, are much more formidable. In the preliminary study, these loci were sketched with the aid of a spirule in order to provide a cross-check against the results obtained by the sensitivity method and to afford the analyst an additional degree of circumspection in comprehending the effects of the variations. The loci are not presented here in order to avoid needless immersion in details which are outside the main stream of thought centered about the real-frequency characterization.

The analysis* via the sensitivity method is initiated by computing $S^T_{K_r}$, $S^T_{H_1}$, etc.

$$S^T_{K_r} = \frac{\Delta^o_{K_r}}{\Delta} = S^T_{K_r} = 1 - \frac{K_r \Delta_{K_r}}{\Delta} = 1 - T \tag{6.15}$$

The change in K_r to cause instability is then

$$\left.\begin{aligned} \frac{\delta_{K_r}}{(K_r)_o} &= \frac{1}{S^T_{K_r} - 1} = -\frac{1}{T} \\ \text{and} \\ \frac{(K_r)_{cr}}{(K_r)_o} &= 1 + \frac{\delta_{K_r}}{(K_r)_o} = 1 - \frac{1}{T} \end{aligned}\right\} \tag{6.16}$$

---

*The reader, not intently concerned with the details of the calculations, may skim lightly over the next few pages, and find the results of the stability analysis summarized in Table 6.1.

From the phase-angle and magnitude plots for T_1 and T_p in Figs. 6.5 and 6.6, $T(j\omega)$ is observed to be real at three frequencies:

(1) At $\omega = o$, $T(o)$ is unity, and $\delta_{K_r}/(K_r)_o = -1$, or $(K_r)_{cr} = 0$. This condition on K_r corresponds to a system pole crossing the $j\omega$ axis at the origin. The root locus reveals an origin pole which crosses into the right-half plane if K_r takes on a negative increment from a zero level.

(2) At $\omega \cong 5.4$, $\angle T(j\omega) = -180^\circ$, with $\angle T_1 = -65^\circ$, and $\angle T_p = -115^\circ$. Since $|T(j\,5.4)| = |T_1(j\,5.4)|\,|T_p(j\,5.4)| = (1.4)(1.27) = 1.78$, the critical value of K_r is $(K_r)_{cr}/(K_r)_o = 1 + 1/(1.78) = 1.56$, or $(K_r)_{cr} = 35.2$.

(3) At $\omega \cong 15.5$, $\angle T = -360^\circ$, with $\angle T_1 = -157^\circ$ and $\angle T_p = -203^\circ$. From Fig. 6.6, $|T(j\,15.5)| = (0.16)(0.09) = 0.0144$. Consequently, $(K_r)_{cr}/(K_r)_o = 1 - 69.5 = -68.5$, or $(K_r)_{cr} = -1540$; this corresponds to the negative feedback case.

If K_r is restricted to positive values, only the second of the three cases is pertinent. The other sensitivities are:

$$S^{T}_{K_p} = \frac{\Delta^{o}_{K_p}}{\Delta} = \frac{(1 + G_1H_1)}{\Delta} = \frac{1}{(1 + G_p)} = \frac{T_p}{G_p} \tag{6.17}$$

A simpler expression is obtained if T_1 is written as

$$\left.\begin{aligned} T_1 &= \frac{K_r G_1}{\Delta} + \frac{K_r G_1 G_p}{\Delta} \\ &= T_\alpha + T_\beta \end{aligned}\right\} \tag{6.18}$$

so that $F'_{K_p} = 1$ with respect to T_α, and $F'_{K_p} = \infty$ with respect to T_β. Hence

$$S^{T_\alpha}_{K_p} = \frac{\Delta^{o}_{K_p}}{\Delta} - 1 = \frac{(1 + G_1H_1)}{(1 + G_p)(1 + G_1H_1)} - 1 = -\frac{G_p}{(1 + G_p)} = -T_p \tag{6.19}$$

The form of Eq. (6.19) is preferable to that of Eq. (6.17) since the stability margins can be obtained directly from the T_p plots. Of course, both equations yield the same margin on K_p as evidenced by

$$\left.\begin{aligned}\frac{(K_p)_{cr}}{(K_p)_o} &= 1 + \frac{1}{S^T_{K_p} - 1} = 1 + \frac{1}{\frac{1}{(1+G_p)} - 1} = \frac{-1}{G_p} \\ &= 1 + \frac{1}{S^{T_a}_{K_p}} = 1 + \frac{1}{\frac{-G_p}{(1+G_p)}} = -\frac{1}{G_p}\end{aligned}\right\} \quad (6.20)$$

The result expressed in Eq. (6.20) could have been anticipated at the outset, since, at the null condition, [Eq. (6.1)], variations in K_p affect only the stability of the power stage, a single-loop, unity-feedback system.

Continuing in this fashion, we find

$$S^T_{H_1} = S^{T_1}_{H_1} = \frac{\Delta^o_{H_1}}{\Delta} - 1$$

$$= -\frac{H_1}{K_r G_p}\Bigg|_{\substack{T \\ H_1 = K_r}} = -\frac{T}{G_p} \quad (6.21)$$

Also,

$$S^T_{K_1} = S^{T_1}_{K_1} = \frac{(1+G_p)}{\Delta} = \frac{1}{(1+G_1H_1)} \quad (6.22)$$

$$\left.\begin{aligned}S^T_a &= S^{G_1}_a S^T_{G_1} = \frac{-a}{(s+a)} \frac{1}{(1+G_1H_1)} = -\frac{a\,s}{K_1H_1} \quad T_1 \\ K_1H_1 &= (6.5)^2\end{aligned}\right\} \quad (6.23)$$

The flow graph is manipulated into the form shown in Fig. 6.7 to display $\underline{a}$ as a simple branch gain. There, it is recognized that $\sum^o_a / \sum = 1$ and the appropriate margin is

$$\frac{\delta_a}{(a)_o} = \frac{1}{S^T_a} \quad (6.24)$$

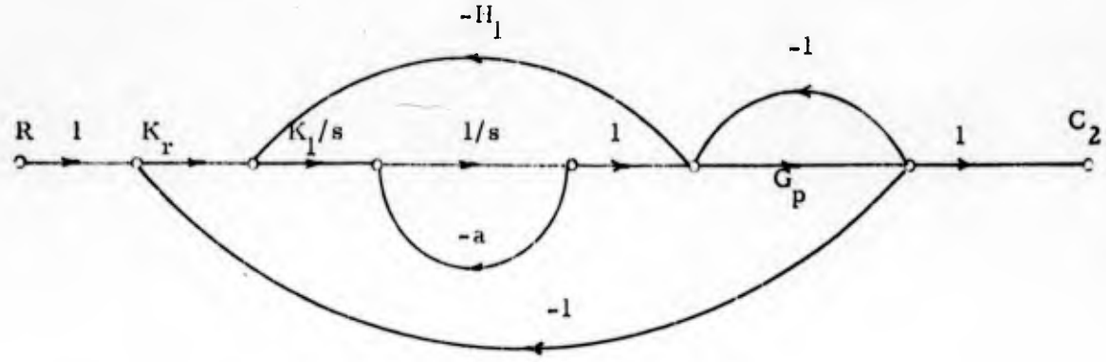

Fig. 6.7 Signal-flow graph with a as a branch transmittance

Similarly,

$$S_b^T = S_b^{G_p} S_{G_p}^T = \frac{-b}{(s+b)} \frac{T_p}{G_p} = \frac{-5\,s(s+20)}{(538)}\, T_p \tag{6.25}$$

A simple flow-graph manipulation reveals $F_b' = 1$ so that

$$\frac{\delta_b}{(b)_o} = \frac{1}{S_b^T} \tag{6.26}$$

The various gain margins are now obtained from an examination of Figs. 6.5 and 6.6 in light of Eqs. (6.16) through (6.26). The margin on K_p is obtained by noting that $\angle T_p = 180^\circ$ at $\omega = 10$, and then by computing the gain margin via Eq. (6.19). Similarly, from Eq. (6.23), $(a)_{cr}$ is found by observing the frequency at which $\angle T_1 = \pm 90^\circ$. On the other hand, $(H_1)_{cr}$ and $(b)_{cr}$ require auxiliary phase plots as indicated by the forms of Eqs. (6.21) and (6.25). These supplementary plots are also shown at the top of Fig. 6.5. For example, $\angle -S_b^T = \left[90^\circ + \angle(j\omega + 20) + \angle T_p\right]$ is sketched by adding $\angle(j\omega + 20)$ to $(90^\circ + \angle T_p)$, and is found to be real (0°) at $\omega \cong 5.1$. The magnitude of S_b^T at this frequency is $|T_p(j\,5.1)|$, [found in Fig. 6.6], multiplied by $(5)(5.1)\,|j\,5.1 + 20|/(538)$. Hence, from Eq. (6.26)

$$\left.\begin{aligned} \frac{\delta_b}{(b)_o} &= -\frac{1}{(1.35)} \frac{538}{(5)(5.1)\,20\sqrt{1 + (5.1/20)^2}} = -0.757 \\ \frac{(b)_{cr}}{(b)_o} &= 1 - 0.757 = 0.243 \\ b_{cr} &= (0.243)(5) = 1.22 \end{aligned}\right\} \tag{6.27}$$

The gain margins and crossover frequencies determined in this manner are listed in Table 6. 1 below. The margins with respect to H_1, a, K_1, and b are comfortably large enough so that incremental variations in these parameters do not cause instability. The most notable aspect of Table 6. 1 is that the smallest gain margin is associated with K_r, the most sensitive element in the system. A method of increasing this margin is the subject of the following section.

Parameter	Nominal Value	Critical Value	Gain Margin	Oscillation Freq.
K_r	22. 5	34. 4	3. 7 db	5. 3
H_1	22. 5	12. 6	-5. 0 db	4. 9
K_p	538	2500	13. 4 db	10. 0
K_1	1. 88	always stable	∞	---
a	5. 2	0	$-\infty$	6. 5
b	5. 0	1. 25	-12 db	5. 0

Table 6. 1 Tabulation of parameter gain margins

The pole sensitivities, and, in particular, the damping sensitivities, provide an alternate -- but not conclusive -- indication of stability for parameters with small variations. Calculation of various pole sensitivities amounts to determination of the residues of the appropriate sensitivity functions, and can be performed graphically on the pole-zero patterns with the aid of a spirule. These sensitivities are summarized in Table 6. 2, and a sample calculation is given in Appendix D. The values obtained for the incrementally varying parameters are not unduly large enough to cause any alarm.

Parameter x	$Q_x^{p_1}$	$S_x^{h_1}$	$S_x^{\rho_1}$	$Q_x^{p_2}$	$S_x^{h_2}$	$S_x^{\rho_2}$
K_r	$5.8\angle -148^\circ$	2.0	-0.14	$7.2\angle 46^\circ$	-3.45	0.63
H_1	$8\angle 55^\circ$	-2.4	0.650	$7.2\angle 225^\circ$	3.5	-0.6
K_p	0	0	0	$2.8\angle 75^\circ$	-0.85	0.46
K_1	$3.4\angle 90^\circ$	-0.46	0.48	0	0	0
a	$-27\angle 23^\circ$	1	0	0	0	0
b	0	0	0	$-2.5\angle 20^\circ$	1.3	0

Table 6.2 Tabulation of pole, radial, and damping sensitivities

6.3 Compensation of the Radar-Tracking System

In the preceding section, it is shown that the gain margin with respect to K_r is 3.7 db, the smallest among all the parameter margins. Since the expected variation of K_r is $\pm$ 9 db,* the system becomes unstable as the signal level varies over wide ranges. Our design objective is to increase the K_r gain margin while maintaining the margins with respect to the other parameters at "reasonable" values -- i.e., all the parameter gain margins should be large enough so that no single variation over its maximum expected range can cause instability. Our attention is focussed primarily on K_r, the most sensitive element in the system, and, to a lesser extent, on K_p with an expected variation of $\pm$ 6 db from its nominal setting. The problem may be stated as: given the constraint of the process, the bandwidth of the data stage, and the general data-recovery and target-tracking objectives mentioned in Sec. 6.1 -- to design the system so that it remains stable despite variations in parameters separately, where the maximum variations are known a priori.

The expected $\pm$ 9 db change in K_r from its nominal value is translated into a range of variation of

$$\frac{1}{2.8} \leq \frac{K_r}{(K_r)_o} \leq 2.8 \tag{6.28}$$

or

$$-0.65 \leq \frac{\delta}{(K_r)} \leq 1.8 \tag{6.29}$$

where

$$K_r = (K_r)_o$$

*This value is deliberately chosen pessimistically. A more realistic variation is about $\pm$ 3 db.

To insure the system stability, $\delta_{cr}/(K_r)_o$ must fall outside the band of variation of Eq. (6.29). Hence, the design calls for

$$\left.\begin{aligned} \frac{\delta_{cr}}{(K_r)_o} &> 1.8 \\ \frac{\delta_{cr}}{(K_r)_o} &< -0.65 \end{aligned}\right\} \qquad (6.30)$$

The sensitivity function with respect to K_r affords a specific translation of the requirements of Eq. (6.30) into frequency specifications for the system transfer functions. From the analysis in Sec. 6.2,

$$S^T_{K_r} = 1 - T_1 T_p = 1 - T \qquad (6.31)$$

and

$$\frac{\delta_{cr}}{(K_r)_o} = \frac{1}{S^T_{K_r} - 1} = -\frac{1}{T} \qquad (6.32)$$

The two cases for which $S^T_{K_r}$ (or T) is real are:

(a) $\angle T = 180^\circ, 540^\circ$, etc. Then $T = -|T|$. Combining Eqs. (6.30) and (6.32) yields

$$\frac{\delta_{cr}}{(K_r)_o} = \frac{1}{|T|} > 1.8 \qquad (6.33)$$

or

$$\left.\begin{aligned} |T| &< \frac{1}{1.8} = 0.55 \\ |T|_{db} &< -5 \text{ db} \end{aligned}\right\} \qquad (6.34)$$

(b) $\angle T = 0^\circ, 360^\circ$, etc. Then $T = |T|$, and the stability margin must be

$$\frac{\delta_{cr}}{(K_r)_o} = -\frac{1}{|T|} < -0.65 \qquad (6.35)$$

or

$$\left.\begin{aligned} |T| &< \frac{1}{0.65} = 1.55 \\ |T|_{db} &< 3.8 \text{ db} \end{aligned}\right\} \qquad (6.36)$$

Now usually $\angle T = 0^\circ$ at $\omega = o$. Hence, Eq. (6.36) states that the d-c gain must be less than 3.8 db. But $T(0) = 1$ is a necessary condition on any servo system which maintains a zero steady-state error to a step input. Consequently, there is no real limitation here. If T has an asymptotic order of 5 or more, at some $\omega > o$, $\angle T$ goes through 360°. At this frequency, the design must insure that $|T| < 3.8$ db. But Eq. (6.34) demands that $|T|$ be less than -5 db, when $\angle T = 180^\circ$. If this condition is satisfied it is very likely that $|T|$ is less than +3.8 db when $\angle T = 360^\circ$. Therefore, the design requirement is to bring $|T|$ below -5db when the phase is 180°.

By a similar line of reasoning, the $\pm$ 6 db gain margin on K_p implies that

whenever

$$\left.\begin{aligned} |G_p| &< -6 \text{ db} \\ \angle G_p &= 180^\circ \end{aligned}\right\} \qquad (6.37)$$

Our first attempt at satisfying Eq. (6.34) involves a modification of the data-stage transmission T_1. Since $T = T_1 T_p$, some improvement can be obtained if the frequency peak in T_1 is reduced. Reduction of ζ and maintenance of the same bandwidth, $\omega_B = 9$ rps, can be achieved if the pole at -a is moved out along the negative real axis. ζ is chosen to be 0.6 which gives a flat frequency response and an 8 percent overshoot to a step input. Suitable forms for G_1 and T_1 are:

$$\left.\begin{aligned} G_1 &= \frac{K_1}{s(s+a)} = \frac{2.66}{s(s+9.3)} \\ T_1 &= \frac{K_r G_1}{1 + H_1 G_1} = \frac{(7.75)^2}{s^2 + 9.3s + (7.75)^2} \end{aligned}\right\} \qquad (6.38)$$

and

$$\left.\begin{aligned} K_r &= H_1 = 22.5, \text{ as before} \\ \omega_n^2 &= K_1 K_r = (7.75)^2 = 60 \end{aligned}\right\}$$

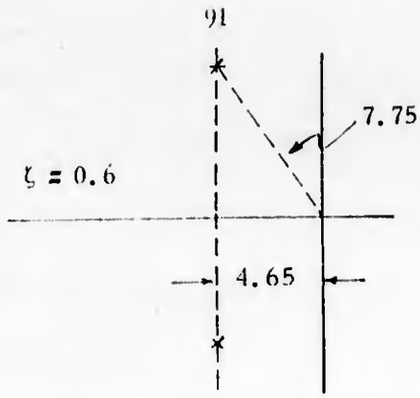

Fig. 6.8 Pole-zero pattern for modified data-stage transmission

The closed-loop pole positions for $T_1(s)$ are indicated in Fig. 6.8, while the gain and phase plots for $T_1(j\omega)$ are drawn in Figs. 6.9 and 6.10. Examination of the phase-angle plots of T_p in Fig. 6.5 and of T_1 in Fig. 6.10 reveals that $T = 180^\circ$ at $\omega = 5.5$, with $T_1 = -60^\circ$, and $T_p = -120^\circ$. From Figs. 6.6 and 6.9 the magnitudes of T_p and T_1 are found to be $|T_p| = 1.2$, and $|T_1| = 1$. The gain margin is

$$\left.\begin{aligned} &\frac{(K_r)_{cr}}{(K_r)_o} = 1 + \frac{1}{|T|} = 1.84 \\ &\text{or} \\ &(GM)_{K_r} = 5.3 \text{ db} \end{aligned}\right\} \qquad (6.39)$$

Although the modification of T_1 increases the gain margin, it still falls short of the required 9 db margin. A close inspection of Figs. 6.9 and 6.10 shows that T_1 falls off rapidly at approximately -40 db/decade for $\omega > 6.5$, and the phase of T_1 only asymptotically approaches -180°. If T_p is altered by adding positive phase shift in the frequency range $\omega > 5$, the crossover frequency can be made to occur at a point where $|T_1|$ is small. For example, at $\omega = 10$, $|T_1| = 0.57$ and $\angle T_1 = -115^\circ$. If $\angle T_p(j\,10) = -65^\circ$ and $|T_p(j\,10)| = 1$, $\angle T = -180^\circ$ and $|T| = 0.57$ which just about satisfies the stability margin on K_r.

The modification of the characteristics of T_p must be effected within the framework of the given configuration, or else a different sensitivity relationship might result. Consequently, a tandem compensation network $G_c(s)$ is placed within the power stage as shown in Fig. 6.11. The various relationships derived previously carry over intact in this new configuration except that $G'_p = G_c G_p$ is substituted for G_p.

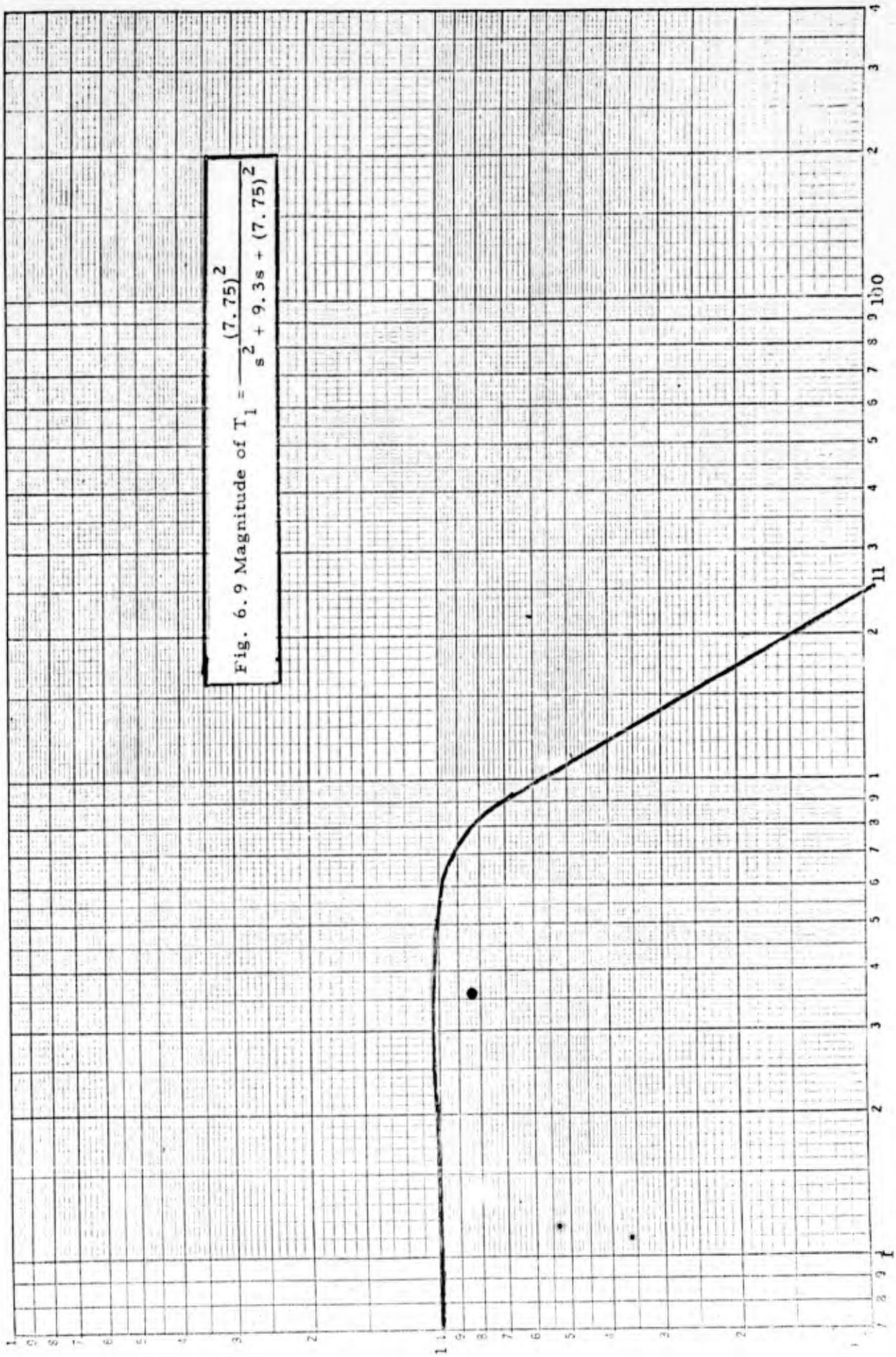

Fig. 6.9 Magnitude of $T_1 = \frac{(7.75)^2}{s^2 + 9.3s + (7.75)^2}$

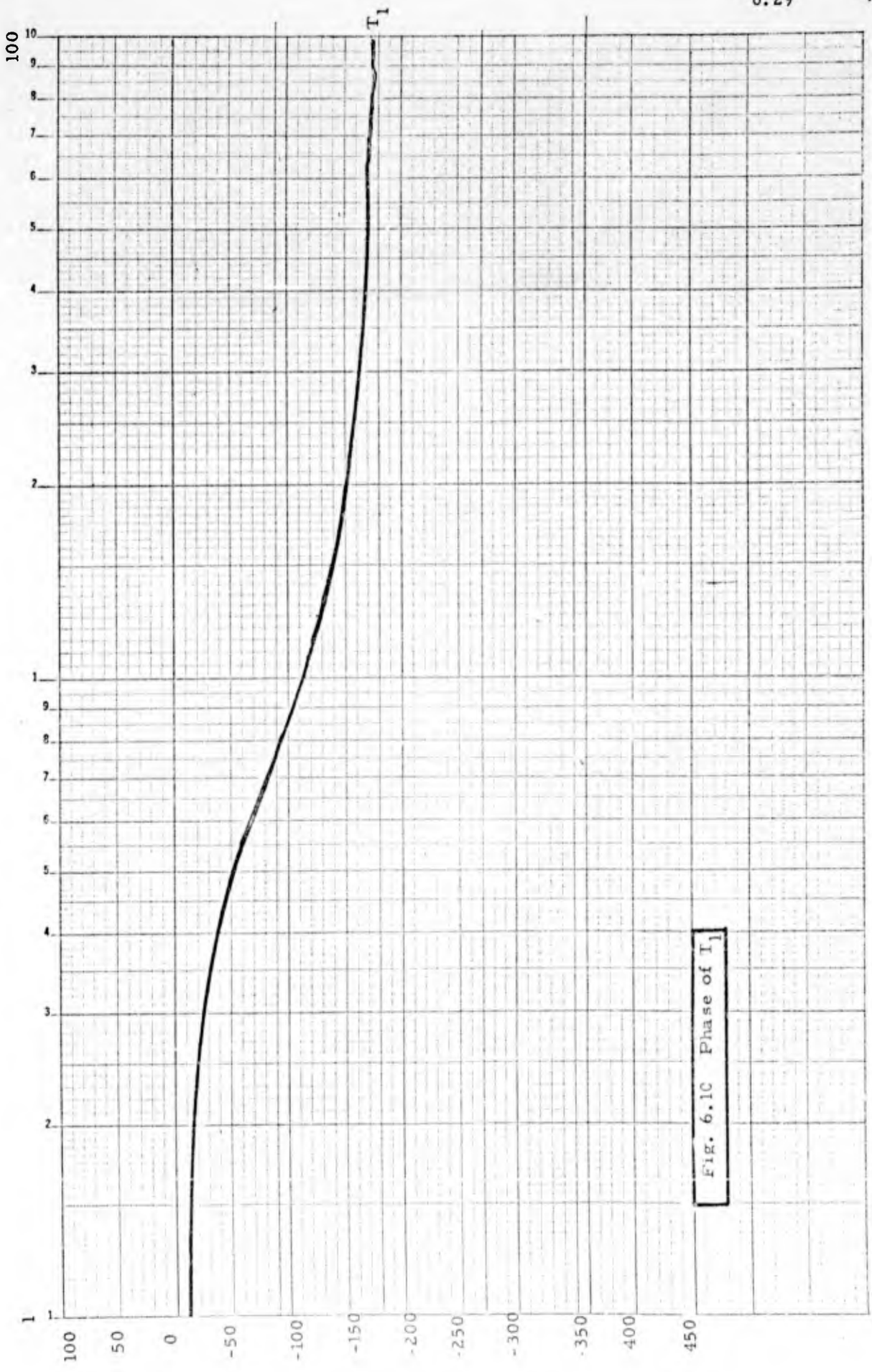

Fig. 6.1C Phase of T_1

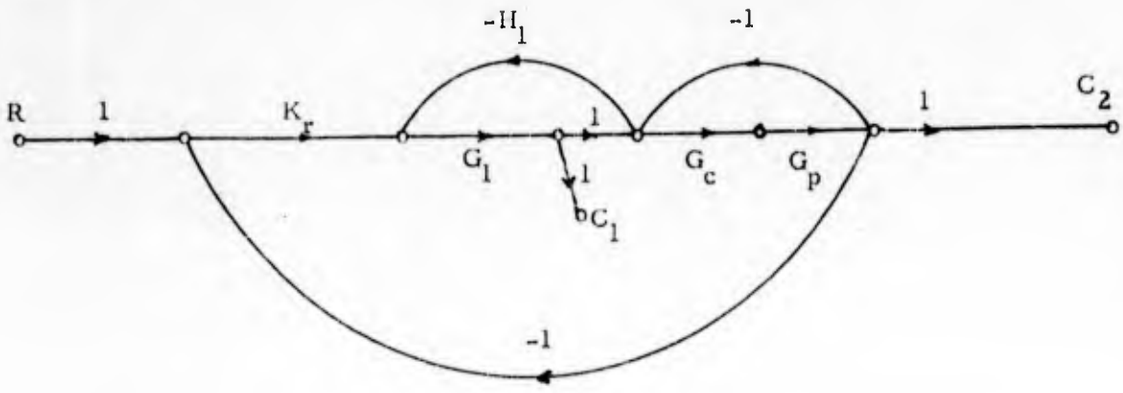

Fig. 6.11 Radar-tracking system with power-stage compensation

A straightforward design procedure involving four steps can be formulated, at least in principle.

(1) The magnitude and phase characteristics for $T_p(j\omega)$ are chosen to yield the appropriate gain margin on K_p; additionally, in conjunction with the given gain-phase plot for $T_1(j\omega)$ of Figs. 6.9 and 6.10, $T_p(j\omega)$ is selected to produce the prescribed gain-margin for K_r. In this sense, the designer picks the crossover frequencies ω_{K_p} and ω_{K_r}. $T_p(j\omega)$ need only be specified at ω_{K_p} and ω_{K_r}, corresponding to crossover of K_p and K_r. But generally, a "well-behaved" $T_p(j\omega)$ would be sketched in the frequency band of interest.

(2) With $T_p(j\omega)$ specified, $G'_p(j\omega)$ can be obtained via the Nichol's Chart; the corresponding Bode plots are sketched.

(3) The frequency characterization of the required compensation $G_c(j\omega)$ is obtained by subtracting the known $G_p(j\omega)$ from $G'_p(j\omega)$ on the log-magnitude and phase-angle plots.

(4) $G_c(j\omega)$ is then approximated by a rational fraction and synthesized by network methods (hopefully!).

A primary drawback of this approach is that the resulting $G_c(j\omega)$ may be either too complex or physically unrealizable. Furthermore, the effect of the compensation on the transient response, the steady-state accuracy, etc., is not evident. As was mentioned at the outset of this chapter, all we expect from the sensitivity functions is a guide to a rational design procedure -- not a complete synthesis technique. For these reasons conventional compensation methods, which are known to be realizable, are employed in shaping the frequency characteristics of $T_p(j\omega)$.

If the crossover frequency, ω_{K_r} is to be increased from its original value of 5.5 rps., T_p must have more positive phase shift in the frequency band about $\omega = 5.5$. Since the asymptotic order of T_p can only be increased or left the same by any realizable compensation network, it appears that the positive phase requirement would imply an increase in the bandwidth of T_p. These considerations suggest that a lead network be tried as $G_c(s)$. In order to simplify calculations, the zero of $G_c(s)$ is picked to cancel the pole of $G_p(s)$ at -5, and a one-decade separation is arbitrarily chosen to separate the pole and zero of $G_c(s)$. Thus,

$$G_c(s) = K \frac{(s+5)}{(s+50)} \tag{6.40}$$

so that

$$G'_p(s) = \frac{KK_p}{s(s+20)(s+50)} = \frac{K'_p}{s(s+20)(s+50)}$$

$$= \frac{K_v}{s\left(\frac{s}{20}+1\right)\left(\frac{s}{50}+1\right)} \tag{6.41}$$

where

$$K_v = \frac{K'_p}{1000} = \frac{538K}{1000} \tag{6.42}$$

From the Routh test or the root locus, the critical value of K_v or K'_p is found to be

$$K'_p = 70,000$$

$$K_v = 70 \tag{6.43}$$

at a frequency $\omega'_{K_p} = \sqrt{1000} = 31.6$

Next, the gain-phase characteristics of $G'_p(s)$ are sketched versus frequency in Fig. 6.12, and on the Nichol's Chart of Fig. 6.13 for $K_v = 10$, 15, and 20. From the latter, the closed-loop response T_p is determined and drawn in Fig. 6.14. Superimposed on these phase characteristics is the plot of $T_1(j\omega)$ of Fig. 6.10. From Fig. 6.14, we find for $K_v = 10$,

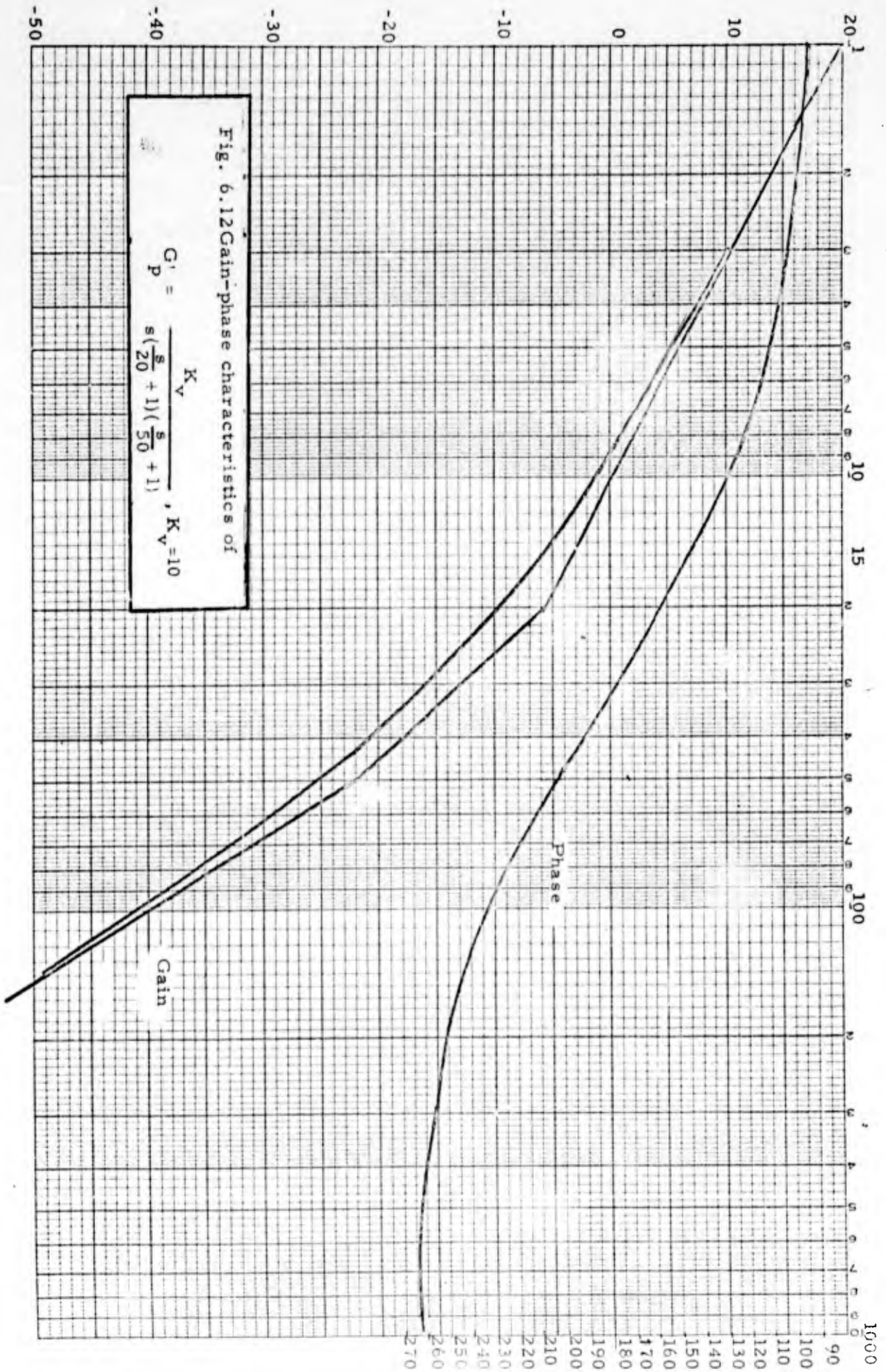

Fig. 6.12 Gain-phase characteristics of

$$G'_p = \frac{K_v}{s\left(\frac{s}{20}+1\right)\left(\frac{s}{50}+1\right)}, \quad K_v = 10$$

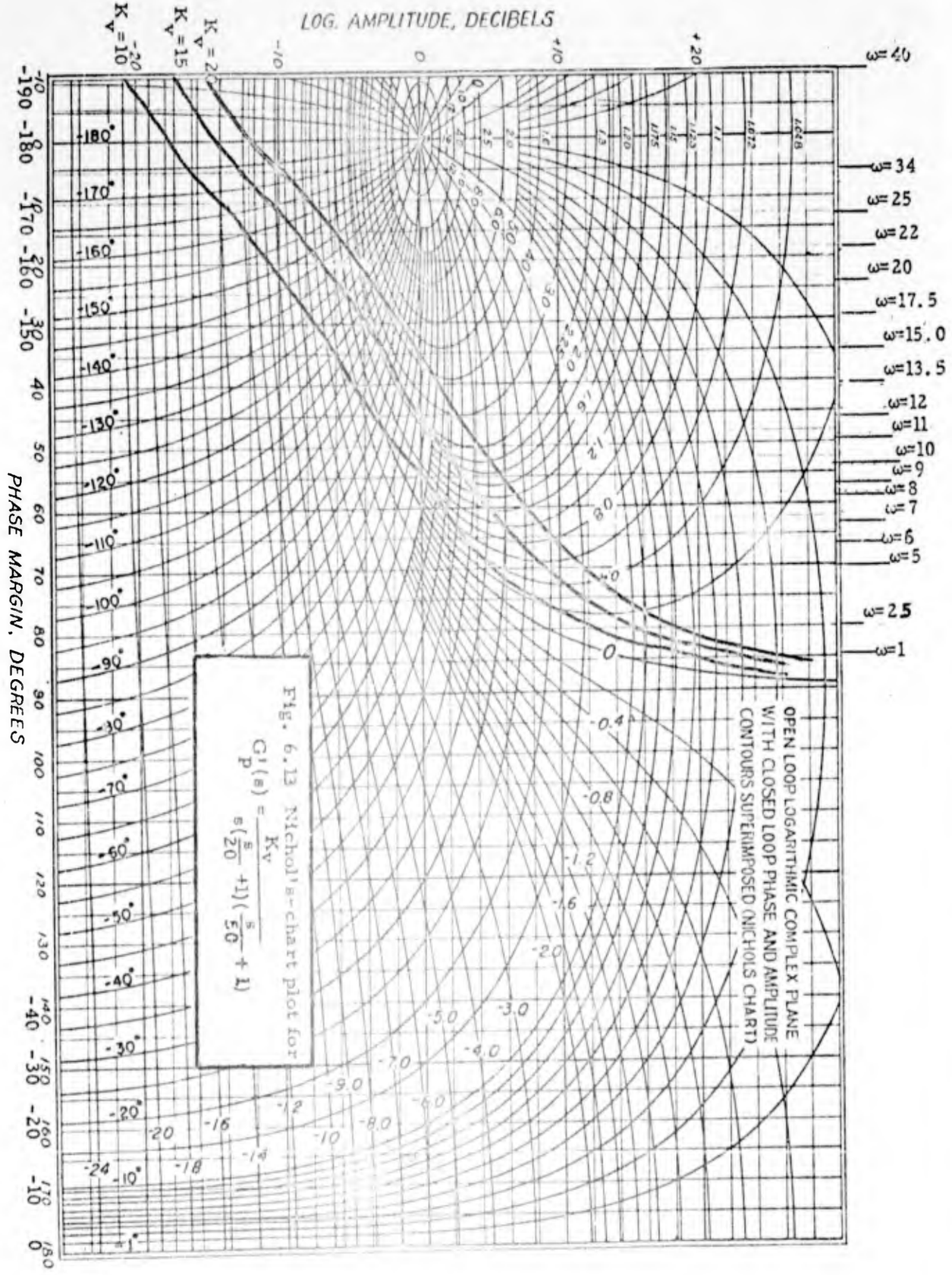
LOG. AMPLITUDE, DECIBELS
PHASE MARGIN, DEGREES
OPEN LOOP LOGARITHMIC COMPLEX PLANE
WITH CLOSED LOOP PHASE AND AMPLITUDE
CONTOURS SUPERIMPOSED (NICHOLS CHART)
Fig. 6.13 Nichol's-chart plot for
$G_p'(s) = \frac{K_v}{s(\frac{s}{20}+1)(\frac{s}{50}+1)}$

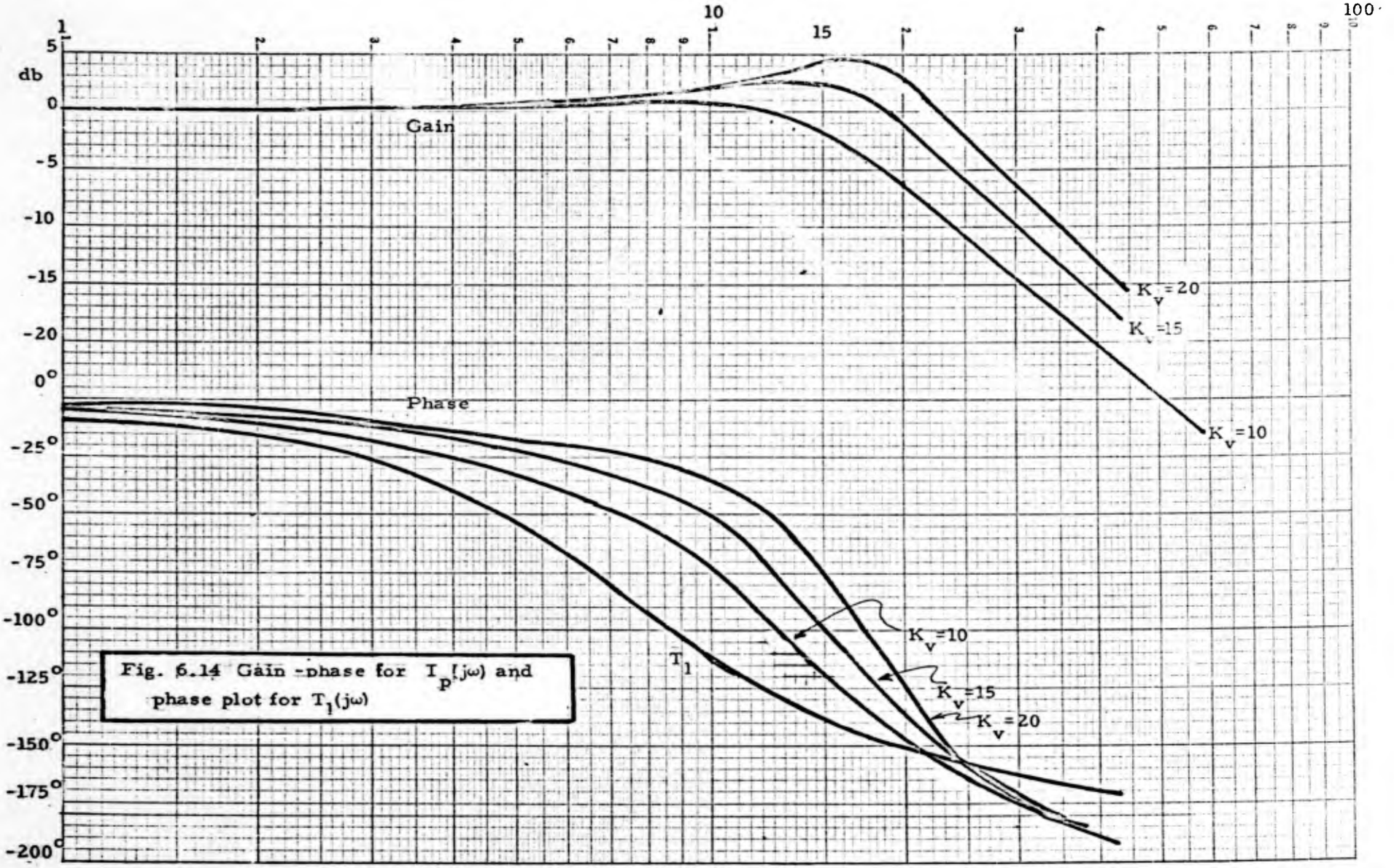

Fig. 6.14 Gain -phase for $T_p(j\omega)$ and phase plot for $T_1(j\omega)$

$$\left.\begin{aligned} (GM)_{K'_p} &= 16 \text{ db} \\ \omega_{K'_p} &= 31.6 \\ (GM)_{K_r} &\cong 8 \text{ db} \\ \omega_{K_r} &\cong 10 \end{aligned}\right\} \quad (6.44)$$

for $K_v = 15$

$$\left.\begin{aligned} (GM)_{K'_p} &= 13.4 \text{ db} \\ \omega_{K'_p} &= 31.6 \text{ (invariant)} \\ (GM)_{K_v} &\cong 8.2 \text{ db} \\ \omega_{K_r} &\cong 11 \end{aligned}\right\} \quad (6.45)$$

for $K_v = 20$

$$\left.\begin{aligned} (GM)_{K'_p} &= 11 \text{ db} \\ \omega_{K'_p} &= 31.6 \\ (GM)_{K_r} &\cong 9 \text{ db} \\ \omega_{K_r} &= 12.2 \end{aligned}\right\} \quad (6.46)$$

The set of margins given by Eq. (6.46) satisfies the required stability margins on K_p and K_r. For the range of K_v considered here, the slight increase in $(GM)_{K_r}$ is traded for a comparatively large decrease in $(GM)_{K'_p}$.

In order to ascertain the effects of a simultaneous variation in K_p and K_r, the Routh test is applied to the graph determinant Δ for two situations: one with $G_c = 1$ or no compensation, and the other with $G_c(s) = K(s + 5)/(s + 50)$.

The graph determinant for the uncompensated system is

$$\Delta = 1 + \frac{K_1 H_1}{s(s+a)} + \frac{K_p}{s(s+b)(s+c)} + K_r K_p \frac{K_1}{s^2(s+a)(s+b)(s+c)} \qquad (6.47)$$

G_o

or

$$\Delta_1 = \frac{\Delta}{G_o} = 1 + \frac{K_p(s+a)}{(s+b)(s+c)(s^2+as+K_1H_1)} + K_pK_r \frac{K_1}{s(s+b)(s+c)(s^2+as+K_1H_1)} \qquad (6.48)$$

The determinant for the compensated system has the same form as Eq. (6.48) except that K_p' replaces K_p and $b' = 50$ takes the role of $b = 5$. It is noted in passing that the determinant Δ_1 is in a form amenable to analysis by means of Meyer's Convex Hull method [Eq. (3.11)].

Application of the Routh test to the zeros of Δ_1 for the two cases yields the stability boundaries in the normalized $K_r - K_p$ plane as shown in Fig. 6.15. The coordinates in this plane are

$$y_1 = \frac{K_r}{22.5}$$

$$y_2 = \frac{K_v}{10} = \begin{cases} \frac{K_p}{100} & \text{for} \quad G_c(s) = 1 \\ \frac{K_p'}{1000} & \text{for} \quad \text{compensated system} \end{cases} \qquad (6.49)$$

The marked improvement in the stability of the system is evident from the curves. Additionally, the curves indicate the wide latitude available to the designer in choosing K_v. For our purposes, $K_v = 20$ is chosen. The gain margins with respect to the other system parameters are computed and tabulated in Table 6.3. The margins are all found to be comfortably " safe" in the sense that no one parameter variation can cause instability. The compensation improves not only the relative stability of the system but also the dynamic and steady-state accuracy, as the velocity constant is increased from 5.38 to 20.0.

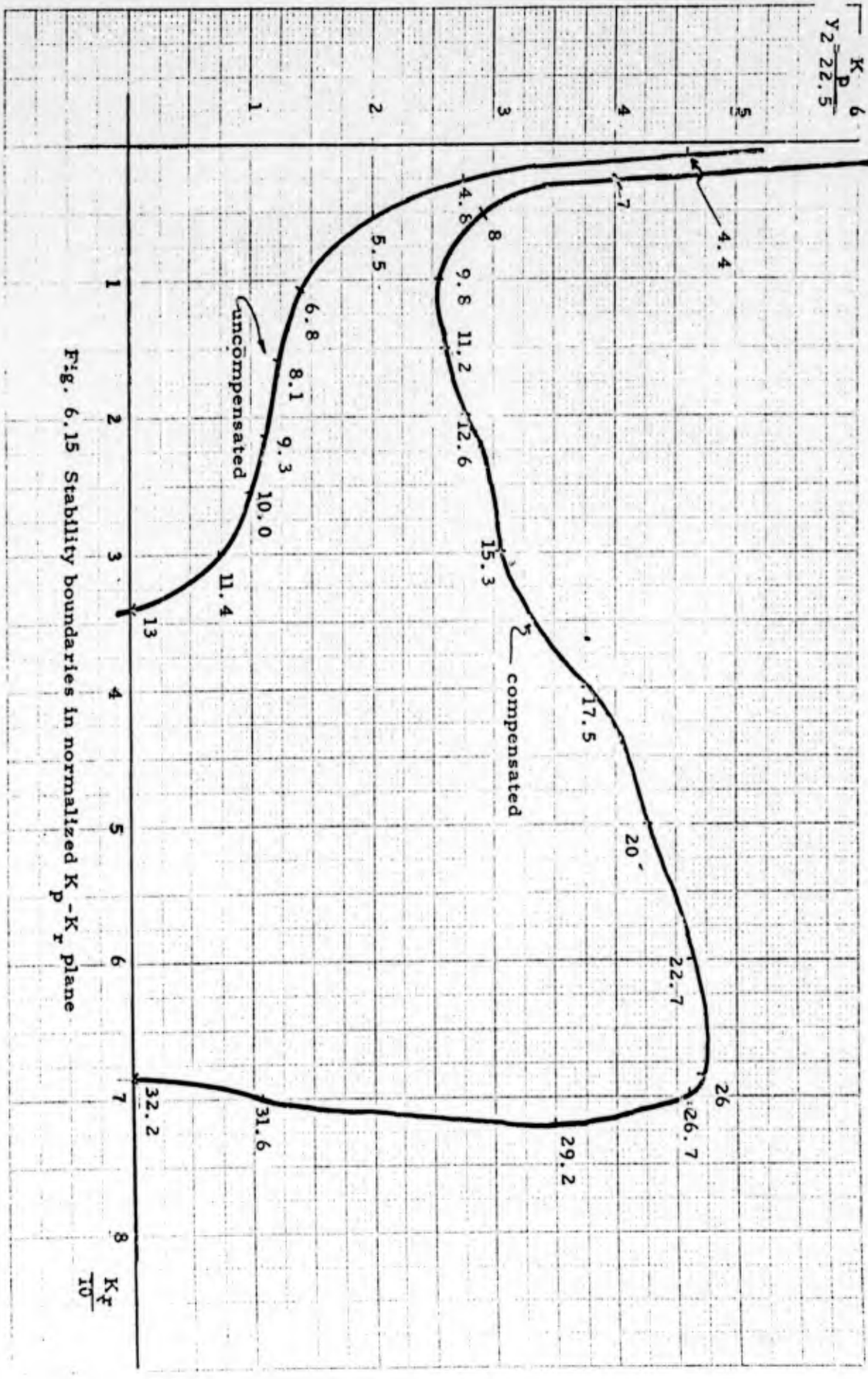

Fig. 6.15 Stability boundaries in normalized K_p-K_r plane

Parameter	Nominal Value	Critical Value	Gain Margin	Oscillation Frequency
K_r	22.5	63	9 db	12.6
H_1	22.5	-29.2		8.5
K_p	538	1890	11 db	31.6
K_1	1.88	∞		∞
a	9.3	0		7.75
b	5.0	-4.3		14.5

Table 6.3 Tabulation of gain margins for compensated system with $K_v = 20$

6.4 Recapitulation

In the preceding three sections, the analysis and the stabilization of a multi-loop system via the sensitivity method are described in some detail. At this point a review of the key steps in the development is needed to set matters in proper focus. The pattern which emerges is:

(1) Analysis. For the given configuration, the parameter gain margins are expressed in terms of the sensitivity functions. The sensitivities in turn are related to the transfer functions of the fixed and adjustable blocks in the system.

(2) Real-frequency specifications. The critical, or unstable, values of the parameter are forced to fall outside the expected range of variation, thereby specifying the parameter gain margin, or, in effect, the magnitude of the sensitivity function at those frequencies where the phase angle of S_x^T is 0° or 180°. The discrete-frequency specification of the sensitivity function is then translated into requirements on the transfer functions of the system blocks. In our system, for example, the two parameters of interest are K_r and K_p, and the required gain margins are $\pm$ 9 db and $\pm$ 6 db, respectively. The sensitivities are expressed as

$$\left.\begin{aligned} S_{K_p}^{T_a} &= -T_p \\ S_{K_r}^{T} &= 1 - T_1 T_p \end{aligned}\right\} \qquad (6.50)$$

From Eq. (6.50) and the gain margin requirement, the specification on T_p and T_1T_p becomes

$$\left.\begin{aligned} |T_p| &< \text{db when } \angle T_p = 180^\circ \\ |T_1 T_p| &< -5\text{db when } \angle T_1 T_p = 180^\circ \end{aligned}\right\} \qquad (6.51)$$

(3) Compensation. The frequency-response characteristics of the component transfer functions are shaped so as to satisfy the real-frequency requirements [e.g., Eq. 6.51)]. Within the bounds of other system specifications such as bandwidth, velocity constant, and the like, the designer is permitted considerable freedom in his choice of appropriate compensation networks. [One caution should be observed in this connection. The graph determinant and the sensitivities must be re-evaluated if the compensation introduces another loop into the system.]

For example, the stabilization of the radar-tracking system is achieved in two steps:

(a) Modification of the frequency response of the adjustable component -- the peak in $|T_1(j\omega)|$ is reduced while maintaining the required bandwidth.

(b) Introduction of compensation -- the lead network inserted in the forward path of the power stage increases the bandwidth of T_p.

In conclusion, the sensitivity method does not constitute a direct synthesis procedure. Rather, the method provides a guide to the stabilization of multiloop systems, and its successful application depends on the experience and ingenuity of the designer.

6.5 Criticism and Limitations of the Sensitivity Method

As was pointed out in Sec. 3.2, the gain margins do not determine the stability of the system if several parameters vary simultaneously. Consequently, design founded upon the sensitivity method can assure stability only if one parameter varies at a time. A consequence of this limitation is illustrated by the stability boundaries in the parameter plane for a system with two varying parameters x and y as shown in Fig. 6.16.

The nominal value of each parameter is unity. Curve (a) represents the uncompensated system with gain margins 20 log $(x_{cr})_1$ and 20 log $(y_{cr})_1$. Curves (b) and (c) indicate two possible stability boundaries which may result from two different compensation networks yielding the same required gain margins, 20 log $(x_{cr})_2$ and

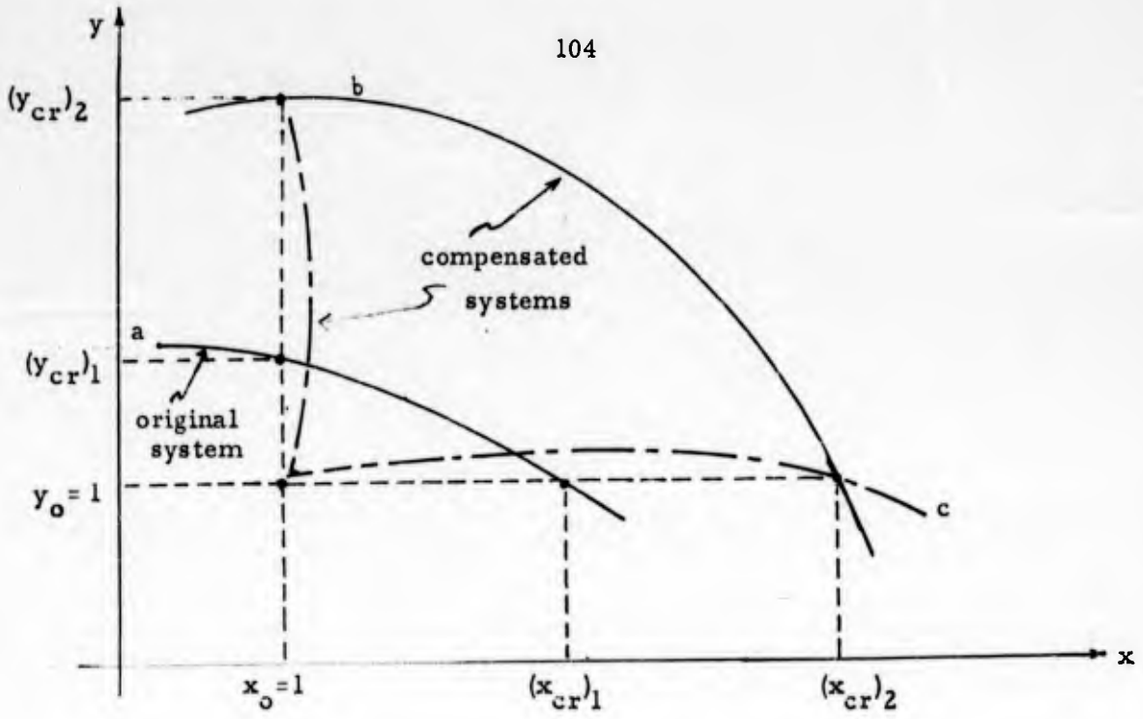

Fig. 6.16 Stability boundaries in parameter plane

20 log $(y_{cr})_2$. As indicated by Curve (c), the compensation actually destabilizes the system when simultaneous variations in the two parameters are considered. In this instance, the pole sensitivities give an indication of the relative stability, although the gain margins are quite misleading.

Consequently, designing for specified gain margins is not sufficient to insure an improvement in the stability of the system. Other methods, such as Routh-Hurwitz and Meyer's Convex Hull, must be employed to check the stability boundaries. Alternately, an analog-computer simulation of the system yields the stability boundaries (at least for the two-parameter case) and can be employed to check the compensation networks suggested by the sensitivity method. Various design possibilities can be studied in this experimental manner until one is found which yields the desired gain margins and improves the stability against simultaneous parameter variations. The sensitivity method, it is stressed, provides but one avenue of attack on the general multiloop, multiparameter problem. Root-locus, Routh-Hurwitz, the Nyquist test, etc., should all be used when applicable.

Chapter VII - Concluding Comments

7.1. Summary

This dissertation presents a novel approach to the stabilization of multi-loop, multiparameter systems. Founded upon the relationships among stability, sensitivity, and flow-graph topology set down in Chaps. II and III, the sensitivity method may be regarded as an evolution from the conventional, real-frequency design techniques so frequently employed for the single-loop, single-parameter system. The parameter gain and phase margins, the design objectives in the multiparameter case, are shown to be generalizations of the gain and phase margin concepts of the servomechanism literature. Whereas the gain and phase margin requirements for the single-loop system specify the loop gain at two frequencies (the so-called "gain and phase crossover" frequencies), the parameter margins for the arbitrary configuration prescribe the sensitivity functions at a set of discrete frequencies.

The sensitivity method not only provides a set of specific design objectives in terms of the parameter gain margins, but also suggests the system modifications to achieve these. The sensitivity approach can always be used in conjunction with other experimental or analytical techniques [e.g., Routh-Hurwitz, computer simulation] to avoid the objectionable situation described in Sec. 6.5.

7.2. Further Research

The criticism of the sensitivity method in Sec. 6.5 points out the need for further study in this general area. Additionally, the developments in the thesis as a whole, generate a number of topics which deserve investigation. These are:

(1) Systematic computer studies of complex systems in conjunction with the sensitivity method to improve the stability against individual and simultaneous variations in parameters.

(2) Fusion of the sensitivity method with some analytical stability theorems which account for multiparameter variations.

(3) Development of direct synthesis procedure which assures realizability of the compensation networks suggested by the sensitivity approach.

(4) Configurational or topological studies to determine if the stability margins can more easily be satisfied by the introduction of additional loops.

(5) Development of the pole-sensitivity into a design, as well as an analytical tool.

(6) Application of the theory presented in this thesis to the identification of internal parameters of a process transfer function.

(7) Extension of the theory to nonlinear systems which are characterized by real describing functions and to the identification of nonlinearities in a system.

APPENDIX

A. Derivation of Eq. (3.78)

Given:
$$\mathrm{Re}\left(\frac{x_o \Delta_x}{\Delta}\right) = \mathrm{Re}\left(\frac{\Delta_x^o}{\Delta}\right) \tag{A.1}$$

Let
$$\left.\begin{aligned} \Delta_x^o(j\omega_p) &= (\Delta_x^o)_r + j(\Delta_x^o)_i \\ \Delta_x(j\omega_p) &= (\Delta_x)_r + j(\Delta_x)_i \\ \Delta(j\omega_p) &= (\Delta_x^o)_r + j(\Delta_x^o)_i + x_o(\Delta_x)_r + jx(\Delta_x)_i \\ &= \underbrace{(\Delta_x^o)_r + x_o(\Delta_x)_r}_{\Delta_r} + j\underbrace{\left[(\Delta_x^o)_i + x_i(\Delta_x)_i\right]}_{j\Delta_i} \end{aligned}\right\} \tag{A.2}$$

Substitution of (A.2) into (A.1) gives

$$\mathrm{Re}\left(\frac{\Delta_x^o}{\Delta}\right) = \mathrm{Re}\left[\frac{(\Delta_x^o)_r + j(\Delta_x^o)_i}{(\Delta_r + j\Delta_i)}\right] = \frac{(\Delta_x^o)_r \Delta_r + (\Delta_x^o)_i \Delta_i}{\Delta_r^2 + \Delta_i^2} = \frac{(\Delta_x^o)_r \Delta_r + (\Delta_x^o)_i \Delta_i}{|\Delta|^2} \tag{A.3}$$

Similarly,

$$\mathrm{Re}\left(\frac{x_o \Delta_x}{\Delta}\right) = \mathrm{Re}\left[\frac{x_o(\Delta_x)_r + j x_o(\Delta_x)_i}{(\Delta_r + j\Delta_i)}\right] = x_o\left[\frac{(\Delta_x)_r \Delta_r + (\Delta_x)_i \Delta_i}{|\Delta|^2}\right] \tag{A.4}$$

If (A.3) is equated to (A.4), and Δ_r and Δ_i expanded, there results

$$\begin{aligned} &(\Delta_x^o)_r\left[(\Delta_x^o)_r + x_o(\Delta_x)_r\right] + (\Delta_x^o)_i\left[(\Delta_x^o)_i + x_o(\Delta_x)_i\right] \\ &\qquad = x_o\left\{(\Delta_x)_r\left[(\Delta_x^o)_r + x_o(\Delta_x)_r\right] + (\Delta_x)_i\left[(\Delta_x^o)_i + x_o(\Delta_x)_i\right]\right\} \end{aligned} \tag{A.5}$$

Eq. (A.5) reduces to

$$(\Delta_x^o)_r^2 + (\Delta_x^o)_i^2 = x_o^2\left[(\Delta_x)_r^2 + (\Delta_x)_i^2\right] \tag{A.6}$$

or
$$|\Delta_x^o|^2 = x_o^2 |\Delta_x|^2 \tag{A.7}$$

B. Derivation of Eqs. (3.92) and (3.93)

(1) Reference is made to Fig. 3.14. If $F_x' = 1$,

$$\left.\begin{aligned} S_x^T(s) &= \frac{-x\Delta_x(s)}{\Delta(s)} \\ T(s) &= \frac{\Sigma_x^o(s)}{\Delta(s)} \end{aligned}\right\} \qquad (B.1)$$

The necessary and sufficient condition for poles of T(s) to cross the line $s = -a$ is that there exist a real β_x, such that

$$S_{x_o}^T(-a + j\beta_x) \text{ is real} \qquad (B.2)$$

Proof: Let $p = s + a$. Since $\Delta(s) = \Delta_x^o(s) + x\Delta_x(s)$,

$$\Delta'(p) = \Delta(p-a) = \Delta_x^o(p-a) + x\Delta_x(p-a) = \Delta_x^{o'}(s) + x\Delta_x'(p) \qquad (B.3)$$

where the prime ($'$) indicates a polynomial of the same order as the original but with different real coefficients generated by the translation of the axes. In terms of the variable p, Eq. (B.1) becomes

$$S_x^T(p-a) = \frac{-x\Delta_x'(p)}{\Delta'(p)} \qquad (B.4)$$

At crossover of the $s = -a$ line, the determinant expressed as a polynomial in p is zero, i.e.,

$$\Delta'(p)\Big|_{\substack{p=j\beta_x \\ x=x_{cr}'}} = \Delta_x^{o\,\prime}(j\beta_x) + (x_o + \delta_{cr}')\Delta_x'(j\beta_x) = 0 \qquad (B.5)$$

Substitution of Eq. (B.5) into Eq. (B.4) yields

$$S_x^T(p-a)\Big|_{\substack{x=x_o \\ p=j\beta_x}} = S_{x_o}^T(-a + j\beta_x) = \frac{-x_o\Delta_x'(j\beta_x)}{-\delta_{cr}'\Delta_x'(j\beta_x)} = \frac{x_o}{\delta_{cr}'} \qquad (B.6)$$

or

$$\frac{\delta_{cr}'}{x_o} = \frac{1}{S_{x_o}^T(-a + j\beta_x)} \qquad (B.7)$$

(2) Reference is made to Fig. 3.15. If $F_x' = \infty$

$$S_x^T(s) = \frac{\Delta_x^o(s)}{\Delta(s)} \tag{B.8}$$

The necessary and sufficient condition for poles of T(s) to cross the constant ζ_m line is that there exist a real β_x such that

$$S_{x_o}^T(j\beta_x e^{j\theta_m}) \text{ is real} \tag{B.9}$$

Proof: Let $S = jpe^{j\theta_m}$. The polynomial, $\Delta'(p)$, (with complex coefficients in this case) is zero at crossover of the ζ_m line, or

$$\Delta'(p)\Big|_{\substack{p=j\beta_x \\ x=x'_{cr}}} = \Delta_x^{o'}(j\beta_x) + (x_o + \delta'_{cr})\,\Delta_x'(j\beta_x) = 0 \tag{B.10}$$

Combining Eqs. (B.8) and (B.10) gives

$$S_x^T(jpe^{j\theta_m})\Big|_{\substack{p=j\beta_x \\ x=x_o}} = \frac{-(x_o + \delta'_{cr})\,\Delta_x'(j\beta_x)}{-\delta_{cr}\,\Delta_x(j\beta_x)} = 1 + \frac{x_o}{\delta_{cr}} \tag{B.11}$$

or

$$\frac{\delta'_{cr}}{x_o} = \frac{1}{S_{x_o}^T(j\beta_x e^{j\theta_m}) - 1} \tag{B.12}$$

C. Derivation of residue sensitivity, Eq. (5.39)

Evaluation of Eq. (5.31) at the nominal values $x = x_o$, $p_k = p_{k_o}$, $x_j = z_{j_o}$ gives

$$r_{k_o} = \frac{\prod_{j=1}^{m}(p_{k_o} - z_{j_o})}{\prod_{\substack{\mu=1 \\ \mu\neq k}}^{m}(p_{k_o} - p_{\mu_o})} \tag{C.1}$$

If x is perturbed from x_o by an amount dx, the poles and zeros shift by dp_k and dz_j respectively. Hence, with the perturbation, the residue is

$$r_k = \frac{\prod\left[(p_{k_o} + dp_k) - (z_{j_o} + dz_j)\right]}{\prod\left[(p_{k_o} + dp_k) - (p_{\mu_o} + dp_\mu)\right]} = r_{k_o} \frac{\prod\left[1 + \frac{dp_k - dz_i}{p_{k_o} - dp_\mu}\right]}{\prod\left[1 + \frac{dp_k - dp_\mu}{p_{\mu_o} - p_{j_o}}\right]} \tag{C.2}$$

Taking the derivative of the logarithm of Eq. (C.2) yields

$$\frac{d}{dx} \ln x = \frac{d}{dx} \left\{ \ln r_{k_o} + \sum \ln\left(1 + \frac{dp_k - dz_i}{p_{k_o} - z_{j_o}} - \sum \ln\left(1 + \frac{dp_k - dp_\mu}{p_{k_o} - z_{j_o}}\right)\right)\right\}$$

$$= \sum \frac{\frac{1}{p_{x_o} - z_{j_o}} \left(\frac{dp_k}{dx} - \frac{dz_j}{dx}\right)}{1 + \frac{dp_k - dz_j}{p_{k_o} - z_{j_o}}} - \sum \frac{\frac{1}{p_{k_o} - p_{\mu_o}} \left(\frac{dp_k}{dx} - \frac{dp_\mu}{dx}\right)}{1 + \frac{dp_k - dp_\mu}{p_{k_o} - p_{\mu_o}}}$$

$$\simeq \sum \frac{\left(\frac{dp_k}{dx} - \frac{dz_j}{dx}\right)}{(p_{k_o} - z_{j_o})} - \sum \frac{\left(\frac{dp_k}{dx} - \frac{dp_\mu}{dx}\right)}{(p_{k_o} - p_{\mu_o})} \tag{C.3}$$

Multiplying through by x_o and identifying $x_o \frac{dp_\mu}{dx}$ with $Q_x^{p_\mu}$ gives the residue sensitivity as

$$x_o \frac{d}{dx} \ln r_k = \frac{dr_k / r_{k_o}}{dx / x_o} = S_{x_o}^{r_k} = \left[\sum_{j=1}^{m} \frac{\left(Q_x^{p_k} - U_x^{z_j}\right)}{(p_k - z_j)} + \sum_{\substack{\mu=1 \\ \mu \neq k}}^{n} \frac{\left(Q_x^{p_k} - Q_x^{p_\mu}\right)}{(p_k - p_\mu)} \right]_{x=x_o} \tag{C.4}$$

D. Sample Calculation of Pole Sensitivity for the System of Fig. 6.1.

The residues at the poles p_1 and p_2 are found from the pole-zero pattern of Fig. 6 to be

$$r_1 = 5.8 \quad 32^\circ$$
$$r_2 = 7.2 \quad 226^\circ \tag{D.1}$$

From the configuration of Fig. 6.1 and the pole-zero pattern the pole sensitivities with respect to H_1 are

$$Q_{H_1}^{p_1} = -\left(\frac{H_1 \Delta_{H_1}}{\Delta}\right) r_1 = -\left(\frac{H_1 G_1}{K_r G_1 G_p}\right) r_1 = -\frac{1}{G_p}\Bigg|_{s = p_1} r_1 = 8.0 \angle 55^\circ \tag{D.2}$$

and

$$Q_{H_1}^{p_2} = -\frac{1}{G_p}\Bigg|_{s = p_2} r_2 = 7.2 \quad 225^\circ \tag{D.3}$$

The other pole sensitivities are computed similarly.

BIBLIOGRAPHY

1. E. J. Angelo, "Design of Feedback Systems", Polytechnic Institute of Brooklyn, Microwave Research Institute, Research Report R-449-55 PIB-379, 1956.
2. S. Darlington, "The Potential Analogue Method of Network Synthesis", Bell System Tech. J., Vol. 30, pp. 315-365, April, 1951.
3. R. F. Hoskins, "Signal Flow-Graph Analysis and Feedback Theory", Institution of Electrical Engineers, July, 1960.
4. W. A. Lynch, "A Formulation of the Sensitivity Function", Correspondence PGCT vol. CT-4, No. 3, p. 289, Sept., 1957.
5. W. A. Lynch and J. G. Truxal, "The Significance of Sensitivity in Feedback SystemsStudies", Polytechnic Institute of Brooklyn, MRI Report PIBMRI-866-60.
6. S. J. Mason, "Feedback Theory--Some Properties of Signal-Flow Graphs", Proc. IRE, Vol. 41, Sept., 1953.
7. S. J. Mason, "Feedback Theory--Further Properties of Signal-Flow Graphs" Proc. IRE, Vol. 44, July, 1956.
8. S. J. Mason and H. J. Zimmerman, "Electronic Circuits, Signals, and Systems", Wiley, New York, 1960.
9. R. B. Meyers, "A Useful Extension of the Nyquist Criterion to Stability Analysis of Multiloop Feedback Amplifiers", Proc. Fourth Midwest Symposium on Circuit Theory,pp. J1-J17, December, 1959.
10. R. B. Meyers, "Two Theorems in Multi-Weighted Sums", Journal of the Society for Industrial and Applied Mathematics, March 1961.
11. E. Mishkin and L. Braun, Jr., Editors, "Adaptive Control Systems ", McGraw-Hill, New York, 1961.
12. J. G. Truxal, "Automatic Feedback Control System Synthesis", McGraw-Hill, Hill, New York, 1955.
13. Hanoch Ur, "Root-Locus Properties and Sensitivity Relations in Control Systems", IRE Trans. on Automatic Control, Jan. 1960.

21 July 1961

TECHNICAL AND FINAL REPORT DISTRIBUTION LIST

PHYSICAL SCIENCES DIRECTORATE

GOVERNMENTAL

No. of Copies	Agency
3	Commander AF Office of Scientific Research ATTN: SRY Washington 25, D. C.
2	Commander AF Office of Scientific Research ATTN: SRGL Washington 25, D. C.
4	Commander Aeronautical Systems Division (ASD) Wright-Patterson Air Force Base Ohio
1	Commander AF Cambridge Research Laboratories ATTN: CRRELA L. G. Hanscom Field Bedford, Massachusetts
2 (Unclassified Only)	Commander EOAR The Shell Building 47 Rue Cantersteen Brussels, Belgium
1	P. O. Box AA Wright-Patterson Air Force Base Ohio
1	Aeronautical Research Laboratories ATTN: Technical Library Building 450 Wright-Patterson Air Force Base Ohio
10	Armed Services Technical Information Agency ATTN: TIPCR Arlington Hall Station Arlington 12, Virginia

1		Commander AF Missile Development Center ATTN: HDOI Holloman Air Force Base New Mexico
1		Commander Army Rocket & Guided Missile Agency ATTN: ORDXR-OTL Redstone Arsenal Alabama
1		Commandant Air Force Institute of Technology (AU) Library MCLI-LIB, Bldg. 125, Area B Wright-Patterson Air Force Base Ohio
2		Commander Air Force Systems Command ATTN: SCRS Andrews Air Force Base Washington 25, D. C.
1		Commanding General U. S. Army Signal Corps Research and Development Laboratory ATTN: SIGFM/EL-RPO Ft. Monmouth, New Jersey
6		National Aeronautics & Space Administration Washington 25, D. C.
1		Advanced Research Projects Agency Washington 25, D. C.
1		Rand Corporation 1700 Main Street Santa Monica, California
1	(Unclassified Only)	Chairman Canadian Joint Staff For DRB/DSIS 2450 Massachusetts Ave., N. W. Washington 25, D. C.
1		Ames Research Center (NASA) ATTN: Technical Library Moffett Field, California
1		High Speed Flight Station (NASA) ATTN: Technical Library Edwards AFB, California
1		Langley Research Center (NASA) ATTN: Technical Library Langley AFB, Virginia

21 July 1961

TECHNICAL AND FINAL REPORT DISTRIBUTION LIST

PHYSICAL SCIENCES DIRECTORATE

GOVERNMENTAL

No. of Copies	Agency
3	Commander AF Office of Scientific Research ATTN: SRY Washington 25, D. C.
2	Commander AF Office of Scientific Research ATTN: SRGL Washington 25, D. C.
4	Commander Aeronautical Systems Division (ASD) Wright-Patterson Air Force Base Ohio
1	Commander AF Cambridge Research Laboratories ATTN: CRRELA L. G. Hanscom Field Bedford, Massachusetts
2 (Unclassified Only)	Commander EOAR The Shell Building 47 Rue Cantersteen Brussels, Belgium
1	P. O. Box AA Wright-Patterson Air Force Base Ohio
1	Aeronautical Research Laboratories ATTN: Technical Library Building 450 Wright-Patterson Air Force Base Ohio
10	Armed Services Technical Information Agency ATTN: TIPCR Arlington Hall Station Arlington 12, Virginia

1	Director of Research and Development Headquarters, USAF ATTN: AFDRD Washington 25, D. C.
1	Office of Naval Research Department of the Navy ATTN: Code 420 Washington 25, D. C.
1	Director, Naval Research Laboratory ATTN: Technical Information Officer Washington 25, D. C.
1	Chief of Research and Development ATTN: Scientific Information Branch Department of the Army Washington 25, D. C.
1	Chief, Physics Branch Division of Research U. S. Atomic Energy Commission Washington 25, D. C.
1	U. S. Atomic Energy Commission Technical Information Extension P. O. Box 62 Oak Ridge, Tennessee
1	National Bureau of Standards Library Room 203, Northwest Building Washington 25, D. C.
1	Physics Program National Science Foundation Washington 25, D. C.
1	Director, Army Research Office, Durham Box CM, Duke Station Durham, North Carolina
1	AEDC (ADQIM) ATTN: AEDC Library Arnold Air Force Station Tullahoma, Tennessee
1	Commander AF Flight Test Center ATTN: FTOTL Edwards Air Force Base California

1		Commander AF Missile Development Center ATTN: HDOI Holloman Air Force Base New Mexico
1		Commander Army Rocket & Guided Missile Agency ATTN: ORDXR-OTL Redstone Arsenal Alabama
1		Commandant Air Force Institute of Technology (AU) Library MCLI-LIB, Bldg. 125, Area B Wright-Patterson Air Force Base Ohio
2		Commander Air Force Systems Command ATTN: SCRS Andrews Air Force Base Washington 25, D. C.
1		Commanding General U. S. Army Signal Corps Research and Development Laboratory ATTN: SIGFM/EL-RPO Ft. Monmouth, New Jersey
6		National Aeronautics & Space Administration Washington 25, D. C.
1		Advanced Research Projects Agency Washington 25, D. C.
1		Rand Corporation 1700 Main Street Santa Monica, California
1	(Unclassified Only)	Chairman Canadian Joint Staff For DRB/DSIS 2450 Massachusetts Ave., N. W. Washington 25, D. C.
1		Ames Research Center (NASA) ATTN: Technical Library Moffett Field, California
1		High Speed Flight Station (NASA) ATTN: Technical Library Edwards AFB, California
1		Langley Research Center (NASA) ATTN: Technical Library Langley AFB, Virginia

1	Lewis Research Center (NASA) ATTN: Technical Library 21000 Brookpark Road Cleveland 35, Ohio
1 (Unclassified Only)	Institute of the Aeronautical Sciences 2 East 64th Street New York 21, New York
1 (Unclassified Only)	Applied Mechanics Reviews Southwest Research Institute 8500 Culebra Road San Antonio 6, Texas
1 (Unclassified Only)	Linda Hall Library ATTN: Document Division 5109 Cherry Street Kansas City 10, Missouri
1	AFOSR (SRLTL) Holloman Air Force Base New Mexico

AF-18(603)-105

SUPPLEMENTAL DISTRIBUTION LIST

Control Theory, Information Theory, and Network Synthesis

Professor Gregory Young
Engineering Center
University of Southern California
Los Angeles 7, California

Professor C T Leondes
Department of Engineering
University of California
Los Angeles, California

Electronics Research Laboratory
College of Engineering
University of California
Berkeley 4, California

Dr. E. I. Jury
Department of Electrical Engineering
University of California
Berkeley 4, California

Dr. Gene F. Franklin
Electronics Research Laboratory
Stanford University
Stanford, California

Dean J. R. Ragazzini
College of Engineering
New York University
University Heights, New York

Columbia University
Electrical Engineering Department
ATTN: G. Kranc
New York 27, New York

University of Illinois
Department of Electrical Engineering
ATTN: M. E. Van Valkenburg
Urbana, Illinois

Polytechnic Institute of Brooklyn
Microwave Research Institute
ATTN: J. G. Truxal
55 Johnson Street
Brooklyn 1, New York

RIAS
1712 Bellona Avenue
Baltimore 12, Maryland

Johns Hopkins University
Department of Mechanics
ATTN: Library (Route to Prof F. H. Clauser)
Baltimore 18, Maryland

9/13/61

UNCLASSIFIED